

Electronic Supplementary Information

**Controlling Photophysics of Styrylnaphthalimides through TICT,
Fluorescence and *E,Z*-Photoisomerization Interplay**

Pavel A. Panchenko,^{*} Antonina N. Arkhipova, Olga A. Fedorova, Yuri V. Fedorov,
Marina A. Zakharko, Dmitry E. Arkhipov, Gediminas Jonusauskas

CONTENTS

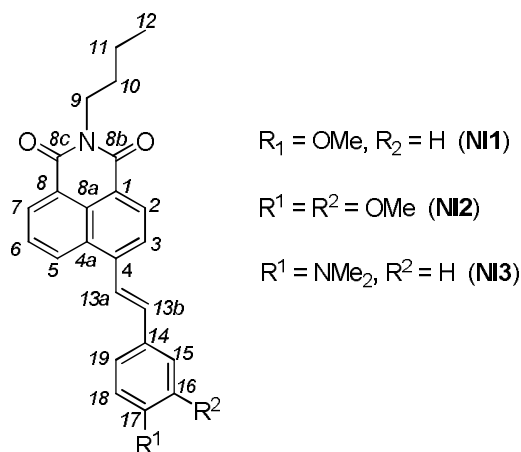
1. Synthesis of the compounds NI1–3	S2
2. Calculation of the absorption spectra of <i>Z</i> -isomers and the ratios of quantum yields $\varphi^{E \rightarrow Z} / \varphi^{Z \rightarrow E}$	S5
3. Light intensity measurement.....	S6
4. Changes in the absorption spectra of NI1–3 upon irradiation.....	S8
5. X-ray data.....	S11
6. Study of <i>E,Z</i> -photoisomerization by NMR spectroscopy.....	S12
7. Steady-state absorption and emission spectra of NI1–3	S22
8. Transient absorption spectroscopy data of NI1–3	S38
9. Plots of fluorescence quantum yield versus excited state lifetime	S56

1. Synthesis of the compounds NI1–3

Materials and general methods. 4-Bromo-1,8-naphthalic anhydride **1**¹ and 4-bromo-*N*-butyl-1,8-naphthalimide **2**² were prepared by literature procedures starting from acenaphthene. All other reagents were purchased from commercial sources and were of the highest grade. Solvents were purified and dried according to standard procedures.

Melting points were measured on Melt-temp melting point electrothermal apparatus and were uncorrected. The reaction course and purity of the final products was followed by TLC on silica gel (DC-Alufolien Kieselgel 60 F₂₅₄, Merck). Column chromatography was conducted over silica gel (Kieselgel 60, particle size 0.063-0.200 mm, Merck). Elemental analyses were carried out in the Microanalysis Laboratory of the A.N. Nesmeyanov Institute of Organoelement Compounds.

NMR measurements. ¹H and ¹³C NMR spectra were recorded on an, Avance 400 and Avance 600 spectrometers (Bruker) operating at 400.13 and 600.22 MHz (for ¹H) and 100.61 and 150.93 MHz (for ¹³C) respectively. The measurements were performed in DMSO-*d*₆ solutions. The chemical shifts (given as δ) were determined with an accuracy of 0.01 ppm relative to the signals corresponding to the residual solvents and recalculated to the internal standard (TMS); the spin-spin coupling constants (*J*) were measured with an accuracy of 0.1 Hz. The numbering of carbon atoms in the compounds **NI1–3** used by us for the description of ¹H and ¹³C NMR spectra below is shown in Scheme S1. The assignment of ¹H and ¹³C signals is based on ¹H COSY, HMBC and HSQC NMR spectra.



Scheme S1. Numbering of carbon atoms in the compounds **NI1–3**

¹ S. D. Ross, M. Finkelstein, R. C. Petersen, *J. Am. Chem. Soc.*, 1958, **80**, 4327-4330; M. Shahid, P. Srivastava, A. Misra, *New J. Chem.*, 2011, **35**, 1690-1700.

² P. Stange, K. Fumino, R. Ludwig, *Chem. Eur. J.*, 2013, **19**, 2990-2994.

Mass spectrometry. LC-ESI-MS analyses were performed on a Finnigan LCQ Advantage mass spectrometer equipped with octopole ion-trap mass-analyzer, MS Surveyor pump, Surveyor auto sampler, Schmidlin-Lab nitrogen generator (Germany) and Finnigan X-Calibur 1.3 software for data collecting and processing. Acetonitrile (Panreac, HPLC-gradient grade) was used as the mobile phase. The isocratic elution was maintained at a flow rate of 50 $\mu\text{L} \cdot \text{min}^{-1}$ without column. The effluent from LC was passed directly into the electrospray ion source without a split. Positive electrospray ionization was achieved using a ionization voltage at 3 kV with temperature at 200 °C. Isotope patterns were calculated with Molecular Weight Calculator, Version 6.37 (Matthew Monroe).

General procedure for the synthesis of compounds NI1–3. A solution of 4-bromo-*N*-butyl-1,8-naphthalimide **2** (1 mmol), Pd(OAc)₂ (0.01 mmol), tris-(*ortho*-tolyl)phosphine (0.06 mmol), triethylamine (1 ml) and corresponding styrene (1.2 mmol) in dry DMF (10 ml) was stirred at 105 °C during 15–24 h under argon atmosphere. The mixture was cooled to ambient temperature then diluted with water and extracted with CH₂Cl₂. The organic layer was dried with MgSO₄ and evaporated in vacuum. The residue was subjected to chromatography on a silica gel by using gradient mixture hexane – ethyl acetate and then recrystallized from ethanol. *2-butyl-6-(4-methoxystyryl)-1H-benzo[d,e]isoquinoline-1,3(2H)-dione (NI1)*. Yield 38%. M.p. 140 – 143°C. ¹H NMR (400.13 MHz, CDCl₃, 22 °C, δ / ppm, J / Hz): 0.99 (t, 3H, H(12), J = 8.4), 1.43 – 1.50 (m, 2H, H(11)), 1.69 – 1.77 (m, 2H, H(10)), 3.88 (s, 3H, OCH₃), 4.20 (t, 2H, H(9), J = 8.4), 6.98 (d, 2H, H(16), H(18), J = 8.6), 7.31 (d, 1H, H(13b), J = 16.0), 7.59 (d, 2H, H(15), H(19), J = 8.6), 7.72 – 7.81 (m, 2H, H(13a), H(6)), 7.98 (d, 1H, H(3), J = 7.7), 8.56 – 8.61 (m, 2H, H(2), H(5)), 8.63 (d, 1H, H(7), J = 8.3). ¹³C NMR (150.93 MHz, CDCl₃, 22°C, δ / м. д., J / Hz): 13.98 (C(12)), 20.89 (C(11)), 30.56 (C(10)), 40.45 (C(9)), 55.16 (OCH₃), 114.56 (C(16), C(18)), 121.56 (C(1)), 121.76 (C(13a)), 123.68 (C(8)), 123.97 (C(3)), 126.84 (C(8a)), 127.23 (C(6)), 129.63 (C(15), C(19)), 129.79 (C(14)), 130.06 (C(4a)), 130.11 (C(5)), 130.23 (C(7)), 131.81 (C(2)), 135.67 (C(13b)), 142.16 (C(4)), 161.07 (C(17)), 163.97 (C(8b)), 164.08 (C(8c)). ESI-MS in MeCN, calculated for [M]⁺, m/z: 385.17; found: 385.21. Elemental analysis: calculated (%) for C₂₅H₂₃NO₃ (MW 385.46): C 77.89, H 6.02, N 3.64; found C 77.94, H 6.11, N 3.70. *2-butyl-6-(3,4-dimethoxystyryl)-1H-benzo[d,e]isoquinoline-1,3(2H)-dione (E-NI2)*. Yield 18%. M.p. 155 – 157°C. ¹H NMR (400.13 MHz, CDCl₃, 21 °C, δ / ppm, J / Hz): 0.99 (t, 3H, H(12), J = 8.4), 1.43 – 1.52 (m, 2H, H(11)), 1.70 – 1.78 (m, 2H, H(10)), 3.96 (s, 3H, OCH₃), 4.02 (s, 3H, OCH₃), 4.20 (t, 2H, H(9), J = 8.4), 6.94 (d, 1H, H(18), J = 8.2), 7.18 – 7.24 (m, 2H, H(15), H(19)), 7.30 (d, 1H, H(13b), J = 16.0), 7.72 – 7.82 (m, 2H, H(13a), H(6)), 7.98 (d, 1H, H(3), J = 7.7), 8.56 – 8.62 (m, 2H, H(2), H(5)), 8.65 (d, 1H, H(7), J = 8.3). ¹³C NMR (150.93 MHz, CDCl₃, 21°C, δ / ppm, J / Hz): 13.98 (C(12)), 20.89 (C(11)), 30.56 (C(10)), 40.45 (C(9)),

55.26 ($2\times$ OCH₃), 109.78 (C(19)), 112.01 (C(18)), 121.63 (C(15)), 121.86 (C(1)), 122.06 (C(13a)), 123.88 (C(8)), 123.97 (C(3)), 127.44 (C(6)), 129.83 (C(8a)), 130.69 (C(14)), 130.86 (C(4a)), 131.11 (C(5)), 131.89 (C(7)), 131.91 (C(2)), 136.07 (C(13b)), 142.16 (C(4)), 149.75 (C(16)), 150.07 (C(17)), 164.37 (C(8b)), 164.48 (C(8c)). ESI-MS in MeCN, calculated for [M]⁺, *m/z*: 415.18; found: 415.22. Elemental analysis: calculated (%) for C₂₆H₂₅NO₄ (MW 415.48): C 75.17, H 6.07, N 3.37; found C 75.21, H 6.13, N 3.43. *2-butyl-6-(4-(dimethylamino)styryl)-1H-benzo[d,e]isoquinoline-1,3(2H)-dione (E-NI3)*. Yield 28%. M.p. 181 – 184°C. ¹H NMR (400.13 MHz, CDCl₃, 23 °C, δ / ppm, *J* / Г_Ц): 0.98 (t, 3H, H(12), *J* = 8.4), 1.42 – 1.51 (m, 2H, H(11)), 1.69 – 1.78 (m, 2H, H(10)), 3.07 (s, 6H, N(CH₃)₂), 4.19 (t, 2H, H(9), *J* = 8.4), 6.73 – 7.00 (m, 2H, H(16), H(18)), 7.33 (d, 1H, H(13b), *J* = 16.0), 7.58 (d, 2H, H(15), H(19), *J* = 8.6), 7.69 – 7.80 (m, 2H, H(6), H(13a)), 7.99 (d, 1H, H(3), *J* = 7.7), 8.55 – 8.65 (m, 3H, H(2), H(5), H(7)). ¹³C NMR (150.93 МГц, CDCl₃, 22°C, δ / ppm, *J* / Г_Ц): 13.02 (C (12)), 20.03 (C (11)), 29.16 (C(10)), 38.76 (C(9)), 38.94 ($2\times$ N(CH₃)₂), 112.06 (C(16), C(18)), 117.96 (C(13a)), 119.87 (C(1)), 122.12 (C(3)), 122.97 (C(8)), 124.84 (C(8a)), 126.23 (C(6)), 129.07 (C(15)), C(19)), 129.79 (C(14)), 130.39 (C(4a)), 130.56 (C(5)), 130.81 (C(7)), 130.89 (C(2)), 136.07 (C(13b)), 142.01 (C(4)), 144.07 (C(17)), 161.97 (C(8b)), 162.08 (C(8c)). ESI-MS in MeCN, calculated for [M]⁺, *m/z*: 398.20; found: 398.27. Elemental analysis: calculated (%) for C₂₆H₂₆N₂O₂ (MW 398.50): C 78.35, H 6.58, N 7.03; found C 78.43, H 6.56, N 7.08.

2. Calculation of the absorption spectra of Z-isomers and the ratios of quantum yields $\varphi^{E \rightarrow Z} / \varphi^{Z \rightarrow E}$

The Fisher method was used to calculate the absorption spectra of Z-isomers. First, we recorded the absorption spectrum of a solution of a dye's E-isomer with a known concentration C_L and the spectra of this solution in E,Z-photostationary states obtained by irradiation with light at two wavelengths $\lambda = 365$ and 436 nm.³ Using the assumption that the ratio of the quantum yields of the Z- and E-isomers ($\varphi^{E \rightarrow Z} / \varphi^{Z \rightarrow E}$) does not depend on the irradiation wavelength, the fraction of the Z-isomer in the photostationary state created by light with $\lambda = 436$ nm was calculated from these spectra using the formula:

$$\alpha_{436} = \frac{\Delta_{365} / D_{365} - \Delta_{436} / D_{436}}{1 + \Delta_{365} / D_{365} - n \times (1 + \Delta_{436} / D_{436})}$$

where Δ_{365} (Δ_{436}) is the difference between the optical density of the solution in the photostationary state created by light with $\lambda = 365$ nm (436 nm) at a wavelength of 365 nm (436 nm) and the optical density of the starting solution of the E-isomer at $\lambda = 365$ nm (436 nm); $n = (D_{436}^{365} - D_{436}^E) / (D_{436}^{436} - D_{436}^E)$, where D_{436}^{365} and D_{436}^{436} are the optical densities of the solution in the photostationary states created by light with $\lambda = 365$ and 436 nm, respectively, at the wavelength where the optical density change is the highest ($\lambda = 436$ nm); D_{436}^E is the optical density of the solution of the starting E-isomer at the wavelength where the same wavelength ($\lambda = 436$ nm).

Once α_{436} was determined, the optical density of the pure Z-isomer was calculated:

$$D_Z(\lambda) = \frac{D^{436}(\lambda) - (1 - \alpha_{436}) \times D_E(\lambda)}{\alpha_{436}}$$

where $D_E(\lambda)$ is the spectrum of the starting solution of the E-isomer; $D^{436}(\lambda)$ is the spectrum of the solution in the photostationary state created by light with $\lambda = 436$ nm.

After that, the ratio of the quantum yields of the direct and reverse photoisomerization reactions was calculated:

$$\frac{\varphi^{E \rightarrow Z}}{\varphi^{Z \rightarrow E}} = \frac{(1 - \alpha_{436}) \varepsilon_E^{436}}{\alpha_{436} \varepsilon_Z^{436}}$$

where ε_E^{436} and ε_Z^{436} are the molar absorption coefficients for the E- and Z-isomer, respectively, at $\lambda = 436$ nm; d is the optical path length that equals 1 cm. In the calculation of the theoretical spectrum of the Z-isomer we assume that the C_L values for the isomers are equal since the entire E-isomer is converted to the Z-isomer.

³ For the compound **Ni3** in cyclohexane, the wavelengths $\lambda = 405$ and 436 nm were used.

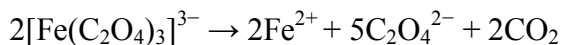
3. Light intensity measurement

The absolute light intensity was measured using a chemical ferrioxalate actinometer. With a chemical actinometer, the number of light quanta is determined from the amount of the photochemical reaction product with a quantum yield known in advance:

$$I = \frac{N}{\Phi \cdot t \cdot (1 - 10^{-D})} \approx \frac{N}{\Phi \cdot t}$$

where N is the number of moles of the product formed; Φ is the quantum yield of product formation; t is the irradiation time; $(1 - 10^{-D})$ is the coefficient representing the fraction of absorbed light (it usually equals 1, since the concentration of the actinometer is most commonly chosen to ensure complete light absorption).

A ferrioxalate actinometer is a solution of the $K_3Fe(C_2O_4)_3 \cdot 3H_2O$ complex salt in 0.1 N sulfuric acid. Under exposure to light, it undergoes the following reaction:



The quantum yield of ferrioxalate decomposition depends on the wavelength. Ferrous iron that is formed upon photolysis gives a colored complex with 1,10-phenanthroline. The complex of 1,10-phenanthroline with Fe^{2+} ions is formed relatively slowly at pH = 2.5 and considerably more quickly at pH 3.5 - 4.2. In this pH range, the resulting complex is stable to UV and visible light, and its absorption at 510 nm changes linearly with variation in the concentration of Fe^{2+} ions.

By measuring the color intensity of this complex, one can determine the amount of Fe^{2+} ions formed and hence the intensity of the light source. To measure the light intensity by the ferrioxalate method, a solution of potassium ferrioxalate is used with a concentration that, as a rule, ensures complete light absorption at the irradiation wavelength.

The following solutions are required to perform the measurements: A) a solution of potassium ferrioxalate in 0.1 N sulfuric acid, where the required concentration of potassium ferrioxalate is selected depending on the irradiation wavelength; B) 0.1% aqueous solution of 1,10-phenanthroline; C) buffer solution: 600 ml of 1 N sodium acetate + 360 ml of 1 N sulfuric acid + water (to dilute the solution to the volume of 1000 ml).

The light intensity is determined as follows. A preset volume (2 ml) of actinometer solution "A" is irradiated with stirring for such a time period t that the optical density changes by 0.1 – 0.6 (e.g., $t = 0, 60, 120, 240, 480$ s). After that, V_2 (e.g., 1.5 ml) of the irradiated solution is transferred into a measuring flask of volume V_3 (e.g., 20 ml), then $(8 - V_2)$ ml of 0.1 N sulfuric acid, 1.6 ml of solution "B" and 4 ml of solution "C" are added into the flask. The solution volume in the flask is brought to the mark with water, stirred and kept in the dark for 30 min in

order to fully complete the complexation reaction. Then, the optical density of the solution of the resulting complex of ferrous iron with 1,10-phenanthroline is measured at 510 nm. The same operations are carried out with V_1 of the non-irradiated actinometer solution used in the reference cell.

The number of moles of ferrous ions formed during photolysis, $N_{Fe^{2+}}$, is determined by the formula:

$$N_{Fe^{2+}} = 10^{-3} \frac{V_1 \cdot V_3 \cdot D}{V_1 \cdot l \cdot \varepsilon}$$

where V_1 is the volume of the irradiated actinometer solution, ml; V_2 is the volume of the irradiated actinometer taken for the analysis, ml; V_3 is the final volume to which the V_2 solution was diluted, ml; D is the solution optical density at 510 nm; l is the optical path length, cm; and ε is the extinction coefficient of the 1,10-phenanthroline–Fe²⁺ complex at 510 nm that equals $1.11 \cdot 10^4 \text{ M}^{-1} \cdot \text{cm}^{-1}$.

If $N_{Fe^{2+}}$, the $\Phi_{Fe^{2+}}$ value at a certain irradiation wavelength and the irradiation time t are known, the intensity of incident light can be calculated as:

$$I = \frac{N_{Fe^{2+}}}{\Phi \cdot t}, [\text{Einstein/s}]$$

4. Changes in the absorption spectra of NI1–3 upon irradiation

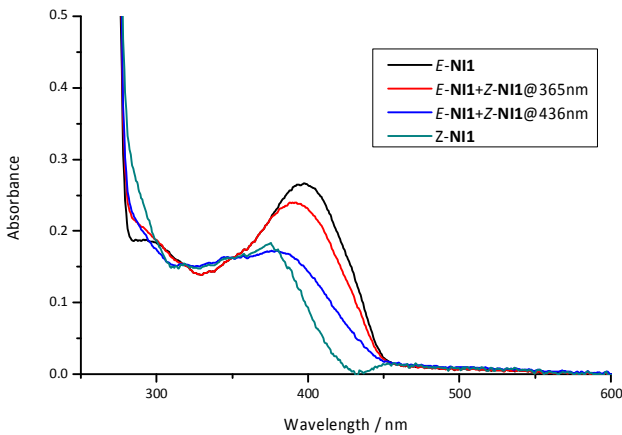


Figure S1. Absorption spectra of *E*- and *Z*-isomers of **NI1** and photoatstationary states obtained using light with $\lambda = 365$ and 436 nm in cyclohexane. The spectrum of *Z*-isomer is calculated by Fisher method. The concentration of **NI1** is $1.2 \cdot 10^{-5}$ M.

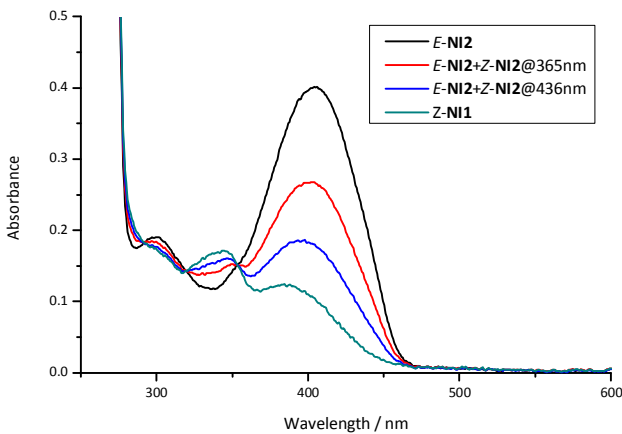


Figure S2. Absorption spectra of *E*- and *Z*-isomers of **NI2** and photoatstationary states obtained using light with $\lambda = 365$ and 436 nm in cyclohexane. The spectrum of *Z*-isomer is calculated by Fisher method. The concentration of **NI2** is $1.2 \cdot 10^{-5}$ M.

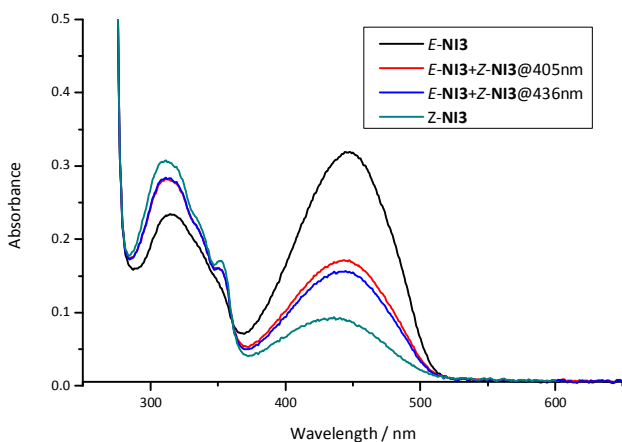


Figure S3. Absorption spectra of *E*- and *Z*-isomers of **NI2** and photoatstationary states obtained using light with $\lambda = 405$ and 436 nm in cyclohexane. The spectrum of *Z*-isomer is calculated by Fisher method. The concentration of **NI2** is $1.2 \cdot 10^{-5}$ M.

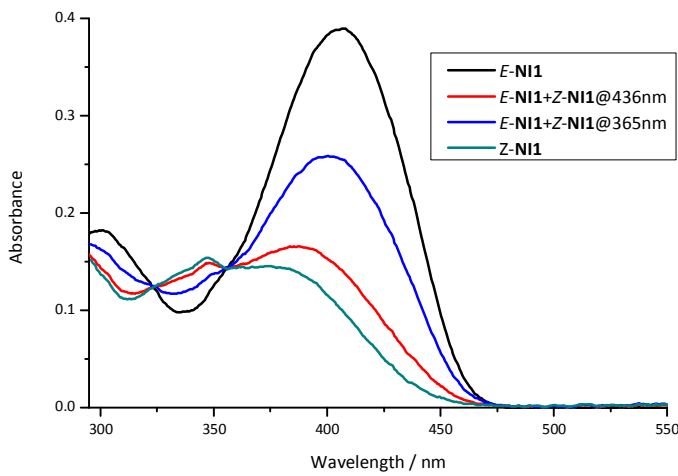


Figure S4. Absorption spectra of *E*- and *Z*-isomers of **NI1** and photoatstationary states obtained using light with $\lambda = 365$ and 436 nm in toluene. The spectrum of *Z*-isomer is calculated by Fisher method. The concentration of **NI1** is $2.0 \cdot 10^{-5}$ M.

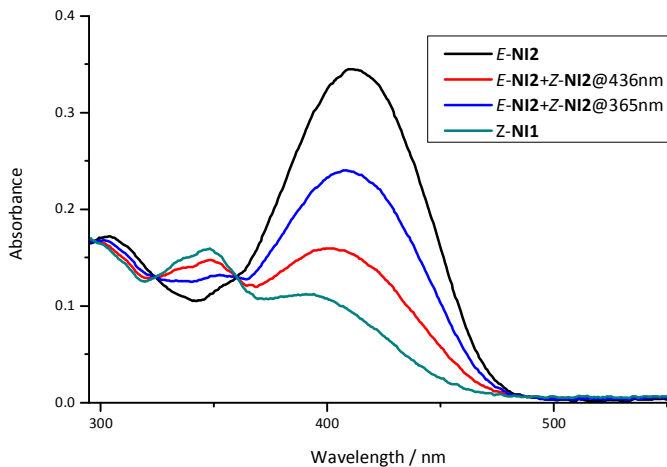


Figure S5. Absorption spectra of *E*- and *Z*-isomers of **NI2** and photoatstationary states obtained using light with $\lambda = 365$ and 436 nm in toluene. The spectrum of *Z*-isomer is calculated by Fisher method. The concentration of **NI2** is $1.3 \cdot 10^{-5}$ M.

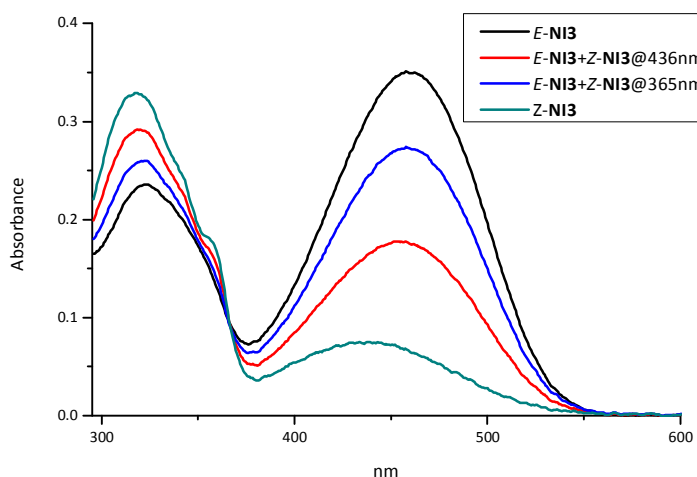


Figure S6. Absorption spectra of *E*- and *Z*-isomers of **NI3** and photoatstationary states obtained using light with $\lambda = 365$ and 436 nm in toluene. The spectrum of *Z*-isomer is calculated by Fisher method. The concentration of **NI3** is $1.2 \cdot 10^{-5}$ M.

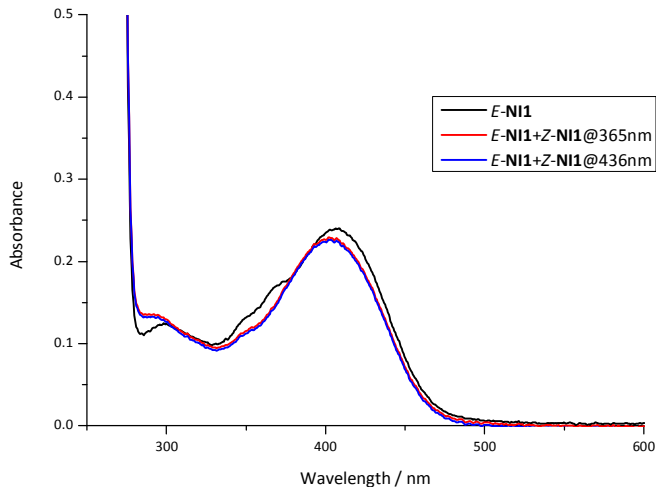


Figure S7. Absorption spectra of *E* -isomers of NI1 and photoatstationary states obtained using light with $\lambda = 365$ and 436 nm in acetonitrile. The concentration of NI1 is $1.1 \cdot 10^{-5}$ M.

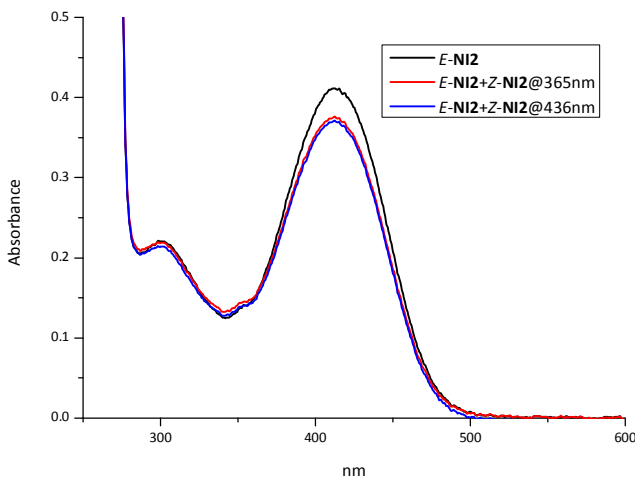


Figure S8. Absorption spectra of *E* -isomers of NI2 and photoatstationary states obtained using light with $\lambda = 365$ and 436 nm in acetonitrile. The concentration of NI2 is $1.4 \cdot 10^{-5}$ M.

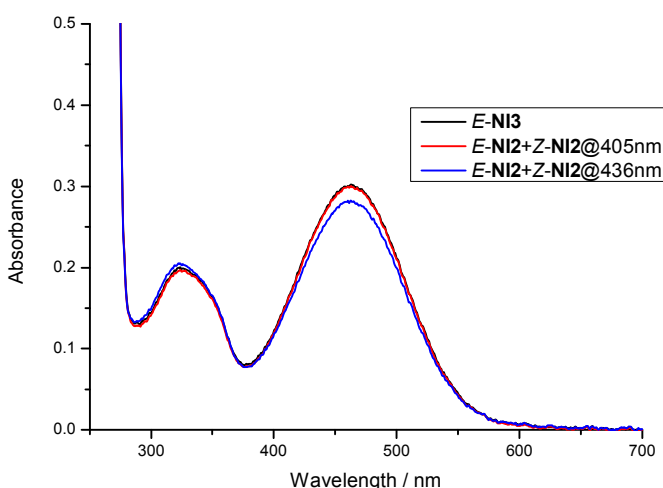


Figure S9. Absorption spectra of *E* -isomers of NI3 and photoatstationary states obtained using light with $\lambda = 405$ and 436 nm in acetonitrile. The concentration of NI3 is $1.0 \cdot 10^{-5}$ M.

5. X-ray data

Table S1. Crystallographic data and refinement parameters for the structures NI1–3

	NI1	NI2	NI3
Formula	C ₂₅ H ₂₃ NO ₃	C ₂₆ H ₂₅ NO ₄	C ₂₆ H ₂₆ N ₂ O ₂
Molecular weight	385.44	415.47	398.49
T, K	120	120	100
Crystal system	Monoclinic	Monoclinic	Triclinic
Space group	P2 ₁ /c	P2 ₁ /n	P-1
Z	4	4	4
a, Å	16.3324(10)	12.6799(7)	7.4660(13)
b, Å	7.7981(5)	9.0474(5)	13.752(2)
c, Å	15.3300(9)	18.8990(10)	20.182(3)
α, °	90.00	90.00	82.470(4)
β, °	101.1780(10)	103.1260(10)	84.186(4)
γ, °	90.00	90.00	89.182(4)
V, Å ³	1915.4(2)	2111.4(2)	2043.6(6)
Density, g·cm ⁻³	1.337	1.307	1.295
μ, cm ⁻¹	0.87	0.88	0.82
F(000)	816	880	848
2θ _{max} , °	60.02	60.10	52.00
Reflections collected	14174	27473	9782
Independent reflections (R _{int})	5579 (0.0443)	6178 (0.0442)	7886 (0.0220)
Number of reflections with I > 2σ(I)	3823	4348	5203
Parameters	264	283	547
R ₁ [I > 2 σ(I)]	0.0506	0.0506	0.0479
wR ₂ (all independent reflections)	0.1573	0.1147	0.1413
GOF	1.022	1.019	1.009
ρ _{min} /ρ _{max} , e·Å ⁻³	0.366/-0.324	0.479/-0.256	0.231/-0.272

6. Study of *E,Z*-photoisomerization by NMR spectroscopy

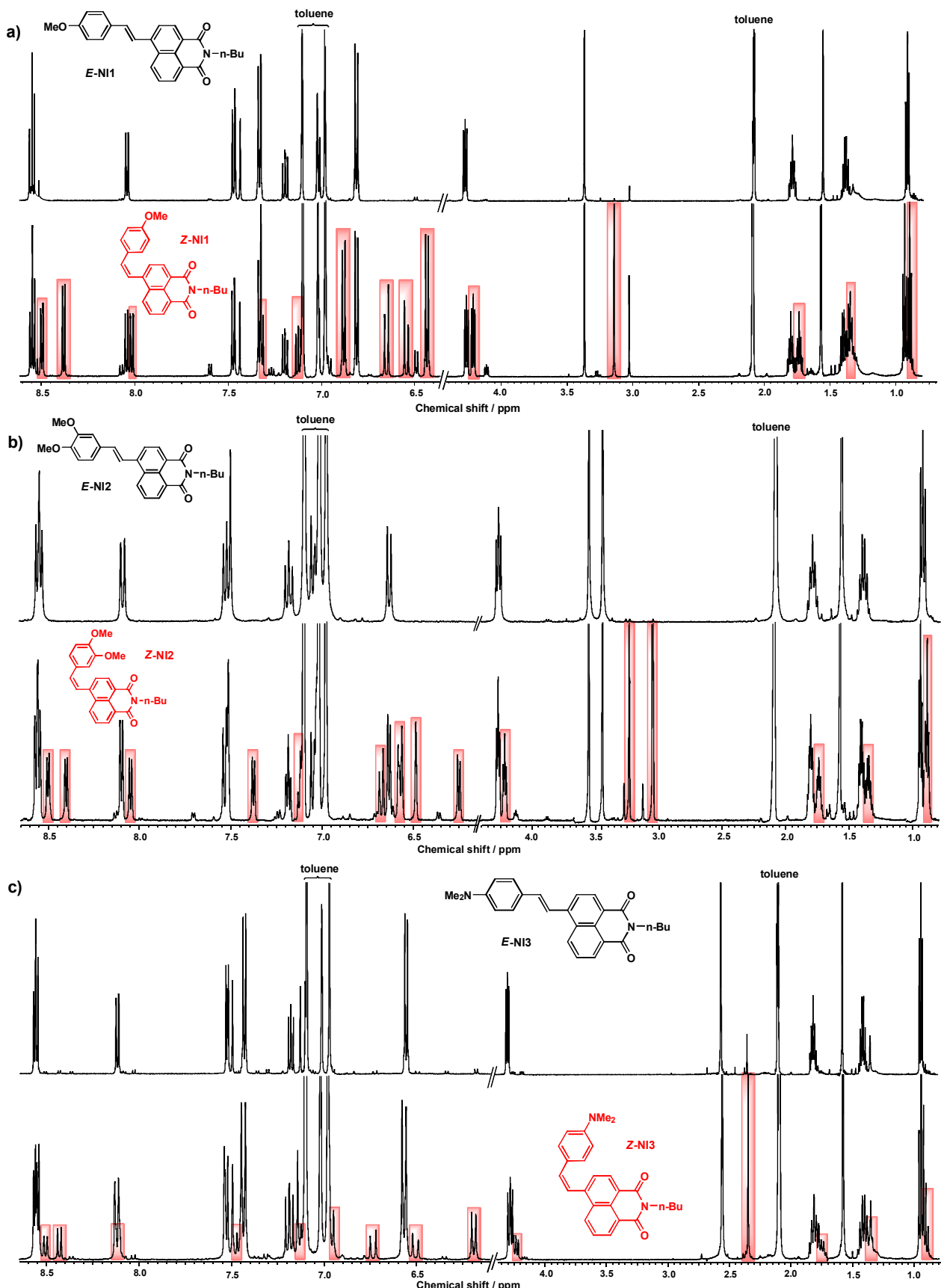


Figure S10. ^1H NMR spectrum of NI1 (a) NI2 (b) and NI3 (c) before (top) and after (bottom) irradiation at 436 nm in toluene- d_8 . The signals of *Z*-isomers are marked with red bars. The concentration of NI1–3 is $2 \cdot 10^{-2}$ M.

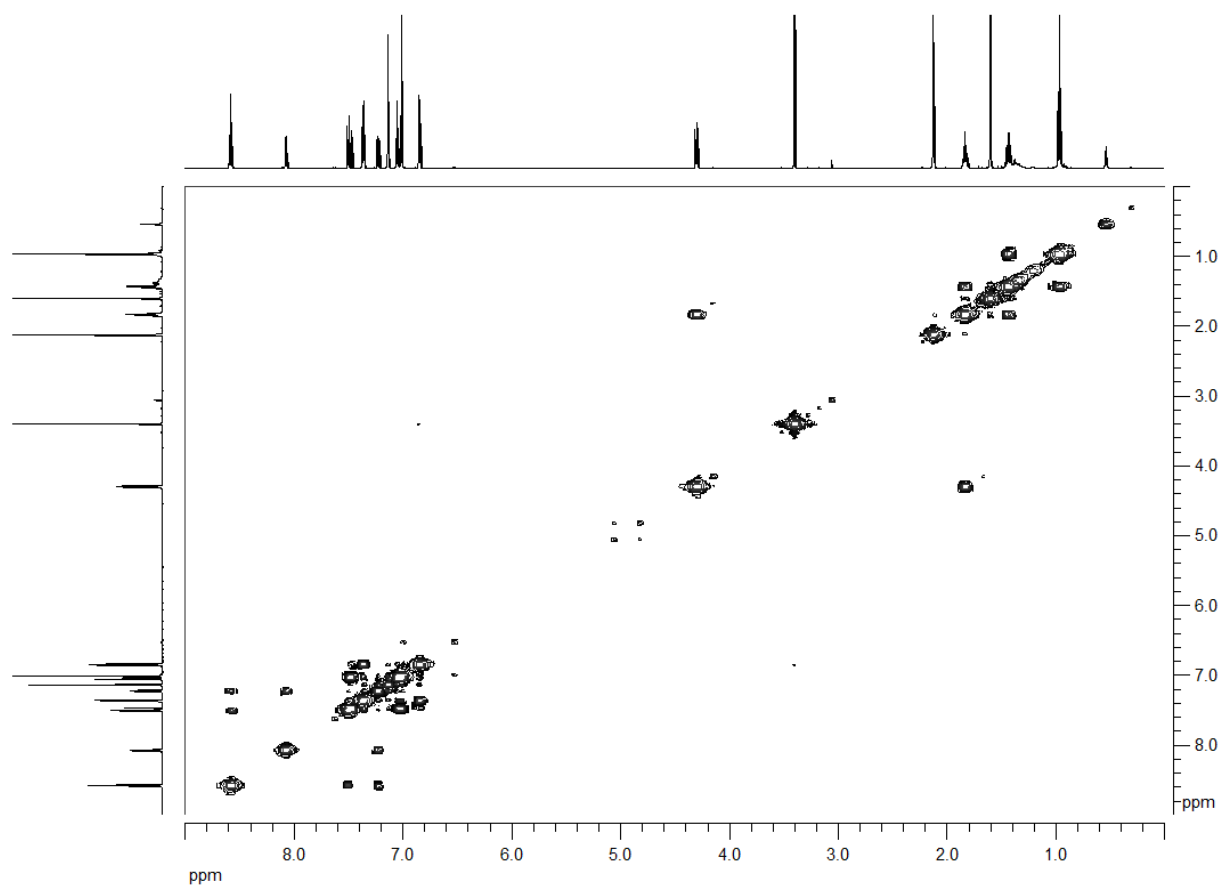


Figure S11. ¹H COSY spectrum of compound NI1 in toluene-*d*₈.

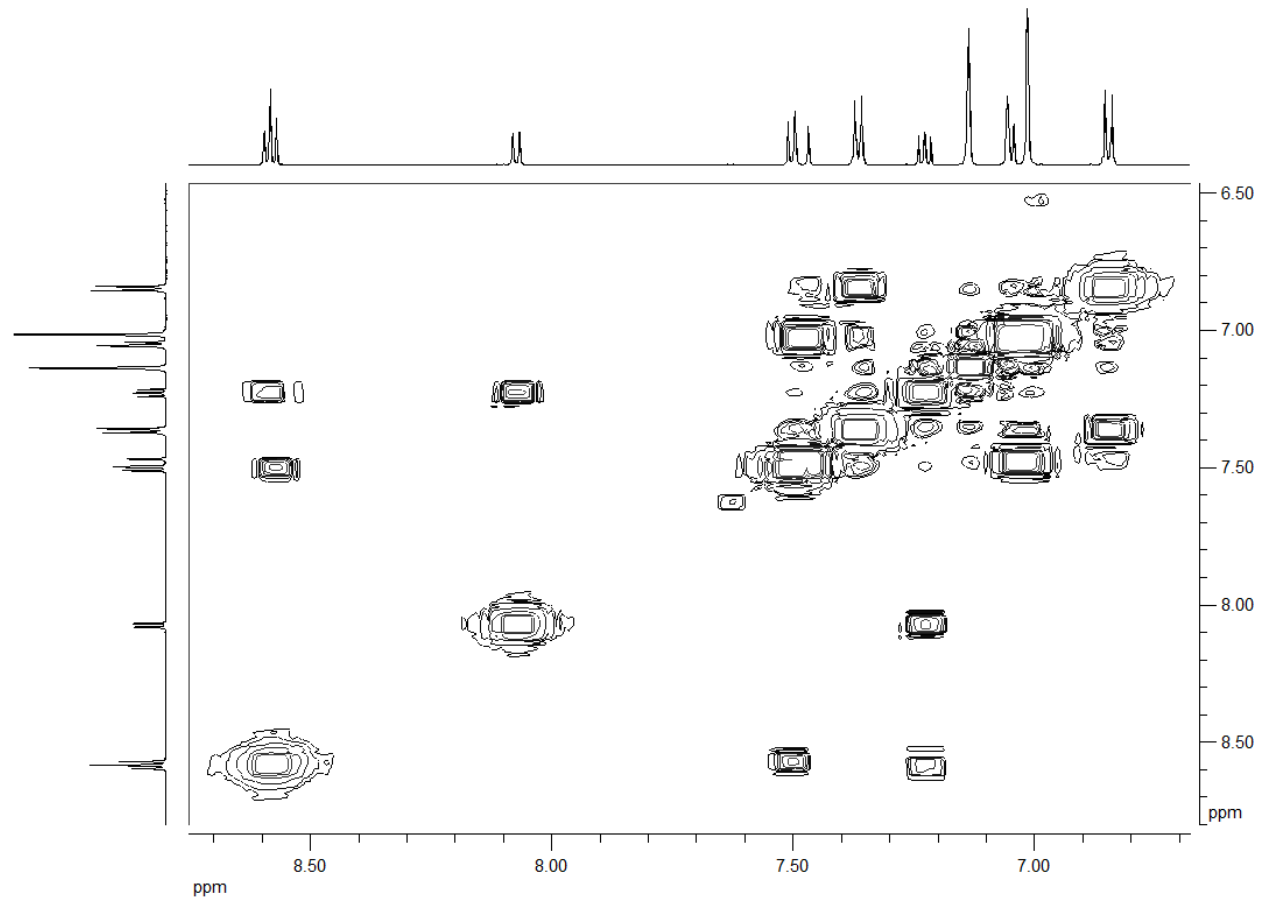


Figure S12. Aromatic part of ¹H COSY spectrum of compound NI1 in toluene-*d*₈.

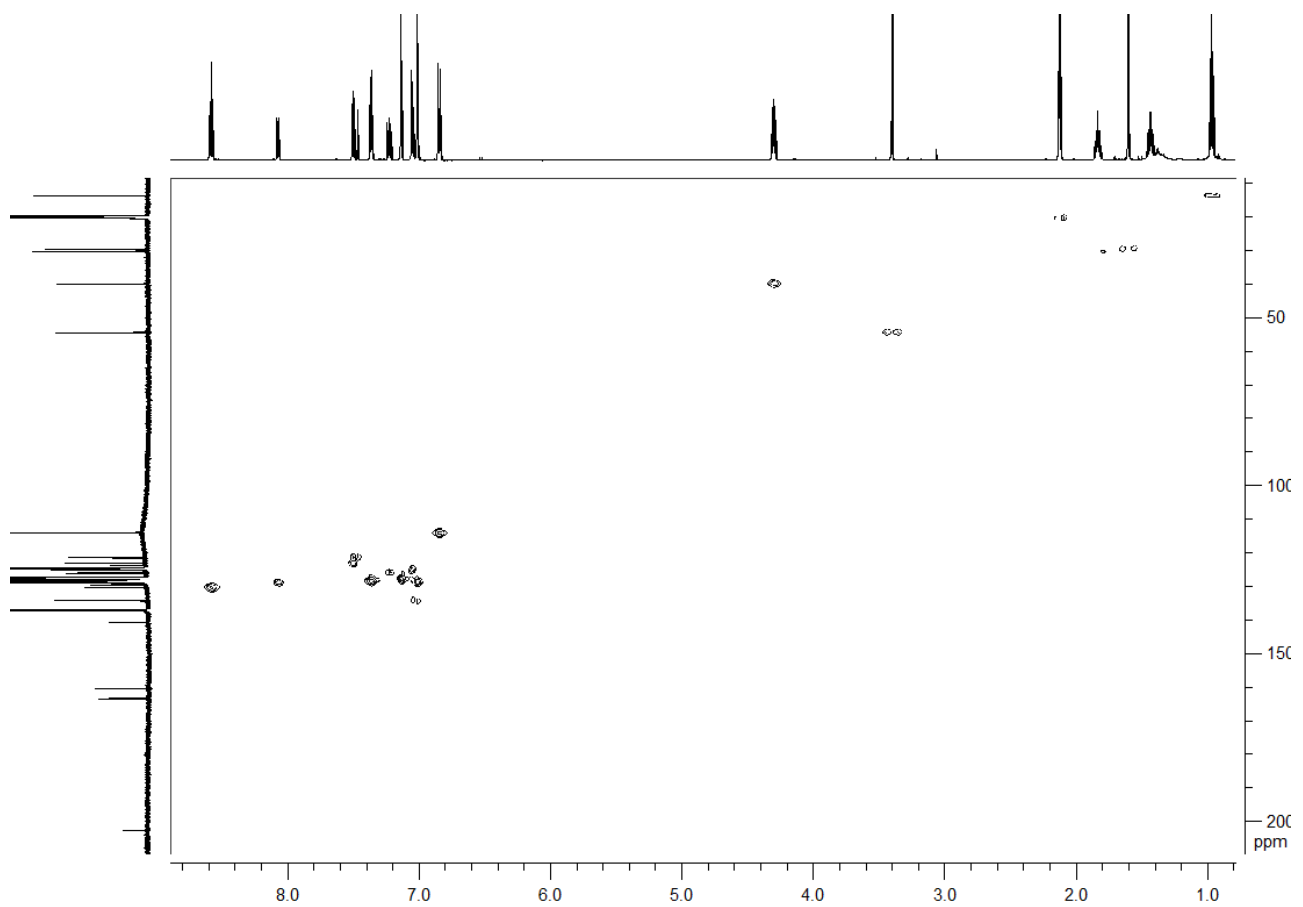


Figure S13. HSQC spectrum of compound NI1 in toluene-*d*₈.

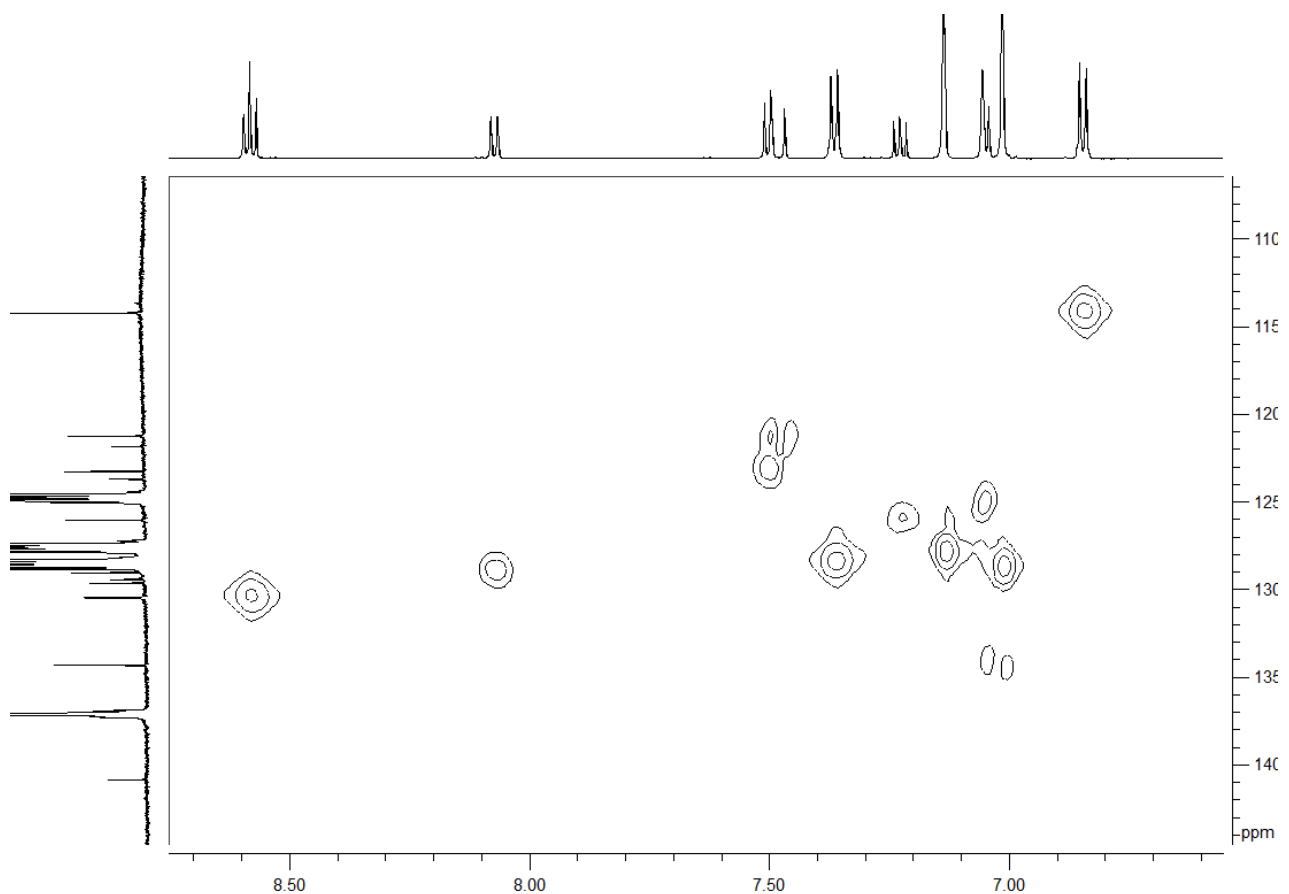


Figure S14. Aromatic part of HSQC spectrum of compound NI1 in toluene-*d*₈.

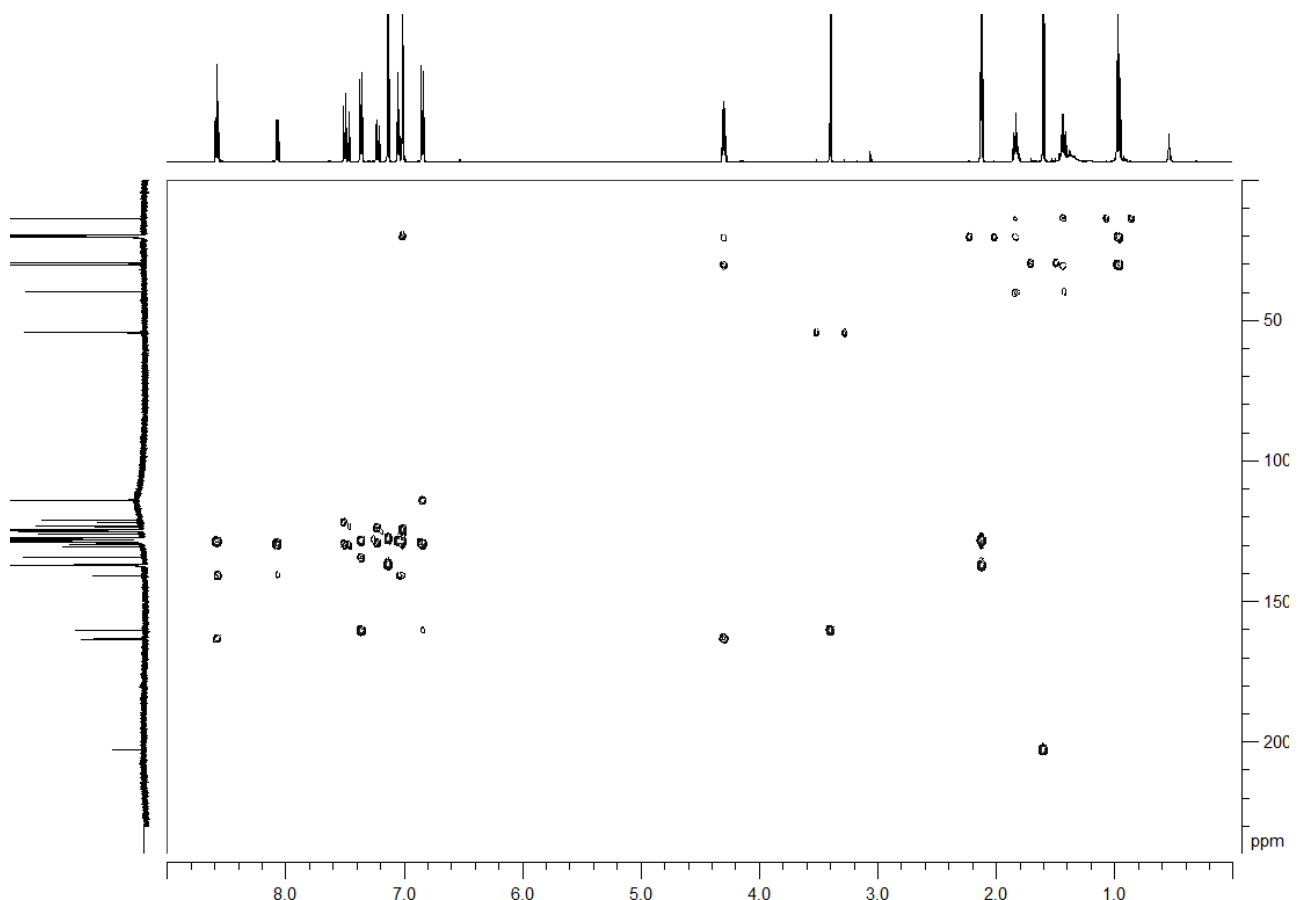


Figure S15. HMBC spectrum of compound NI1 in toluene- d_8 .

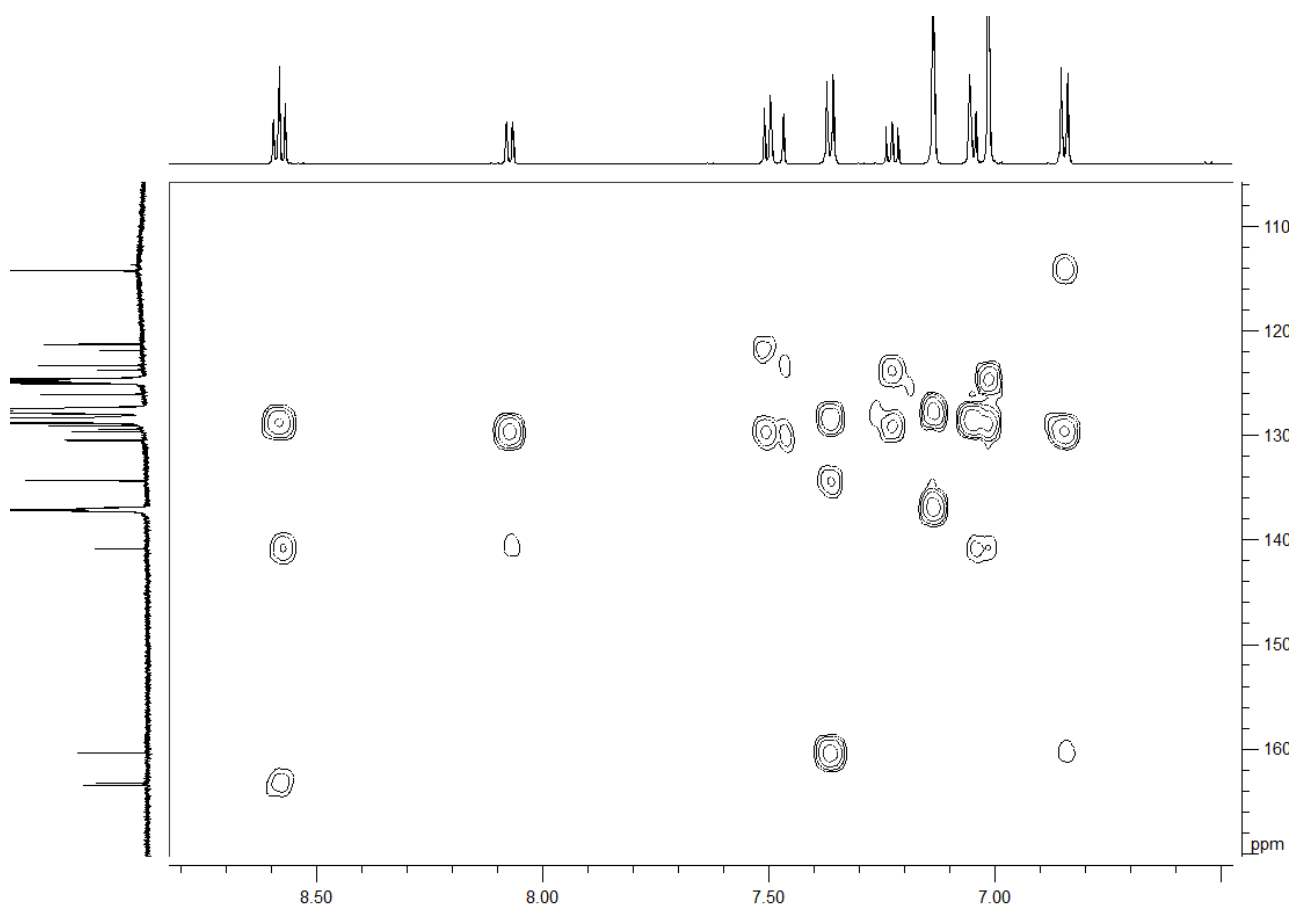


Figure S16. Aromatic part of HMBC spectrum of compound NI1 in toluene- d_8 .

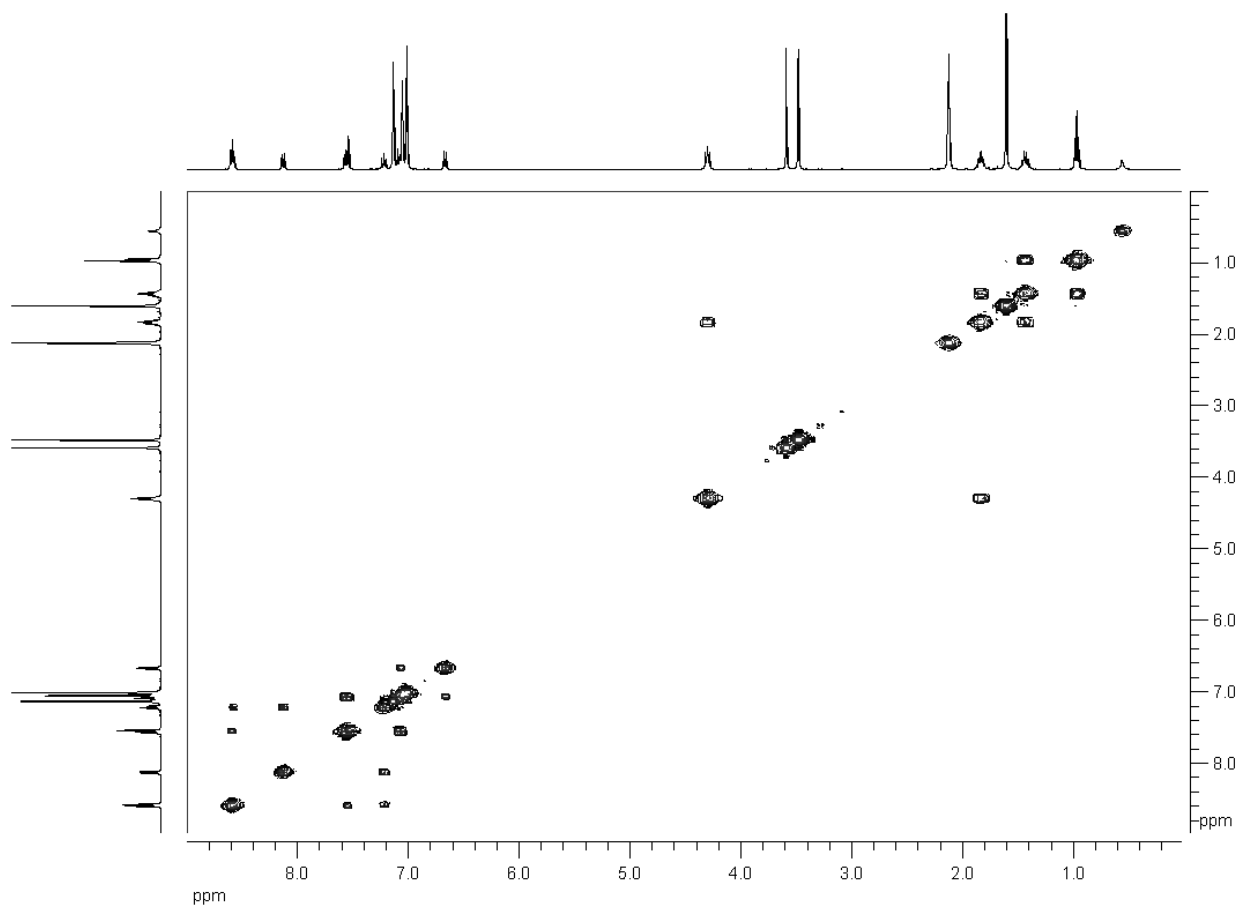


Figure S17. ^1H COSY spectrum of compound **NI2** in toluene- d_8 .

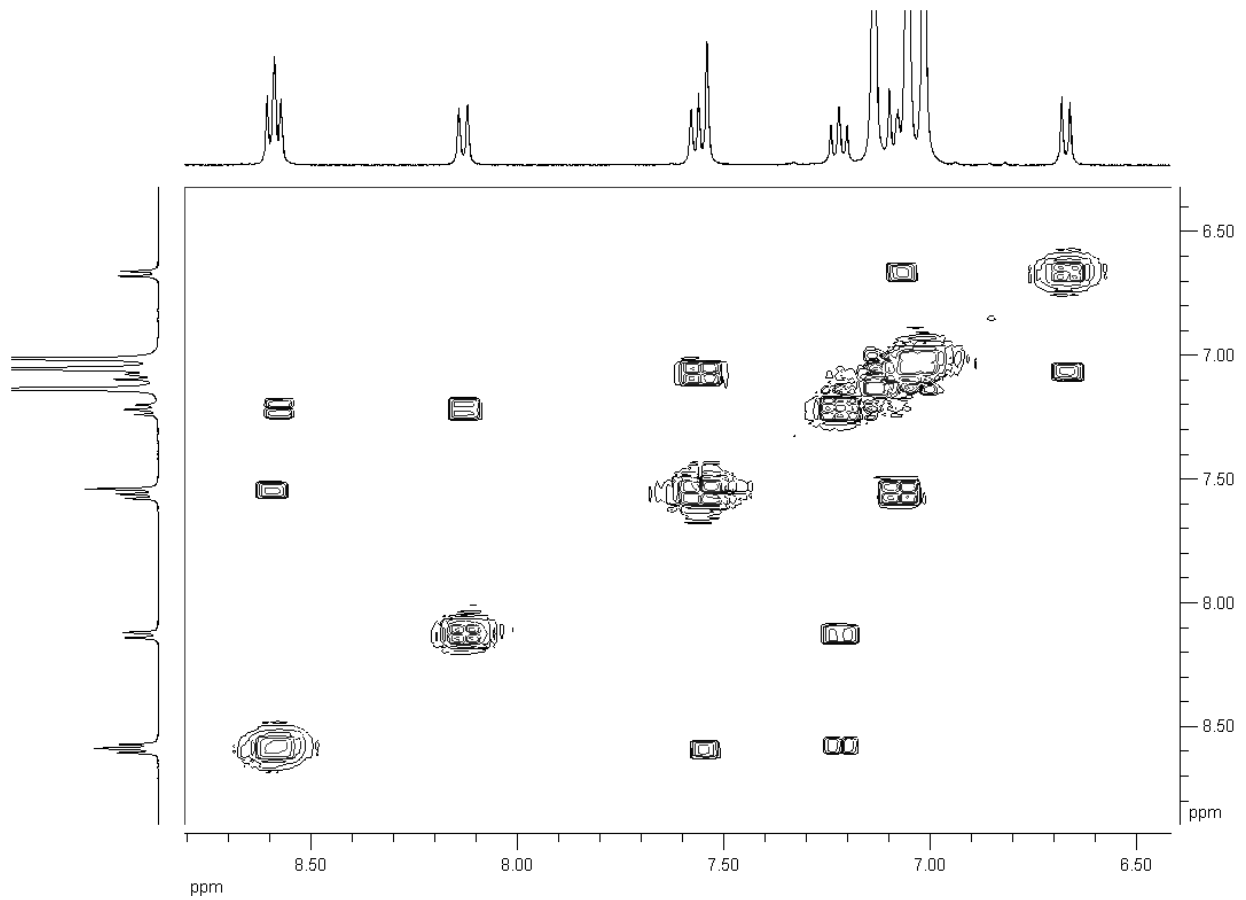


Figure S18. Aromatic part of ^1H COSY spectrum of compound **NI2** in toluene- d_8 .

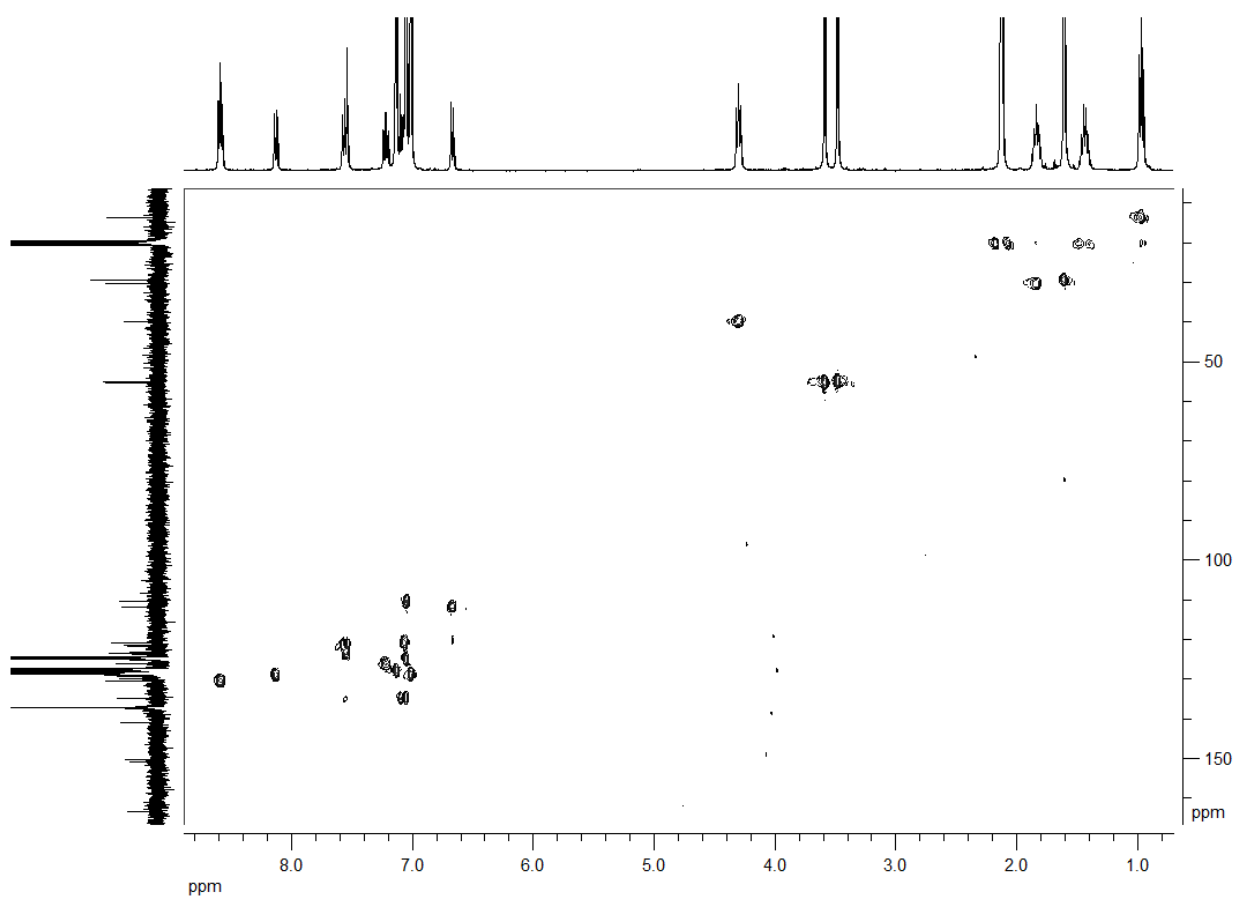


Figure S19. HSQC spectrum of compound NI2 in toluene-*d*₈.

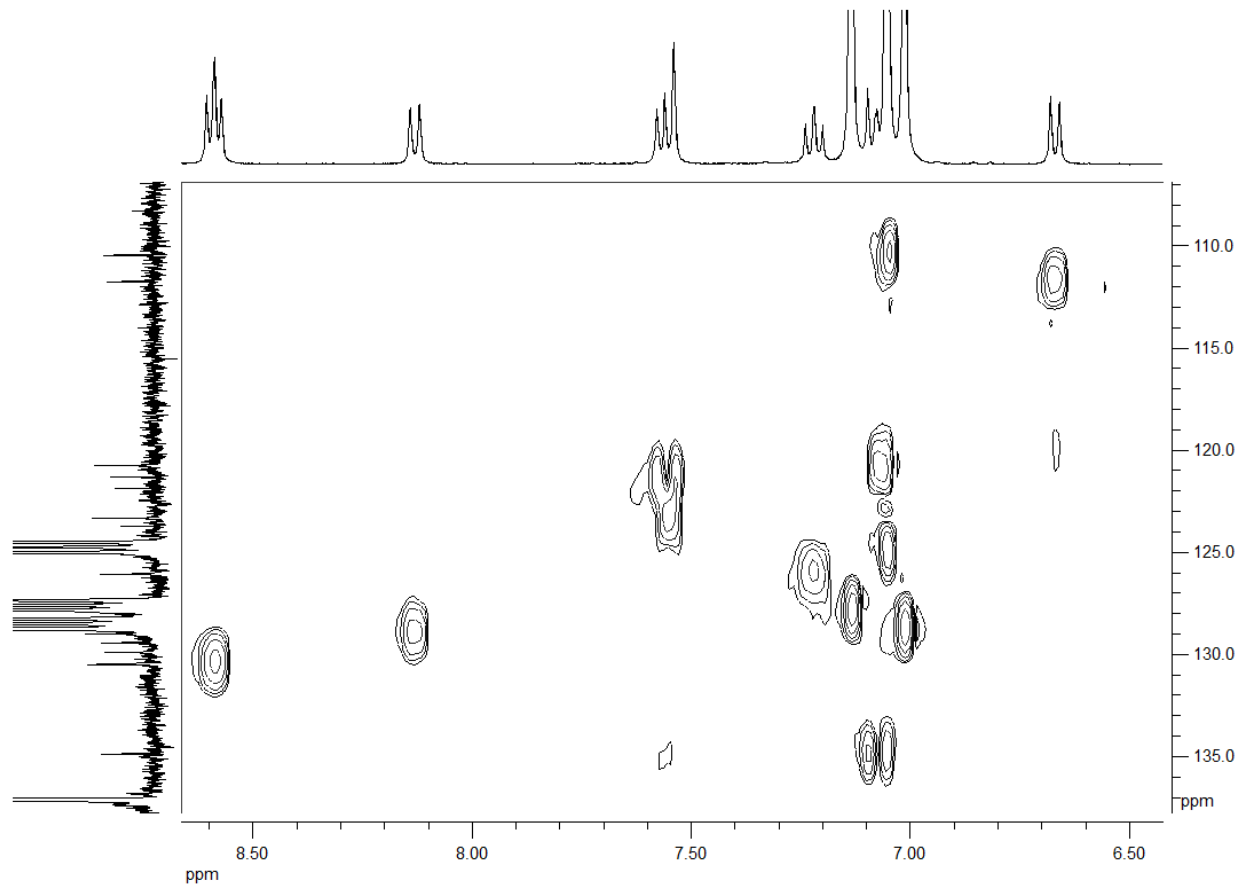


Figure S20. Aromatic part of HSQC spectrum of compound NI2 in toluene-*d*₈.

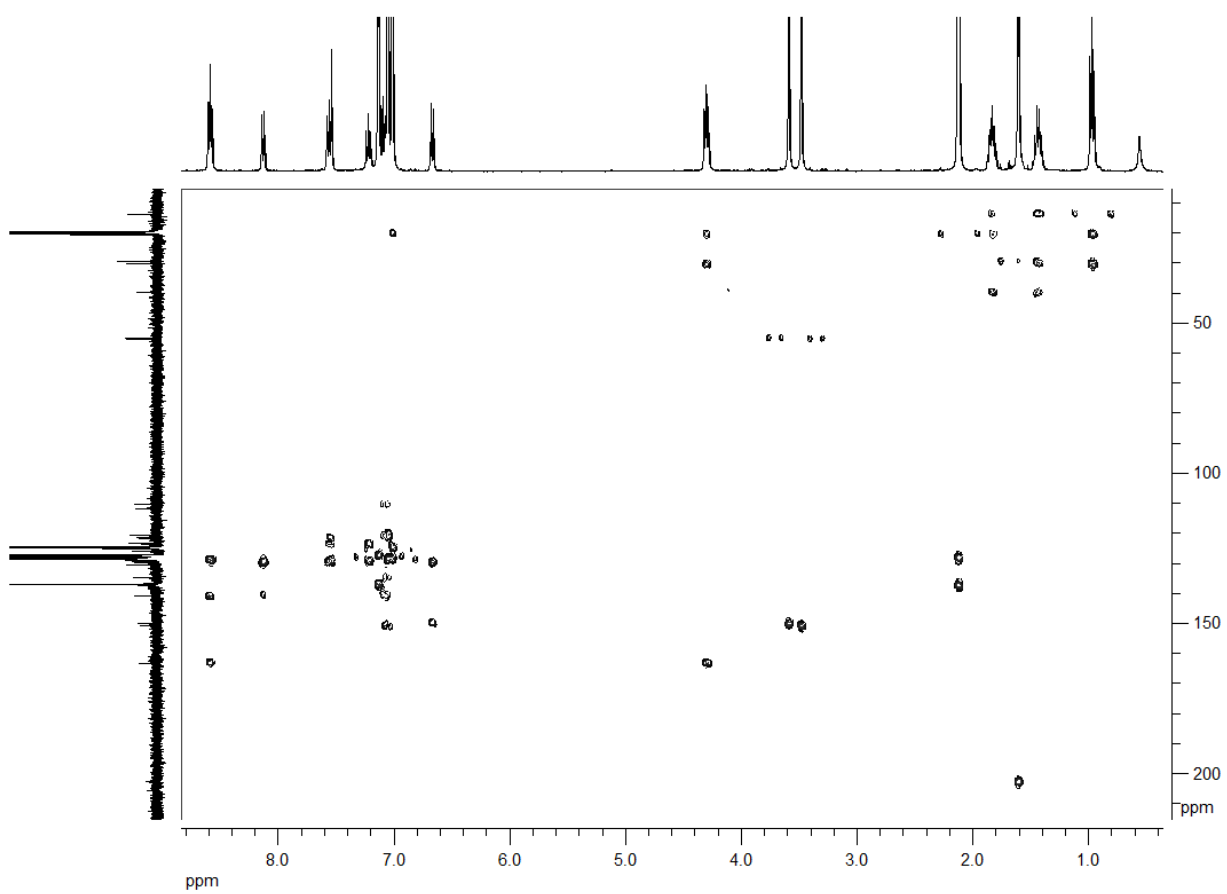


Figure S21. HMBC spectrum of compound NI2 in toluene-*d*₈.

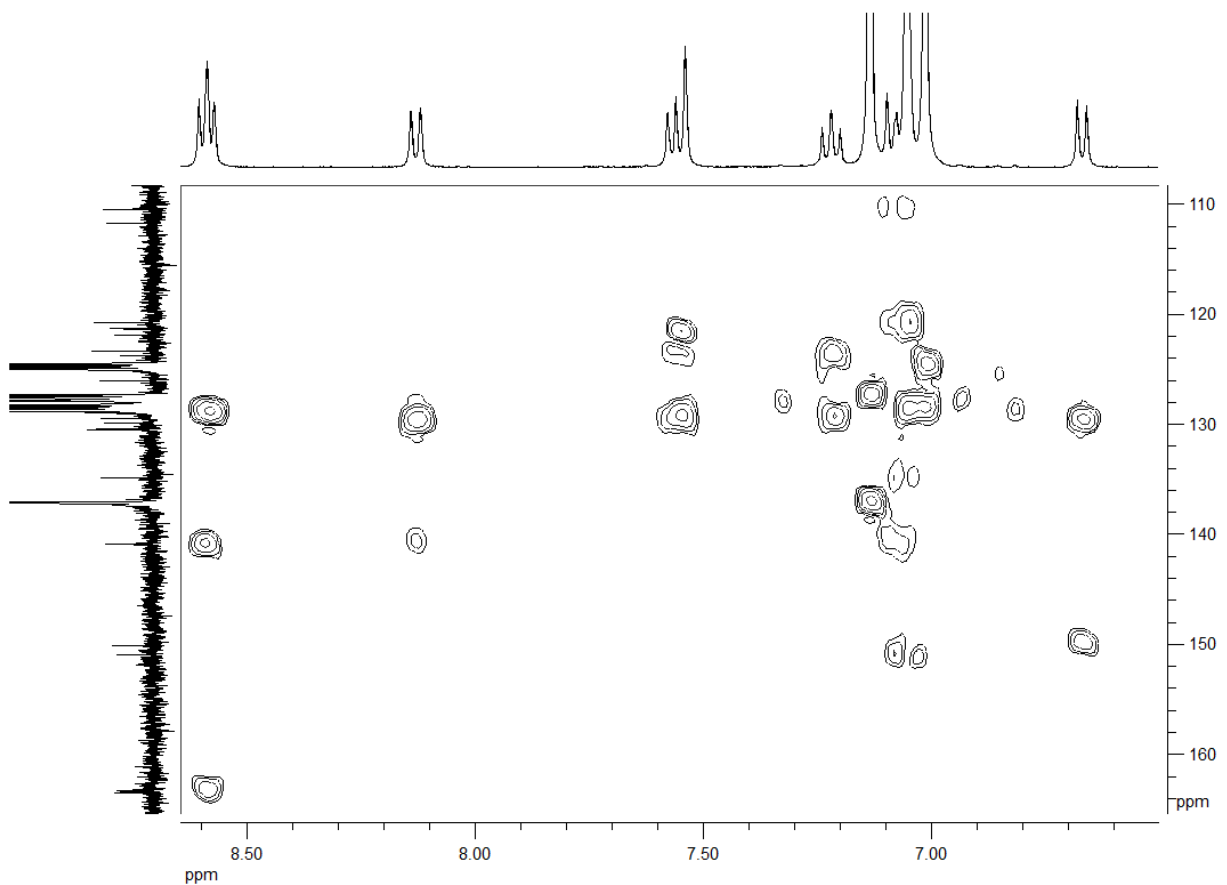


Figure S22. Aromatic part of HMBC spectrum of compound NI2 in toluene-*d*₈.

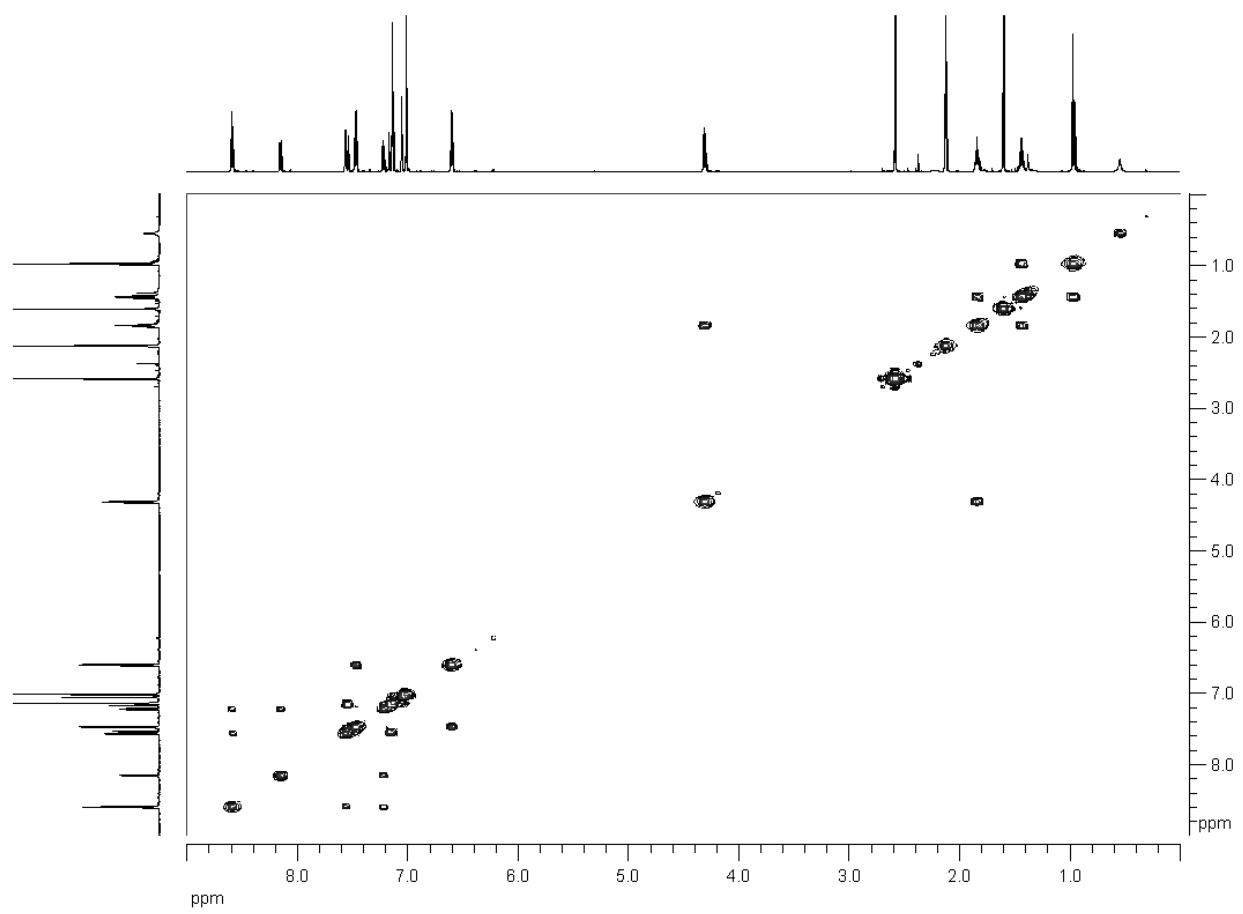


Figure S23. ^1H COSY spectrum of compound NI3 in toluene- d_8 .

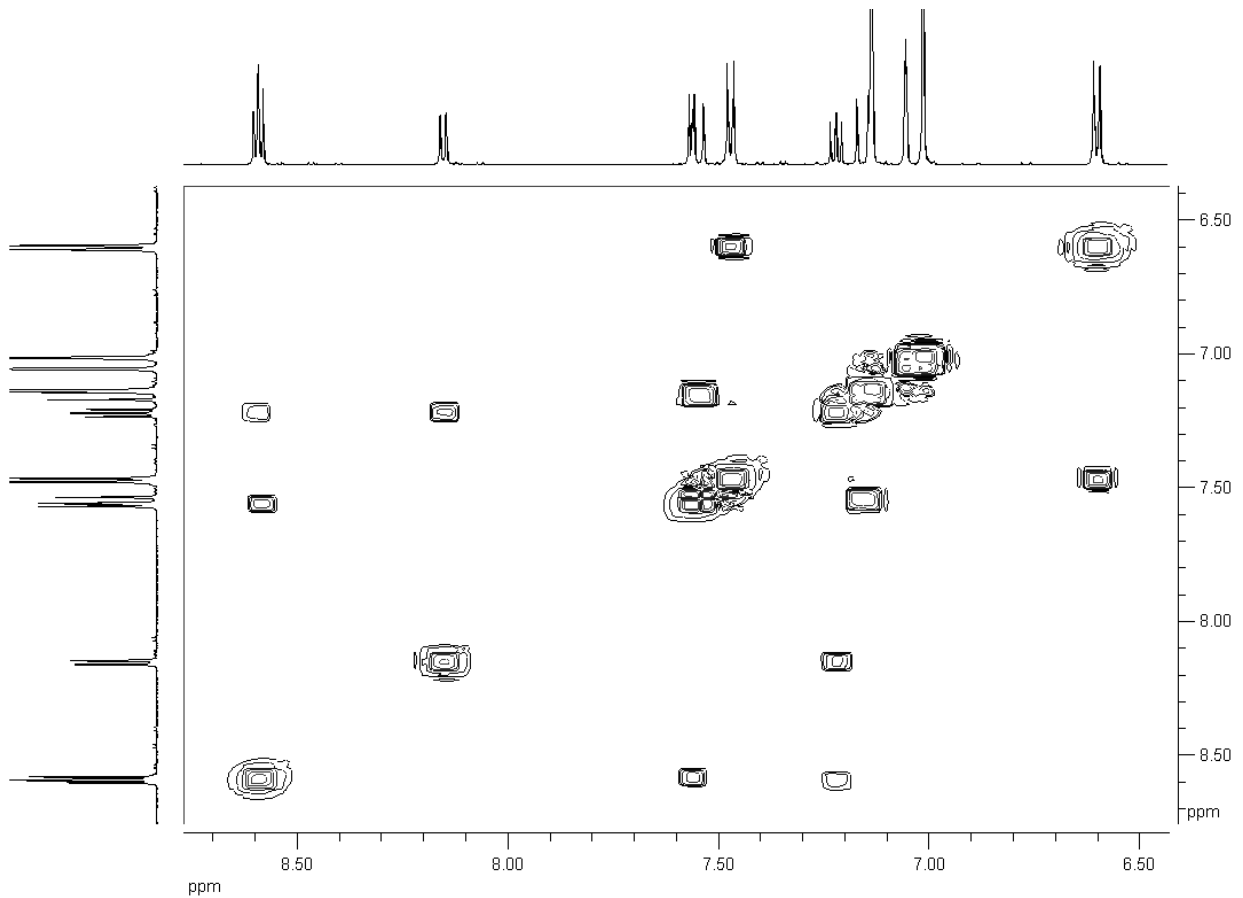


Figure S24. Aromatic part of ^1H COSY spectrum of compound NI3 in toluene- d_8 .

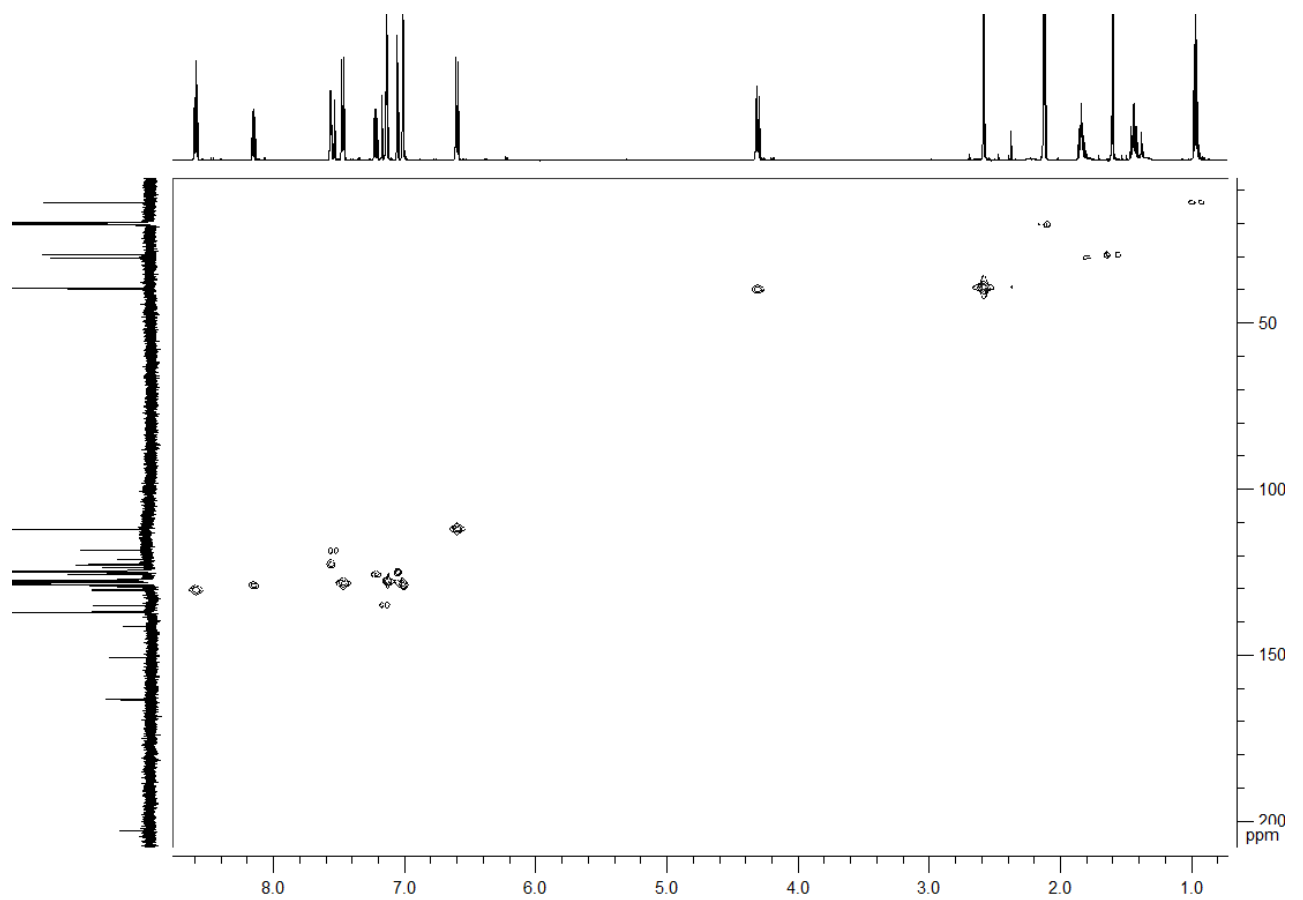


Figure S25. HSQC spectrum of compound NI3 in toluene- d_8 .

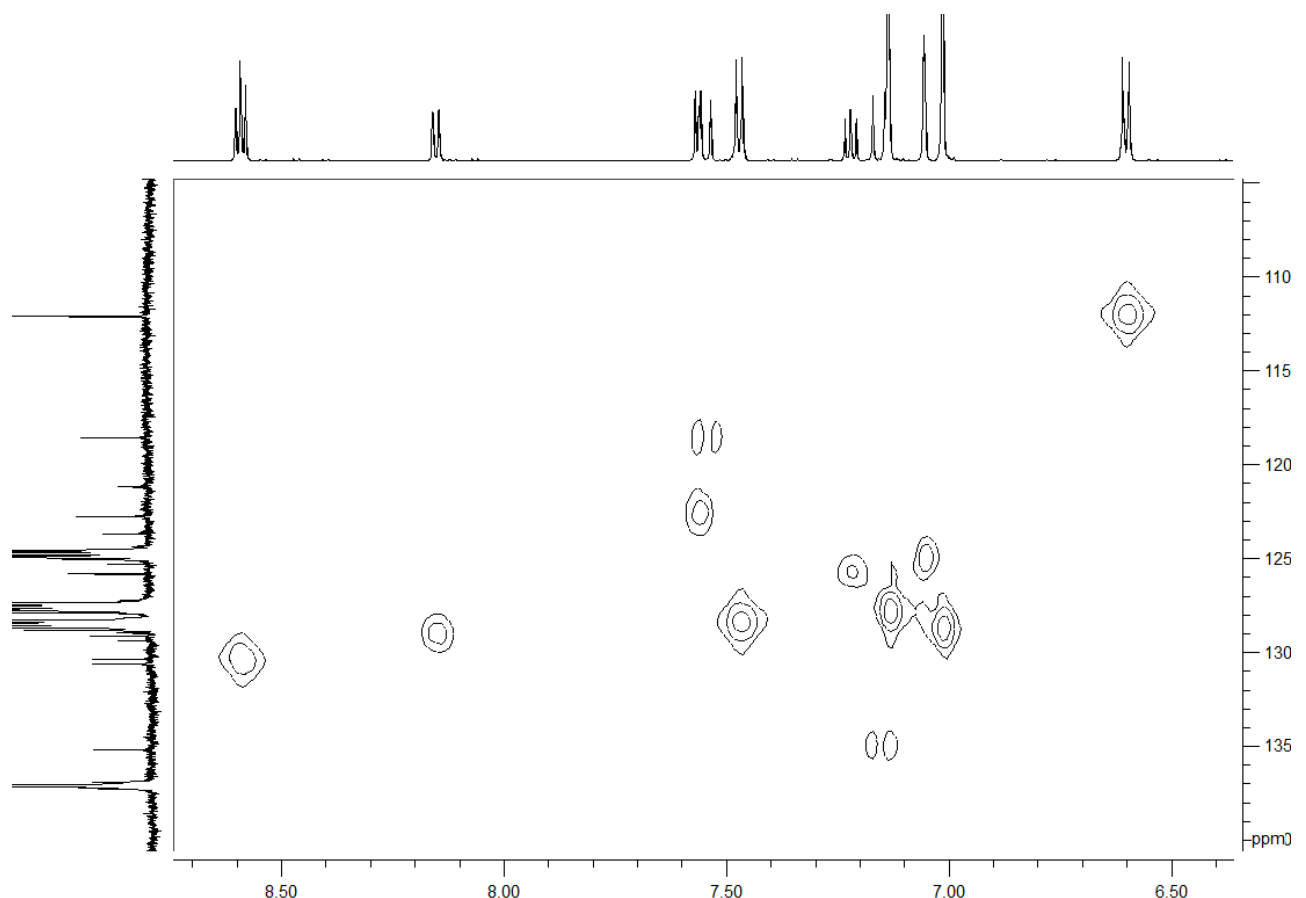


Figure S26. Aromatic part of HSQC spectrum of compound NI3 in toluene- d_8 .

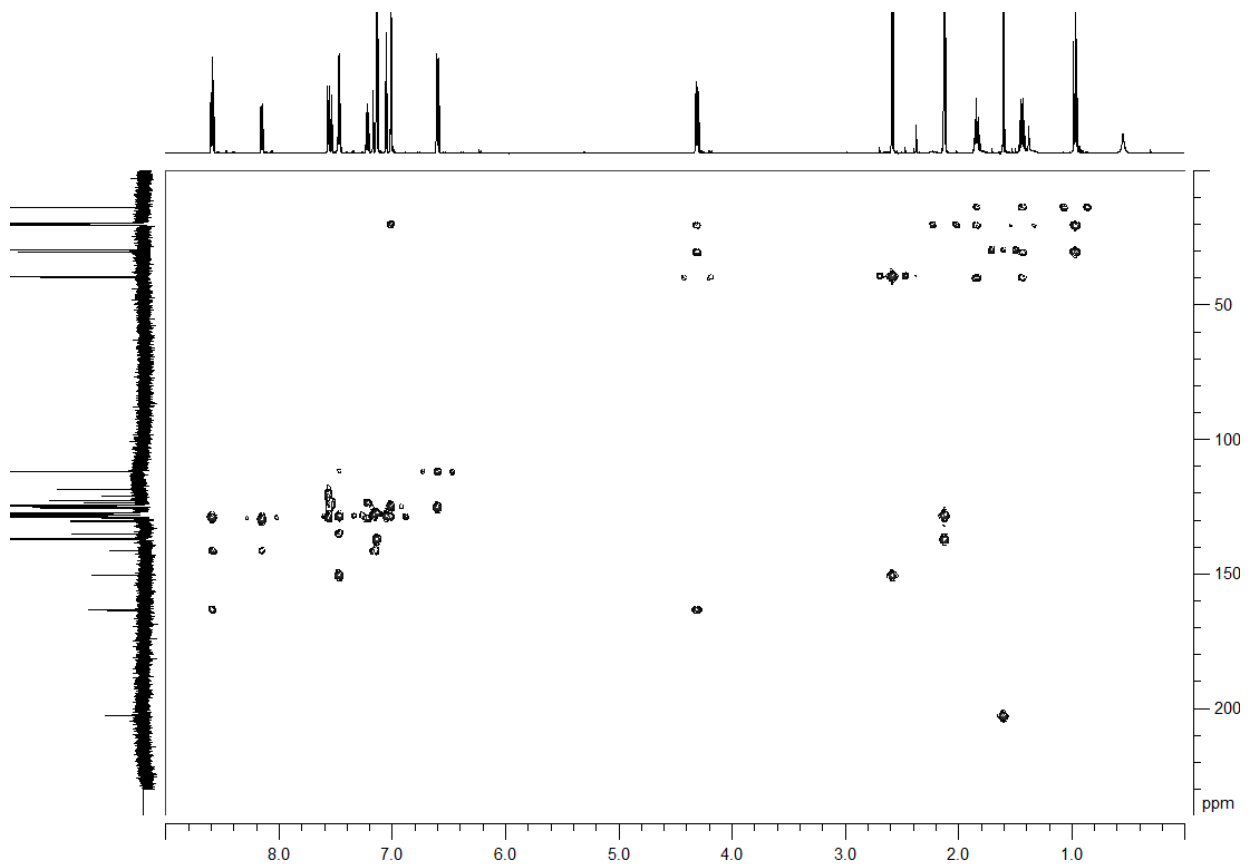


Figure S27. HMBC spectrum of compound NI3 in toluene-*d*8.

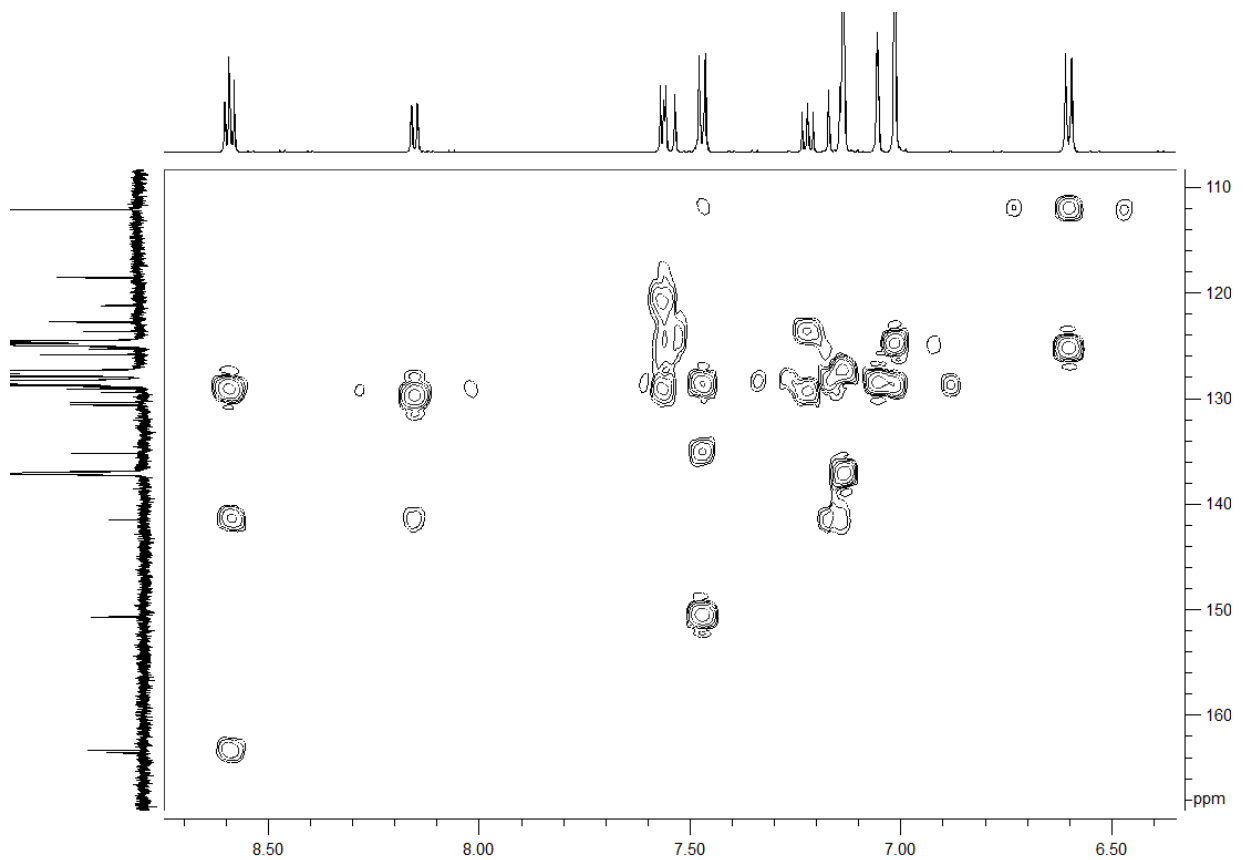


Figure S28. Aromatic part of HMBC spectrum of compound NI3 in toluene-*d*8.

7. Steady-state absorption and emission spectra of NI1–3

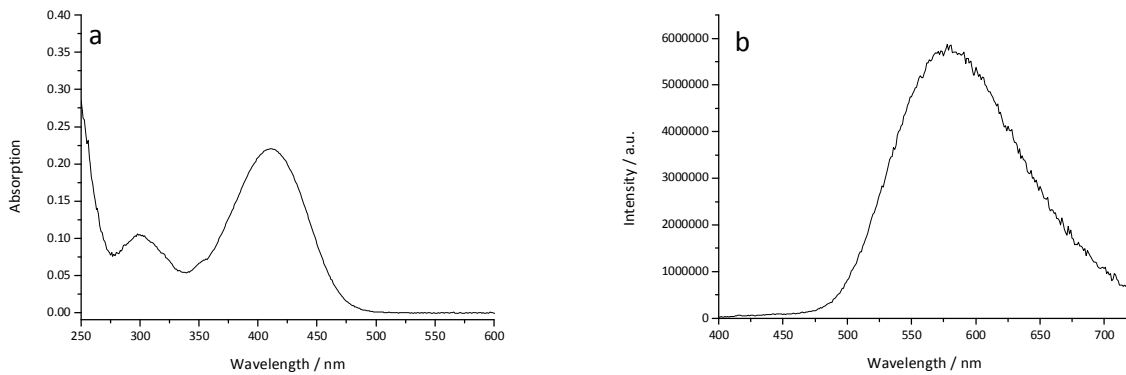


Figure S29. Absorption (a) and emission (b) spectrum of compound **NI1** in propylene carbonate. The concentration of **NI1** is $1.0 \cdot 10^{-5}$ M. Excitation wavelength 370 nm.

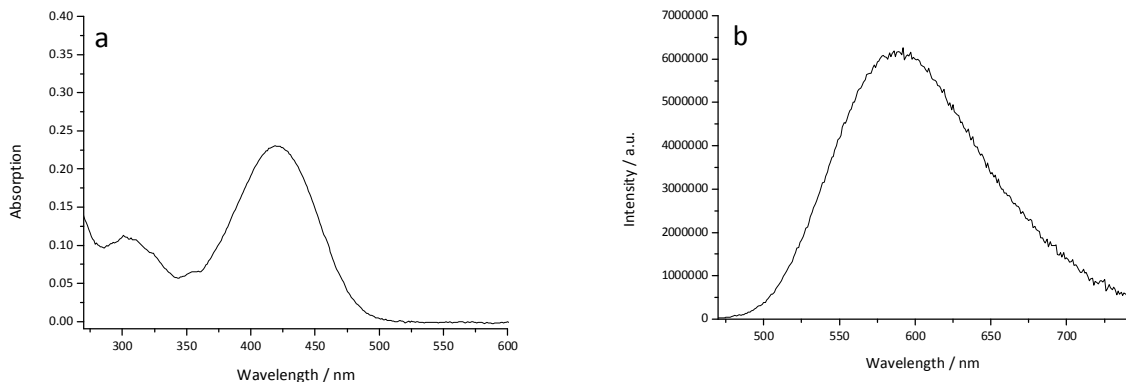


Figure S30. Absorption (a) and emission (b) spectrum of compound **NI1** in DMSO. The concentration of **NI1** is $1.0 \cdot 10^{-5}$ M. Excitation wavelength 420 nm.

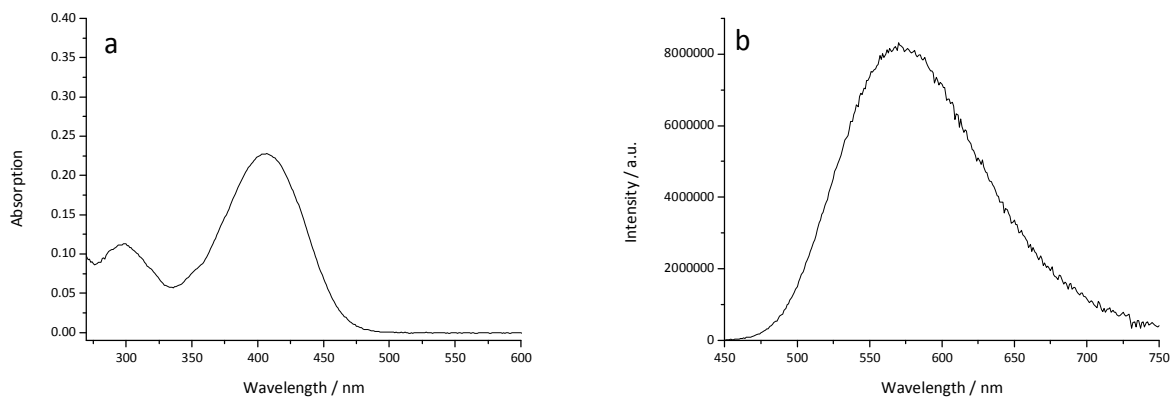


Figure S31. Absorption (a) and emission (b) spectrum of compound **NI1** in acetonitrile. The concentration of **NI1** is $1.0 \cdot 10^{-5}$ M. Excitation wavelength 365 nm.

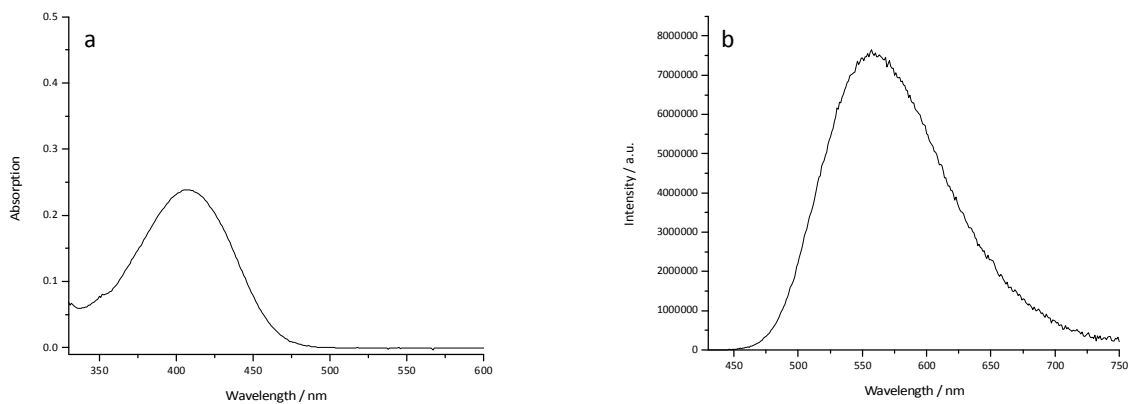


Figure S32. Absorption (a) and emission (b) spectrum of compound **NI1** in acetone. The concentration of **NI1** is $1.0 \cdot 10^{-5}$ M. Excitation wavelength 400 nm.

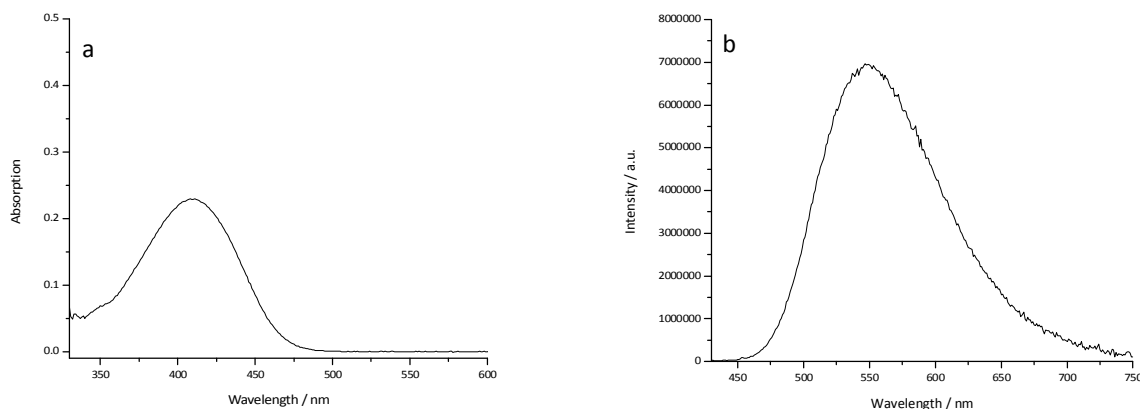


Figure S33. Absorption (a) and emission (b) spectrum of compound **NI1** in 3-methylbutanone-2. The concentration of **NI1** is $1.0 \cdot 10^{-5}$ M. Excitation wavelength 400 nm.

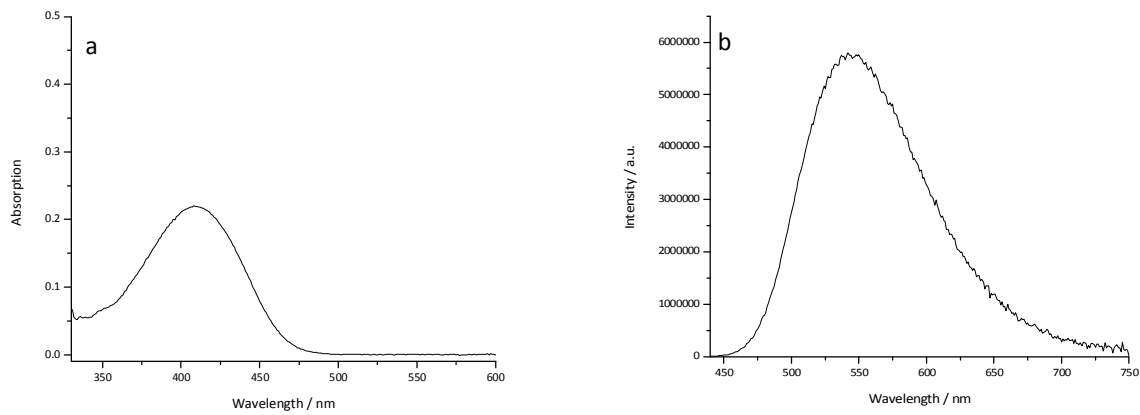


Figure S34. Absorption (a) and emission (b) spectrum of compound **NI1** in 4-methylpentanone-2. The concentration of **NI1** is $1.0 \cdot 10^{-5}$ M. Excitation wavelength 435 nm.

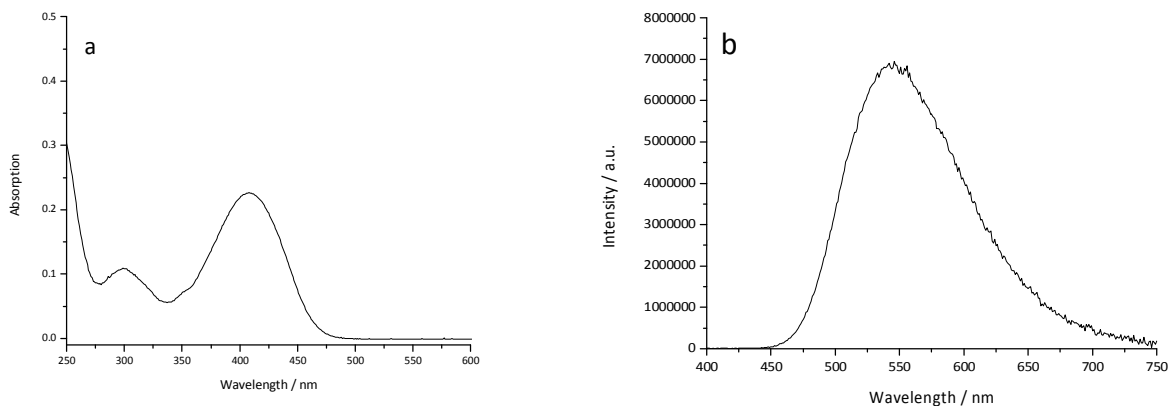


Figure S35. Absorption (a) and emission (b) spectrum of compound **NI1** in 1,2-dimethoxyethane. The concentration of **NI1** is $1.0 \cdot 10^{-5}$ M. Excitation wavelength 350 nm.

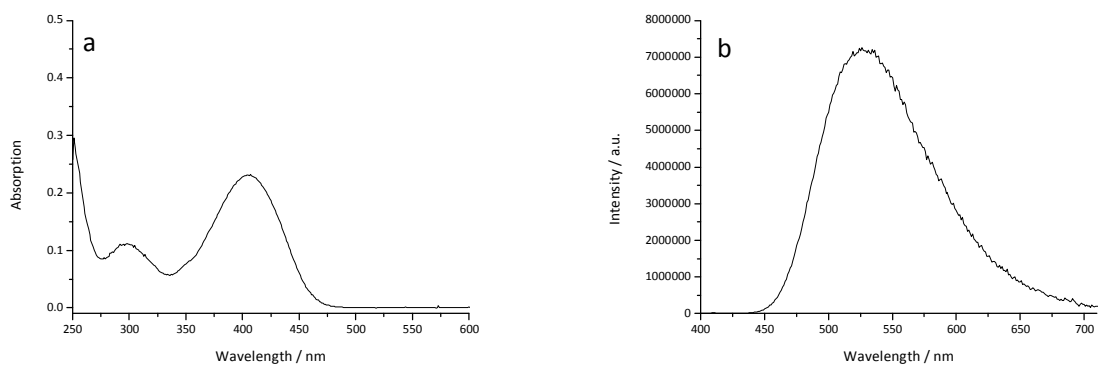


Figure S36. Absorption (a) and emission (b) spectrum of compound **NI1** in ethylacetate. The concentration of **NI1** is $1.0 \cdot 10^{-5}$ M. Excitation wavelength 365 nm.

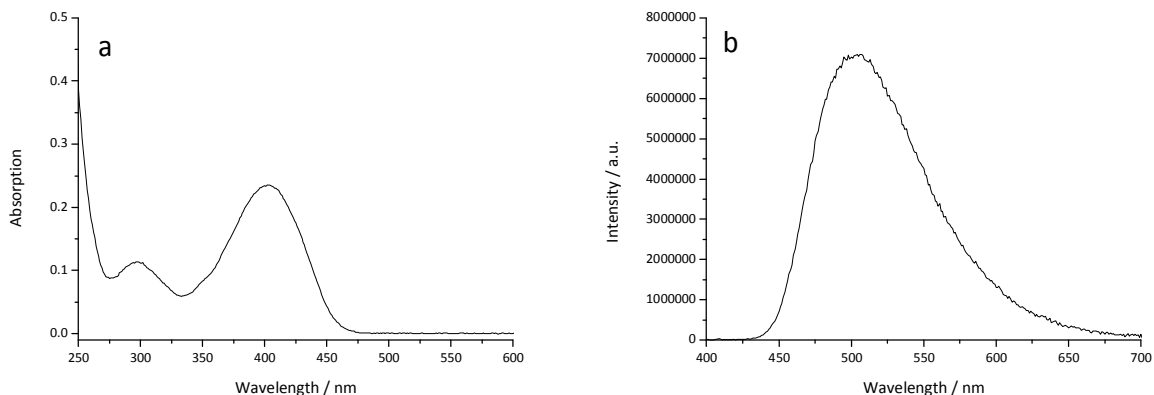


Figure S37. Absorption (a) and emission (b) spectrum of compound **NI1** in diethyl ether. The concentration of **NI1** is $1.0 \cdot 10^{-5}$ M. Excitation wavelength 365 nm.

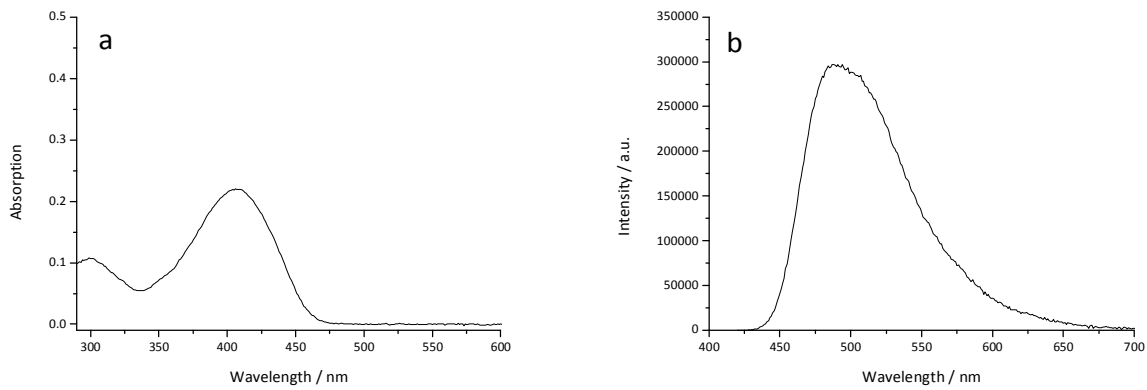


Figure S38. Absorption (a) and emission (b) spectrum of compound **NI1** in toluene. The concentration of **NI1** is $1.0 \cdot 10^{-5}$ M. Excitation wavelength 4150 nm.

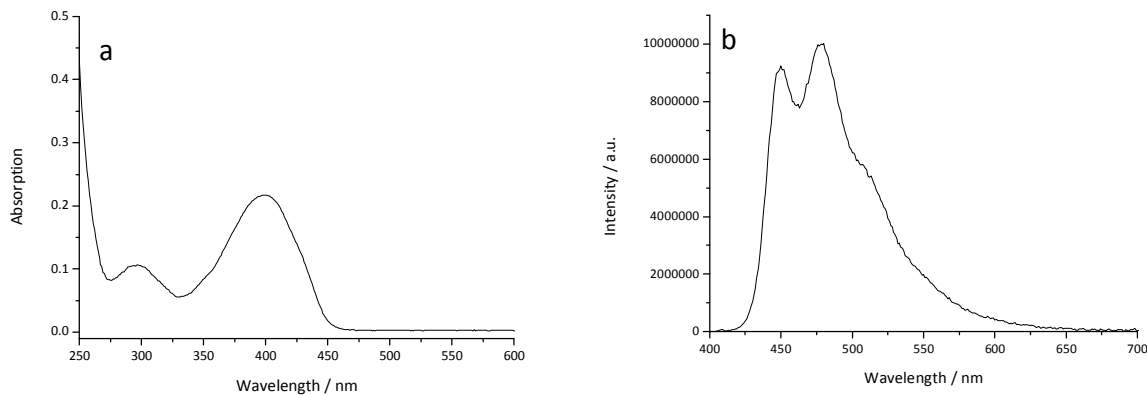


Figure S39. Absorption (a) and emission (b) spectrum of compound **NI1** in cyclohexane. The concentration of **NI1** is $1.0 \cdot 10^{-5}$ M. Excitation wavelength 365 nm.

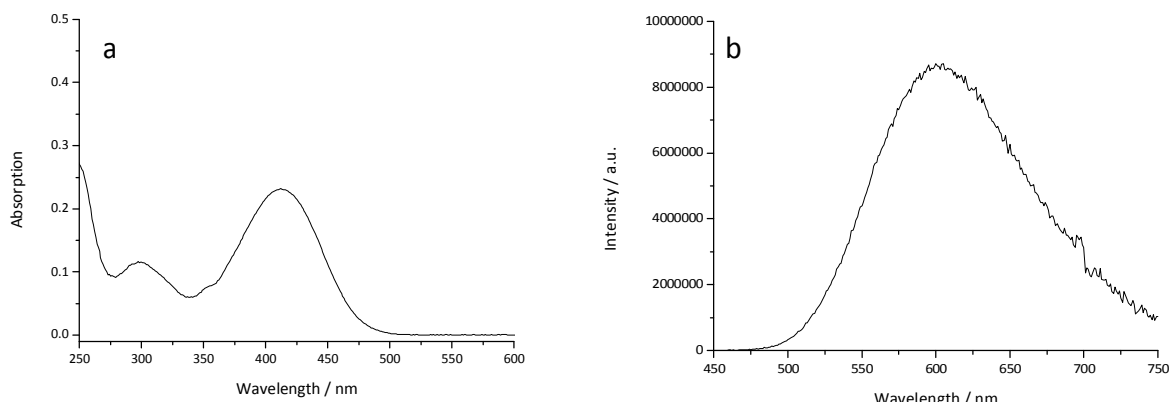


Figure S40. Absorption (a) and emission (b) spectrum of compound **NI1** in methanol. The concentration of **NI1** is $1.0 \cdot 10^{-5}$ M. Excitation wavelength 350 nm.

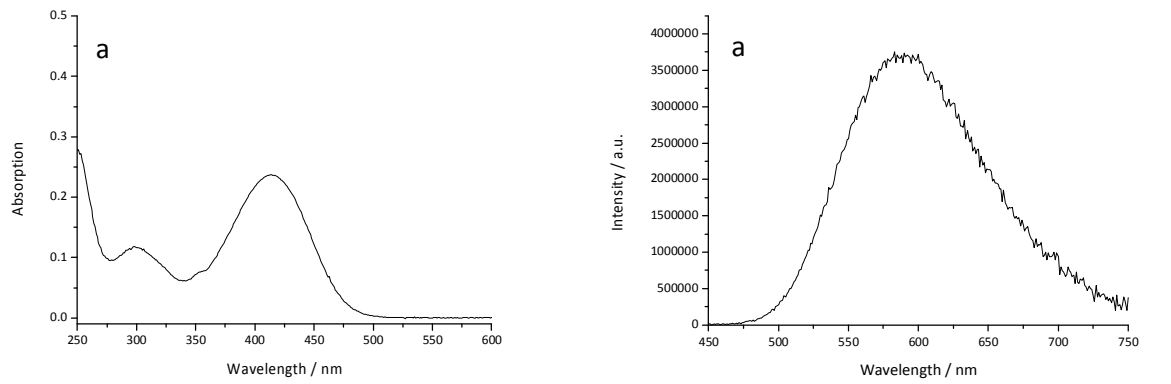


Figure S41. Absorption (a) and emission (b) spectrum of compound **NI1** in ethanol. The concentration of **NI1** is $1.0 \cdot 10^{-5}$ M. Excitation wavelength 350 nm.

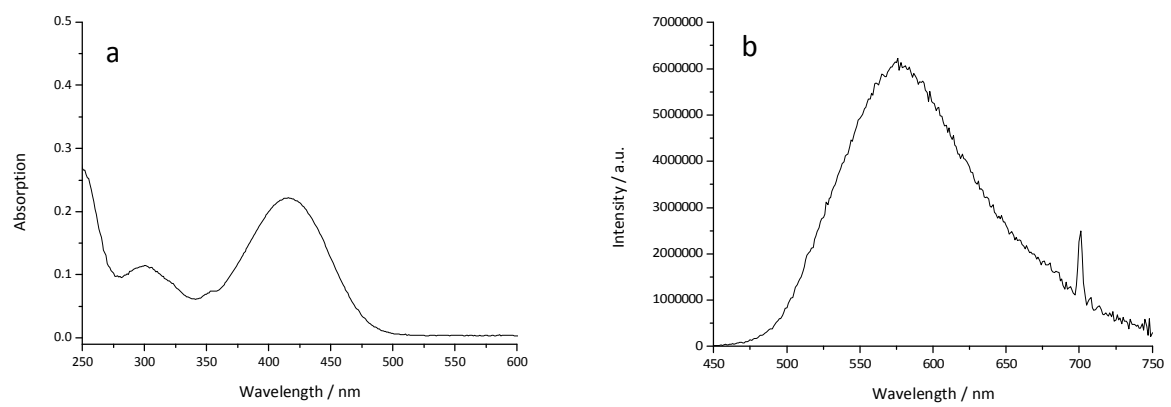


Figure S42. Absorption (a) and emission (b) spectrum of compound **NI1** in *n*-butanol. The concentration of **NI1** is $1.0 \cdot 10^{-5}$ M. Excitation wavelength 350 nm.

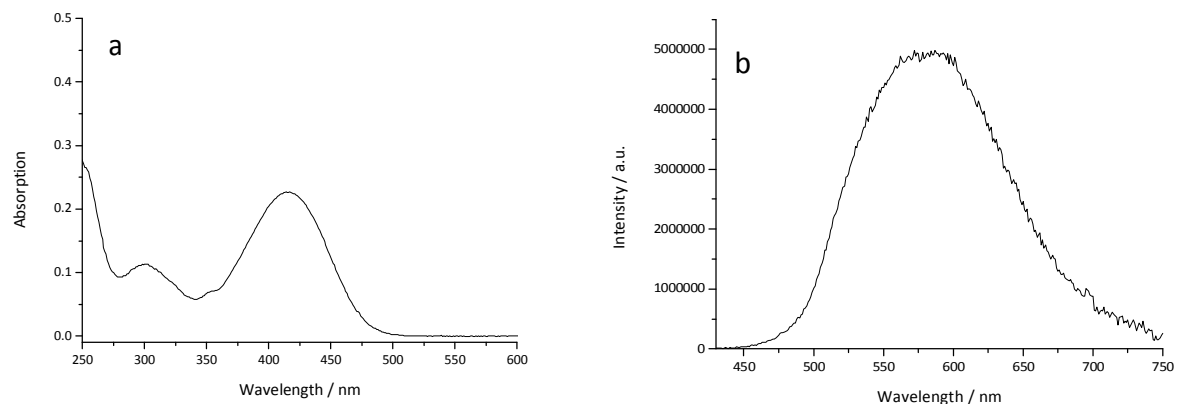


Figure S43. Absorption (a) and emission (b) spectrum of compound **NI1** in *n*-hexanol. The concentration of **NI1** is $1.0 \cdot 10^{-5}$ M. Excitation wavelength 350 nm.

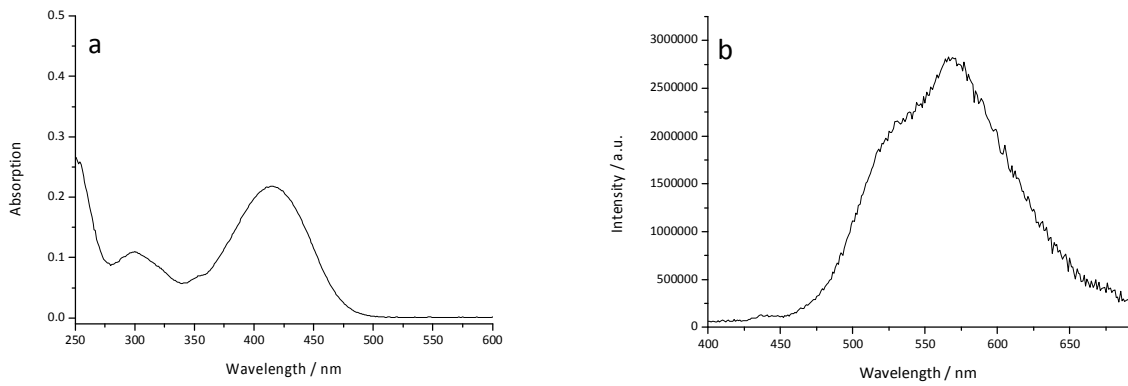


Figure S44. Absorption (a) and emission (b) spectrum of compound **NI1** in *n*-decanol. The concentration of **NI1** is $1.0 \cdot 10^{-5}$ M. Excitation wavelength 350 nm.

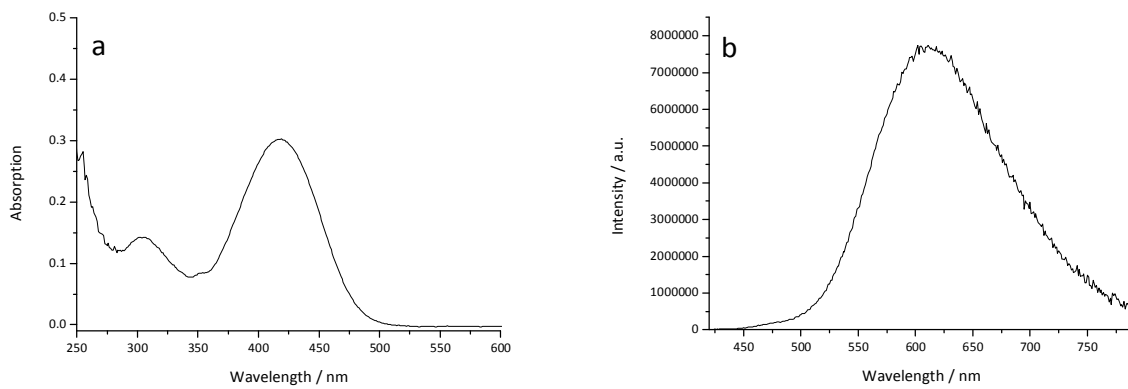


Figure S45. Absorption (a) and emission (b) spectrum of compound **NI2** in propylene carbonate. The concentration of **NI2** is $1.0 \cdot 10^{-5}$ M. Excitation wavelength 400 nm.

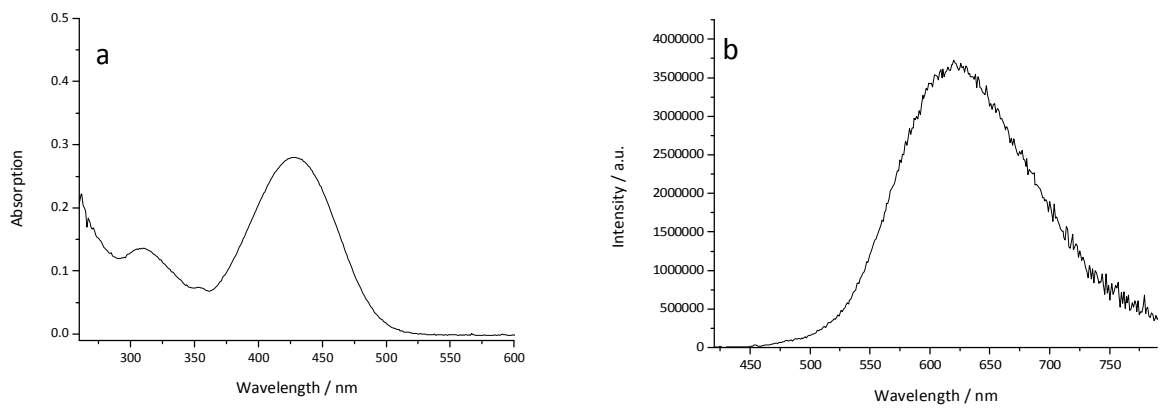


Figure S46. Absorption (a) and emission (b) spectrum of compound **NI2** in DMSO. The concentration of **NI2** is $1.0 \cdot 10^{-5}$ M. Excitation wavelength 400 nm.

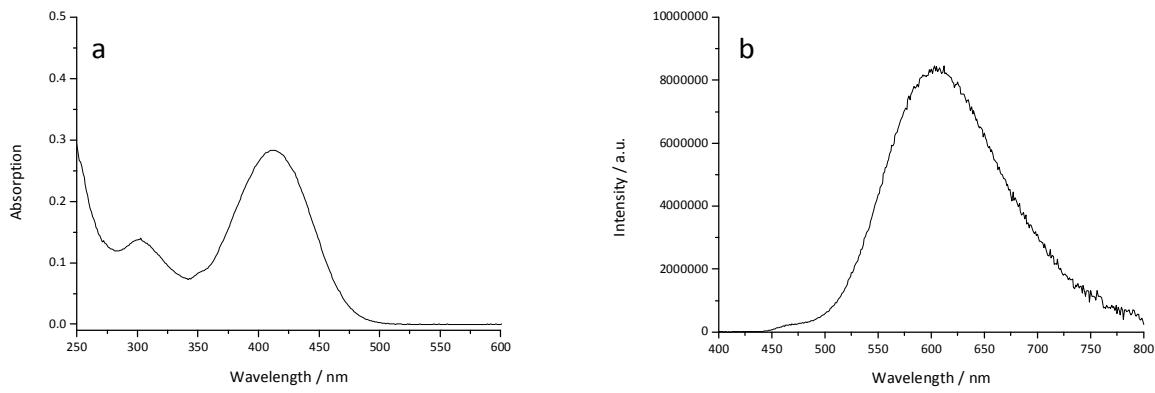


Figure S47. Absorption (a) and emission (b) spectrum of compound **NI2** in acetonitrile. The concentration of **NI2** is $1.0 \cdot 10^{-5}$ M. Excitation wavelength 380 nm.

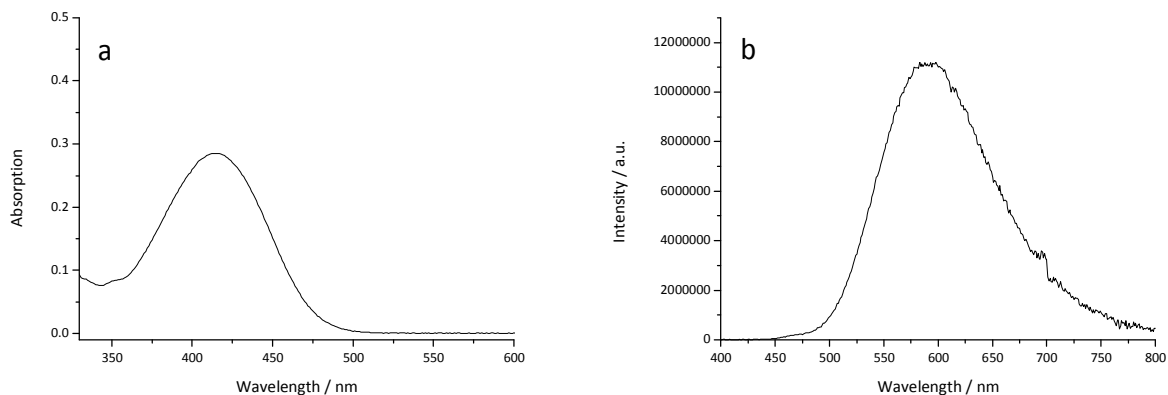


Figure S48. Absorption (a) and emission (b) spectrum of compound **NI2** in acetone. The concentration of **NI2** is $1.0 \cdot 10^{-5}$ M. Excitation wavelength 350 nm.

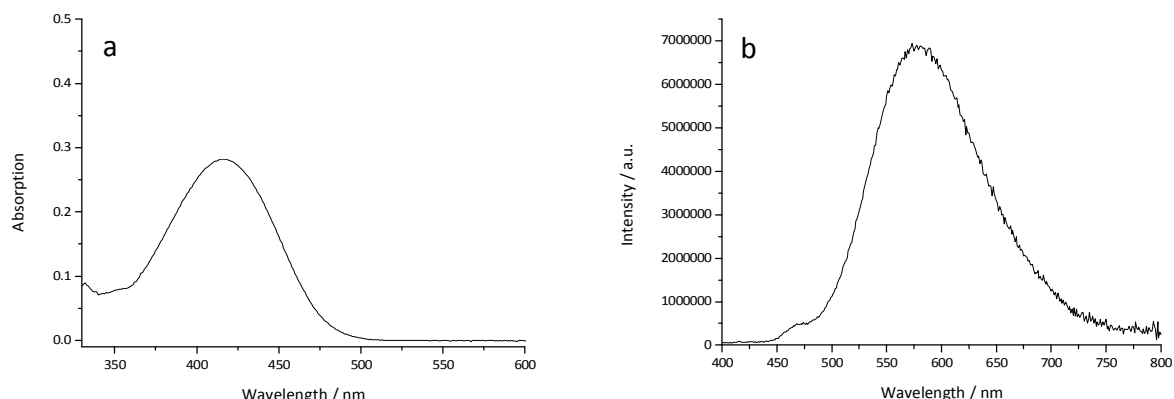


Figure S49. Absorption (a) and emission (b) spectrum of compound **NI2** in 3-methylbutanone-2. The concentration of **NI2** is $1.0 \cdot 10^{-5}$ M. Excitation wavelength 370 nm.

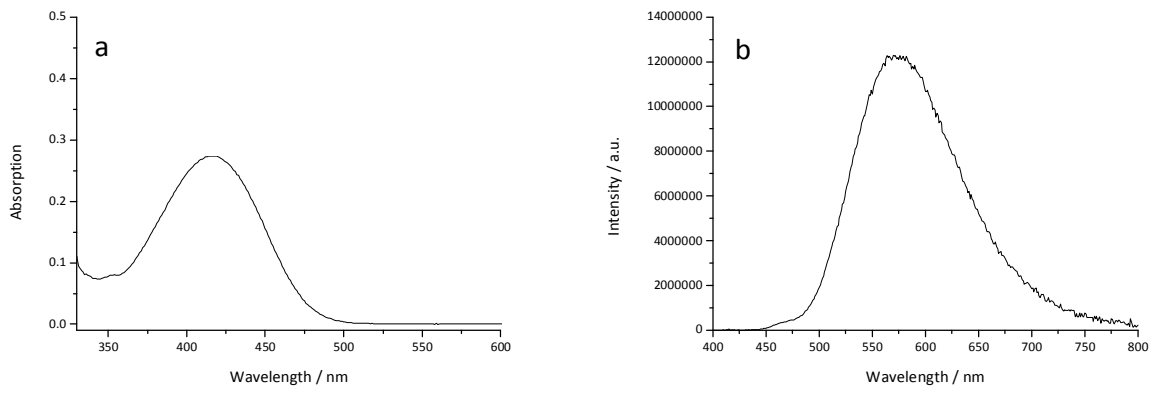


Figure S50. Absorption (a) and emission (b) spectrum of compound **NI2** in 4-methylpentanone-2. The concentration of **NI2** is $1.0 \cdot 10^{-5}$ M. Excitation wavelength 370 nm.

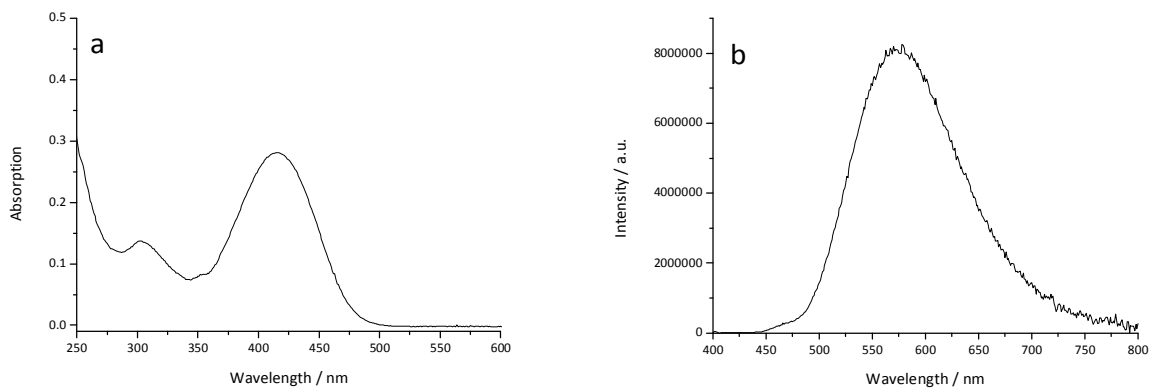


Figure S51. Absorption (a) and emission (b) spectrum of compound **NI2** in 1,2-dimethoxyethane. The concentration of **NI2** is $1.0 \cdot 10^{-5}$ M. Excitation wavelength 360 nm.

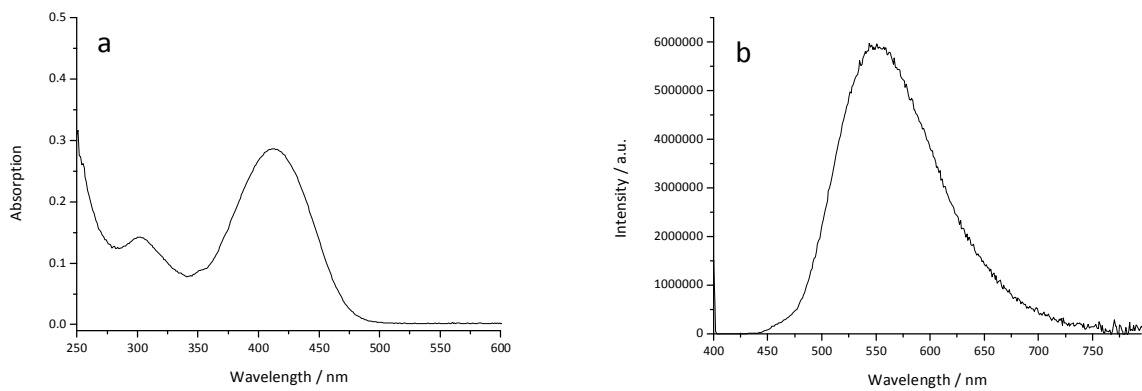


Figure S52. Absorption (a) and emission (b) spectrum of compound **NI2** in ethylacetate. The concentration of **NI2** is $1.0 \cdot 10^{-5}$ M. Excitation wavelength 400 nm.

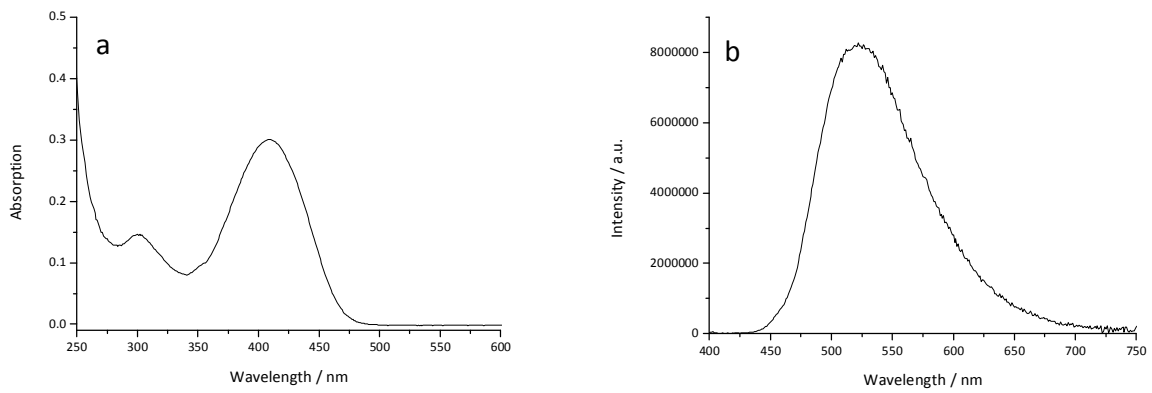


Figure S53. Absorption (a) and emission (b) spectrum of compound **NI2** in diethyl ether. The concentration of **NI2** is $1.0 \cdot 10^{-5}$ M. Excitation wavelength 360 nm.

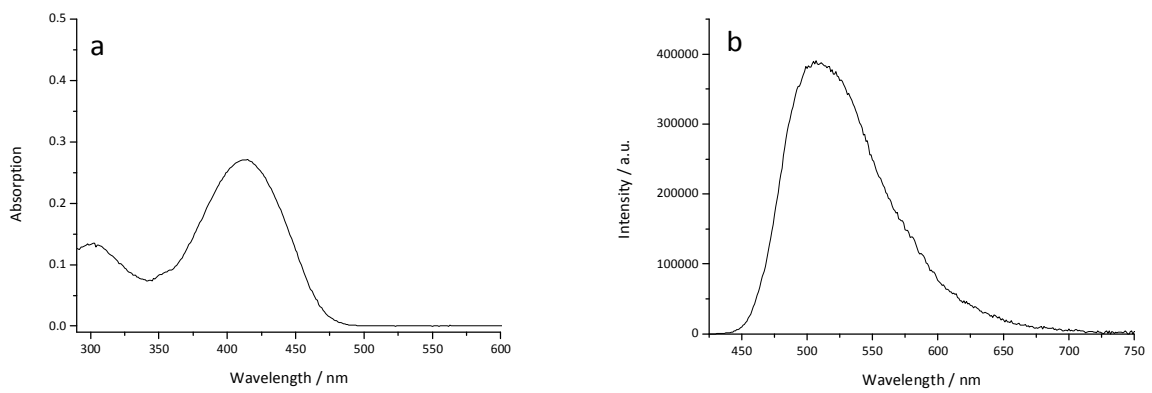


Figure S54. Absorption (a) and emission (b) spectrum of compound **NI2** in toluene. The concentration of **NI2** is $1.0 \cdot 10^{-5}$ M. Excitation wavelength 415 nm.

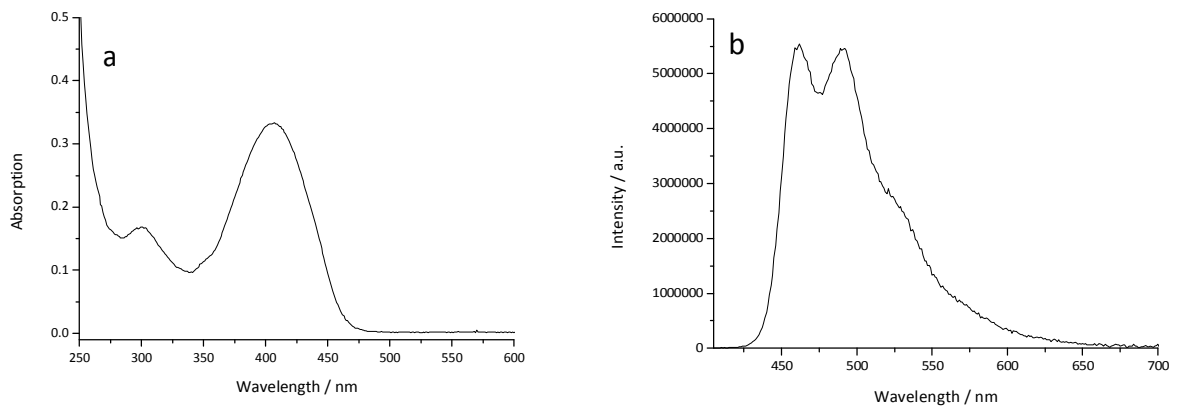


Figure S55. Absorption (a) and emission (b) spectrum of compound **NI2** in cyclohexane. The concentration of **NI2** is $1.0 \cdot 10^{-5}$ M. Excitation wavelength 400 nm.

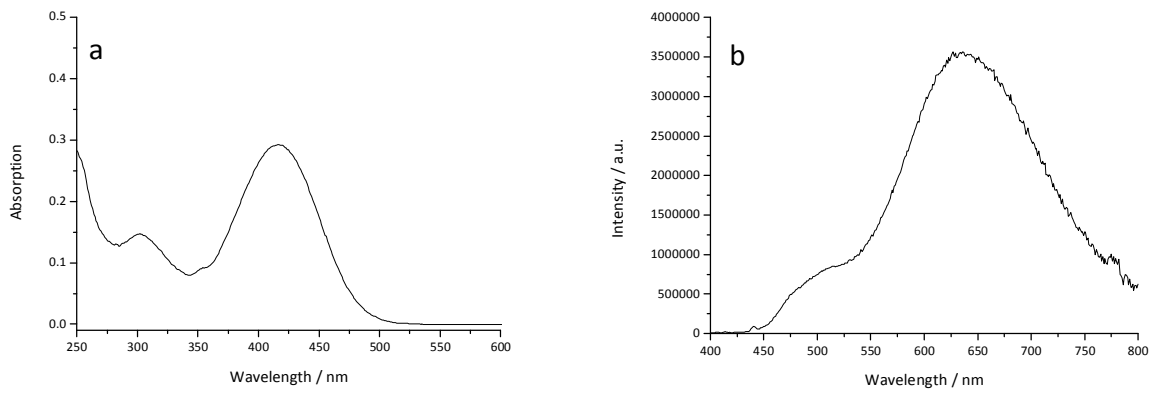


Figure S56. Absorption (a) and emission (b) spectrum of compound **NI2** in methanol. The concentration of **NI2** is $1.0 \cdot 10^{-5}$ M. Excitation wavelength 390 nm.

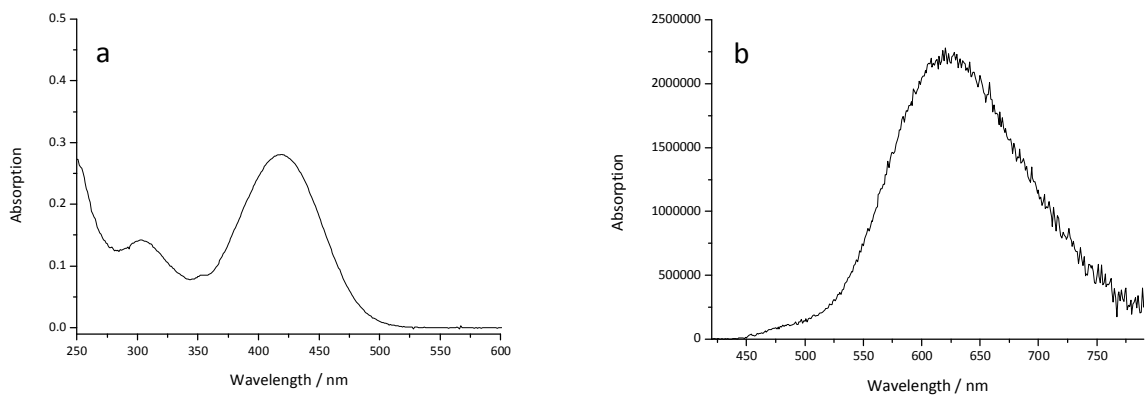


Figure S57. Absorption (a) and emission (b) spectrum of compound **NI2** in ethanol. The concentration of **NI2** is $1.0 \cdot 10^{-5}$ M. Excitation wavelength 400 nm.

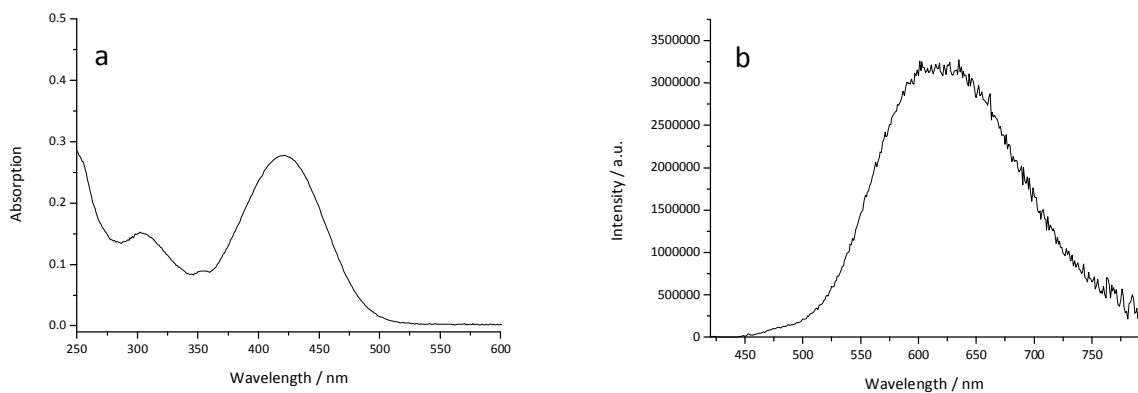


Figure S58. Absorption (a) and emission (b) spectrum of compound **NI2** in *n*-butanol. The concentration of **NI2** is $1.0 \cdot 10^{-5}$ M. Excitation wavelength 400 nm.

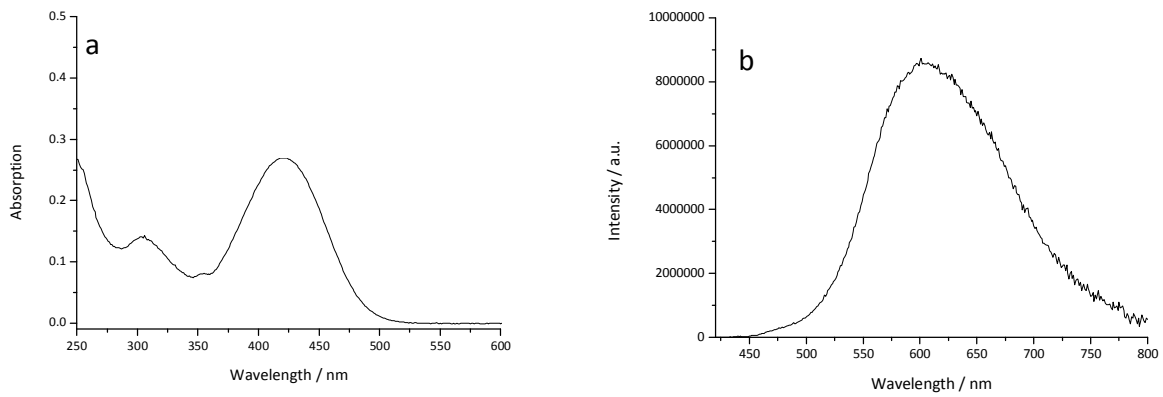


Figure S59. Absorption (a) and emission (b) spectrum of compound **NI2** in *n*-hexanol. The concentration of **NI2** is $1.0 \cdot 10^{-5}$ M. Excitation wavelength 390 nm.

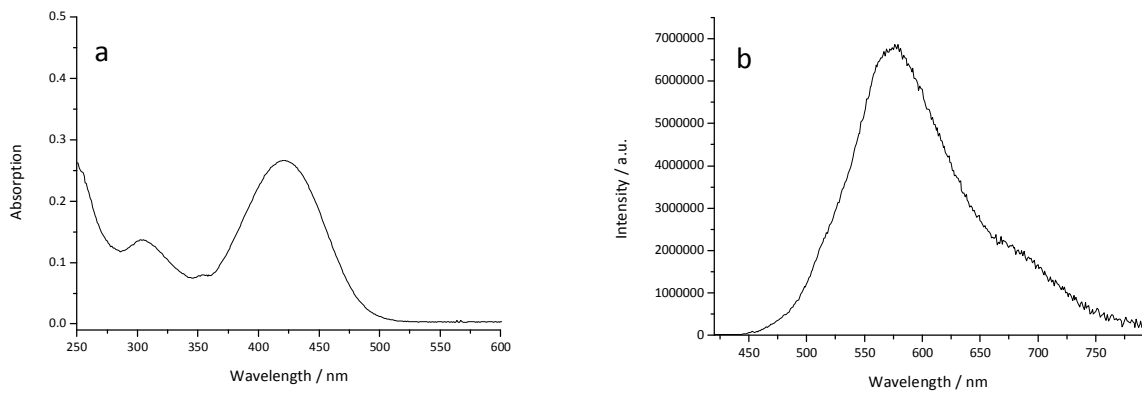


Figure S60. Absorption (a) and emission (b) spectrum of compound **NI2** in *n*-decanol. The concentration of **NI2** is $1.0 \cdot 10^{-5}$ M. Excitation wavelength 400 nm.

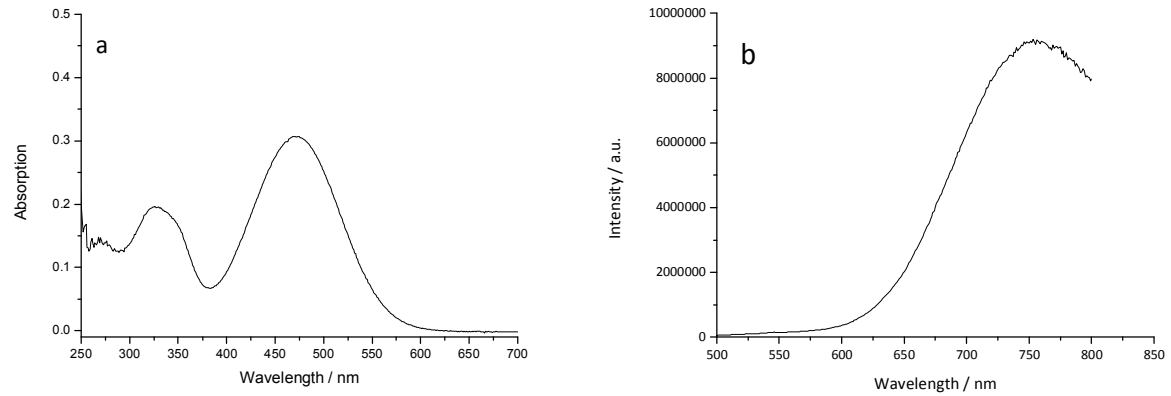


Figure S61. Absorption (a) and emission (b) spectrum of compound **NI3** in propylene carbonate. The concentration of **NI3** is $1.0 \cdot 10^{-5}$ M. Excitation wavelength 469 nm.

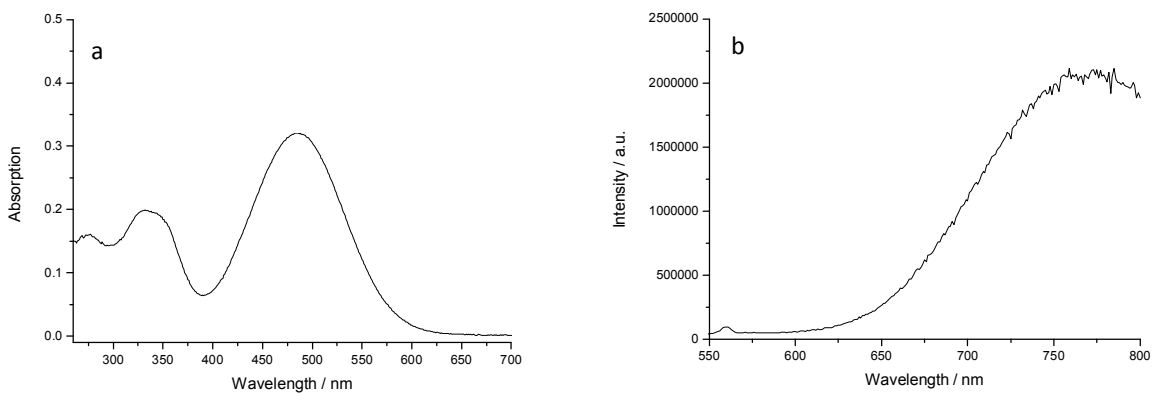


Figure S62. Absorption (a) and emission (b) spectrum of compound **NI3** in DMSO. The concentration of **NI3** is $1.0 \cdot 10^{-5}$ M. Excitation wavelength 480 nm.

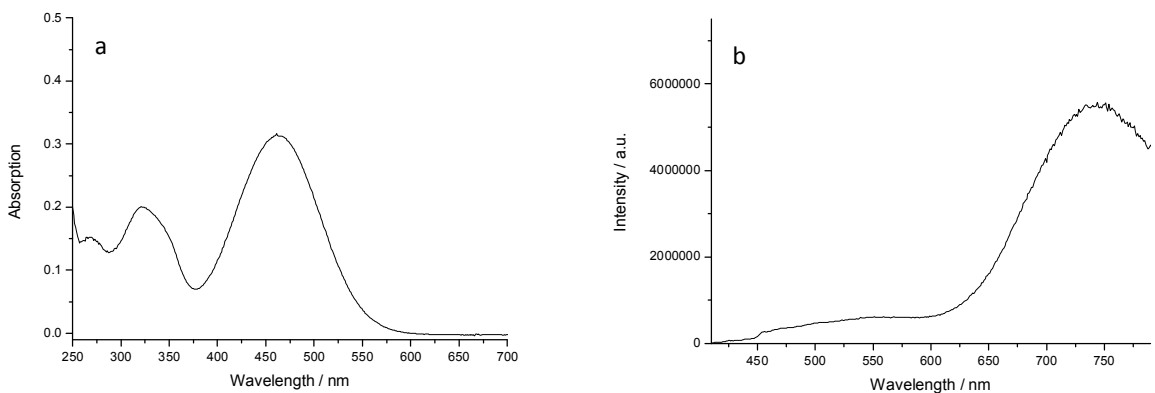


Figure S63. Absorption (a) and emission (b) spectrum of compound **NI3** in acetonitrile. The concentration of **NI3** is $1.0 \cdot 10^{-5}$ M. Excitation wavelength 400 nm.

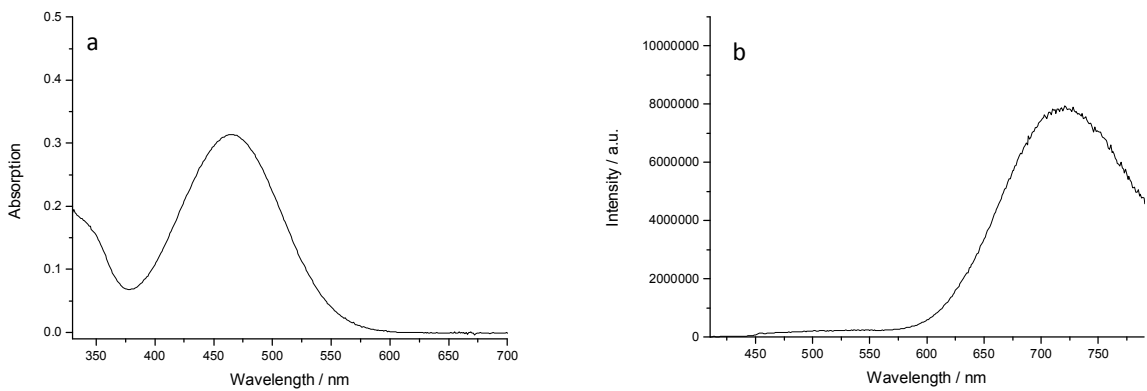


Figure S64. Absorption (a) and emission (b) spectrum of compound **NI3** in acetone. The concentration of **NI3** is $1.0 \cdot 10^{-5}$ M. Excitation wavelength 400 nm.

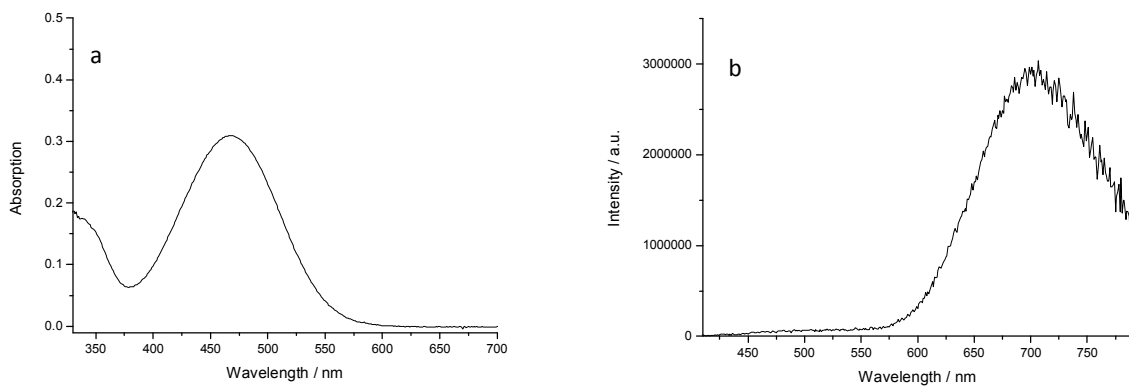


Figure S65. Absorption (a) and emission (b) spectrum of compound **NI3** in 3-methylbutanone-2. The concentration of **NI3** is $1.0 \cdot 10^{-5}$ M. Excitation wavelength 400 nm.

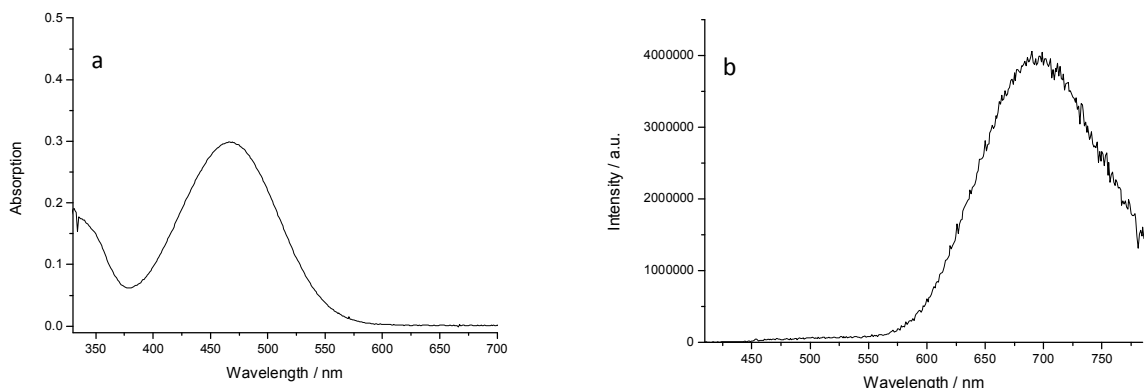


Figure S66. Absorption (a) and emission (b) spectrum of compound **NI3** in 4-methylpentanone-2. The concentration of **NI3** is $1.0 \cdot 10^{-5}$ M. Excitation wavelength 400 nm.

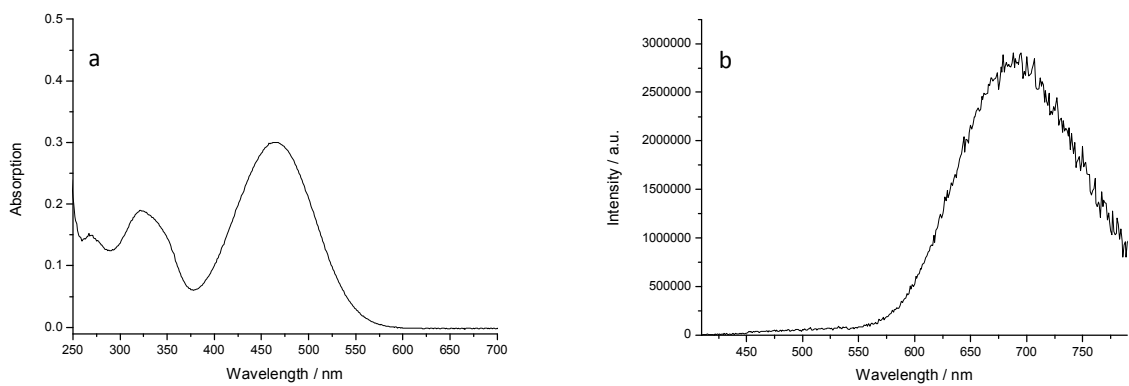


Figure S67. Absorption (a) and emission (b) spectrum of compound **NI3** in 1,2-dimethoxyethane. The concentration of **NI3** is $1.0 \cdot 10^{-5}$ M. Excitation wavelength 400 nm.

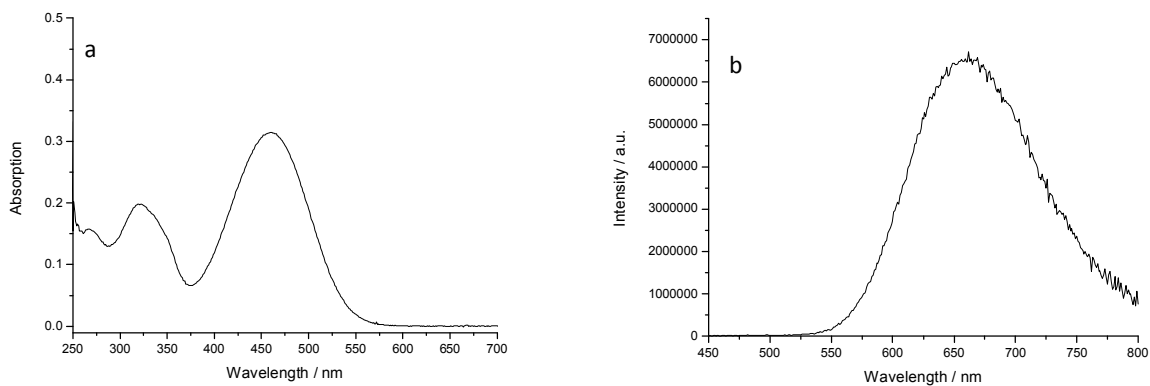


Figure S68. Absorption (a) and emission (b) spectrum of compound **NI3** in ethylacetate. The concentration of **NI3** is $1.0 \cdot 10^{-5}$ M. Excitation wavelength 425 nm.

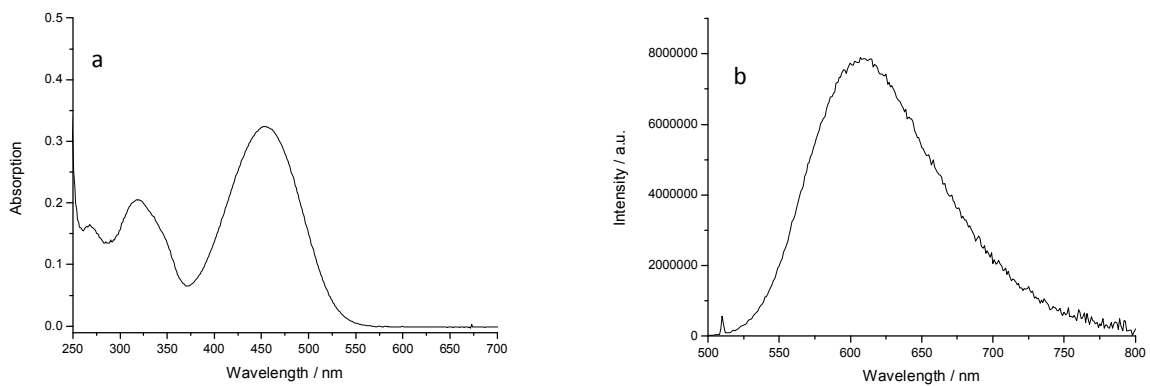


Figure S69. Absorption (a) and emission (b) spectrum of compound **NI3** in diethyl ether. The concentration of **NI3** is $1.0 \cdot 10^{-5}$ M. Excitation wavelength 510 nm.

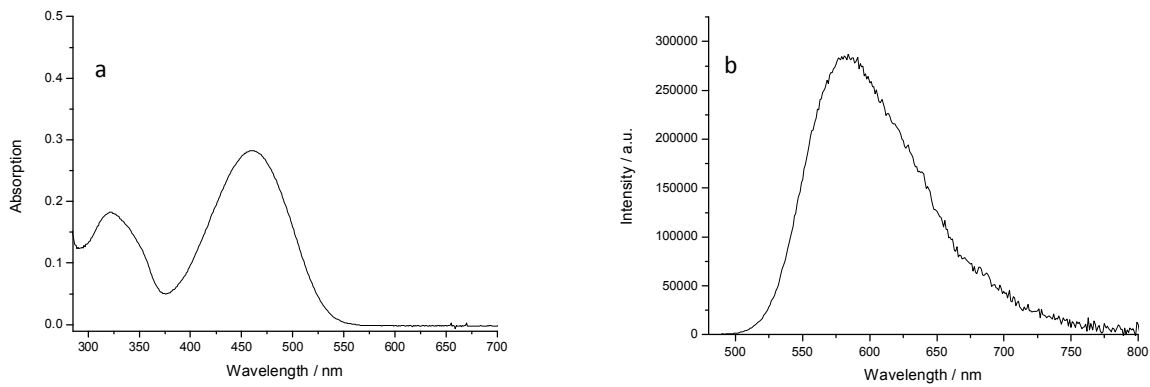


Figure S70. Absorption (a) and emission (b) spectrum of compound **NI3** in toluene. The concentration of **NI3** is $1.0 \cdot 10^{-5}$ M. Excitation wavelength 460 nm.

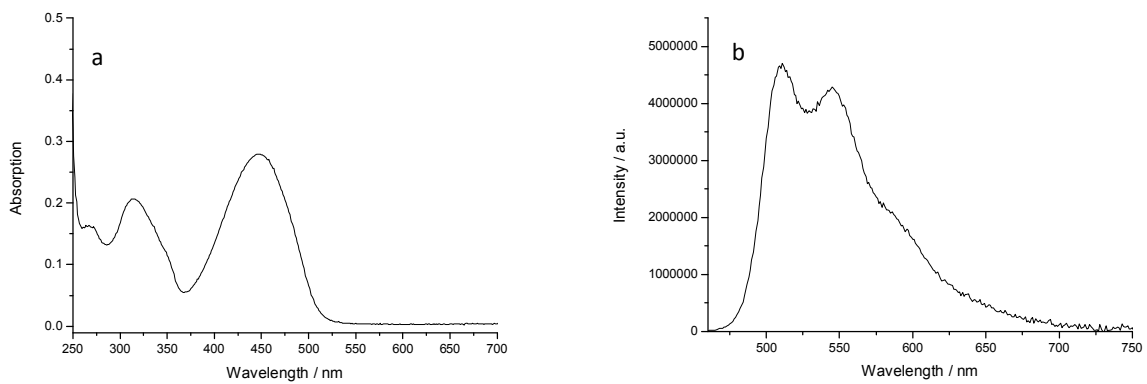


Figure S71. Absorption (a) and emission (b) spectrum of compound **NI3** in cyclohexane. The concentration of **NI3** is $1.0 \cdot 10^{-5}$ M. Excitation wavelength 450 nm.

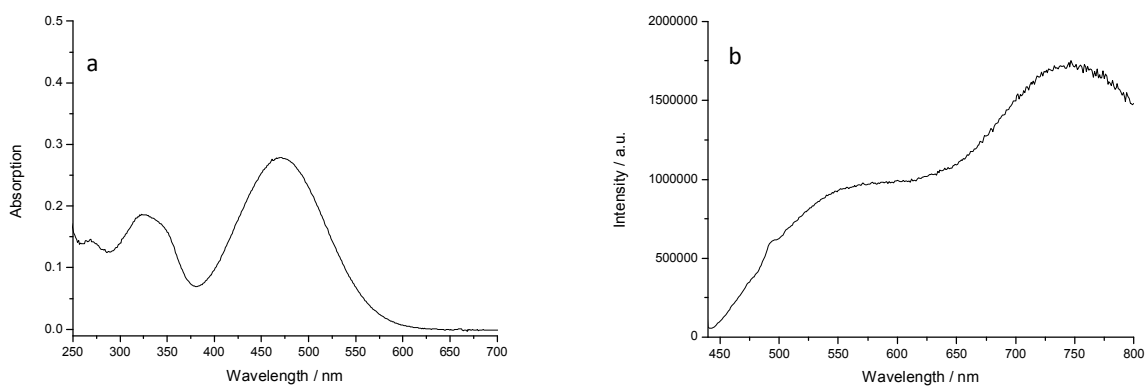


Figure S72. Absorption (a) and emission (b) spectrum of compound **NI3** in methanol. The concentration of **NI3** is $1.0 \cdot 10^{-5}$ M. Excitation wavelength 430 nm.

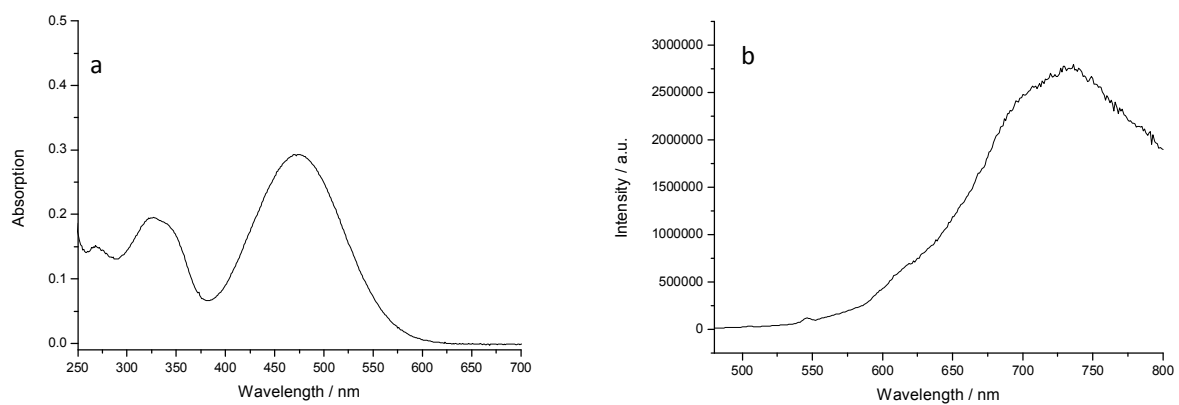


Figure S73. Absorption (a) and emission (b) spectrum of compound **NI3** in ethanol. The concentration of **NI3** is $1.0 \cdot 10^{-5}$ M. Excitation wavelength 470 nm.

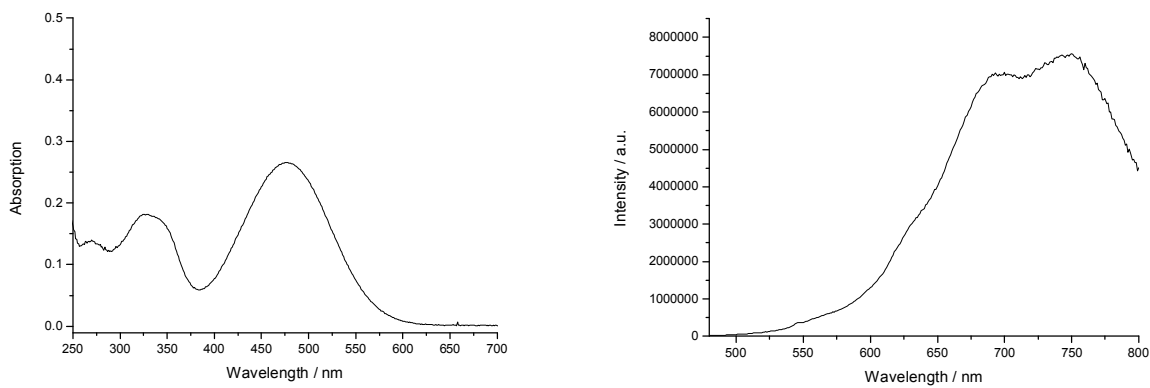


Figure S74. Absorption (a) and emission (b) spectrum of compound **NI3** in *n*-butanol. The concentration of **NI3** is $1.0 \cdot 10^{-5}$ M. Excitation wavelength 470 nm.

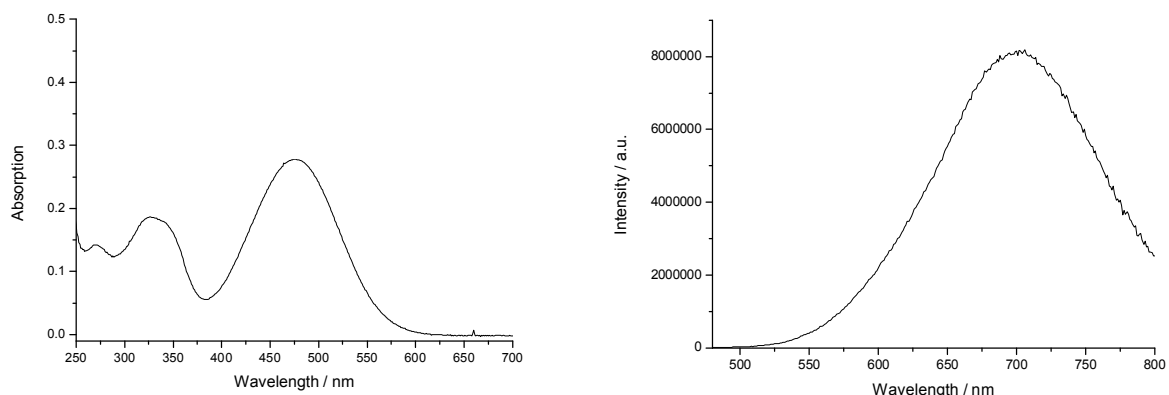


Figure S75. Absorption (a) and emission (b) spectrum of compound **NI3** in *n*-hexanol. The concentration of **NI3** is $1.0 \cdot 10^{-5}$ M. Excitation wavelength 470 nm.

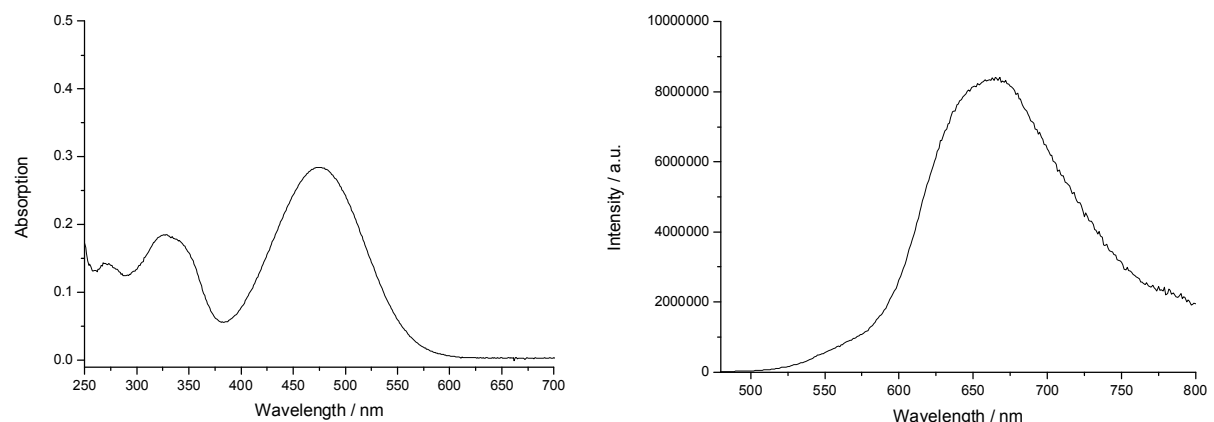
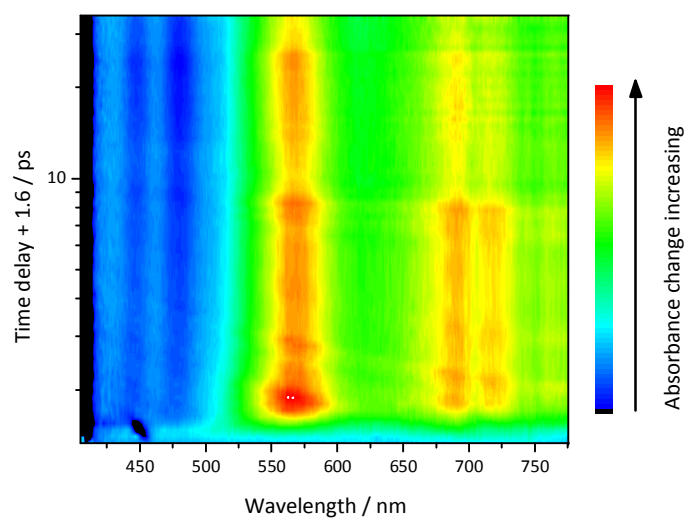


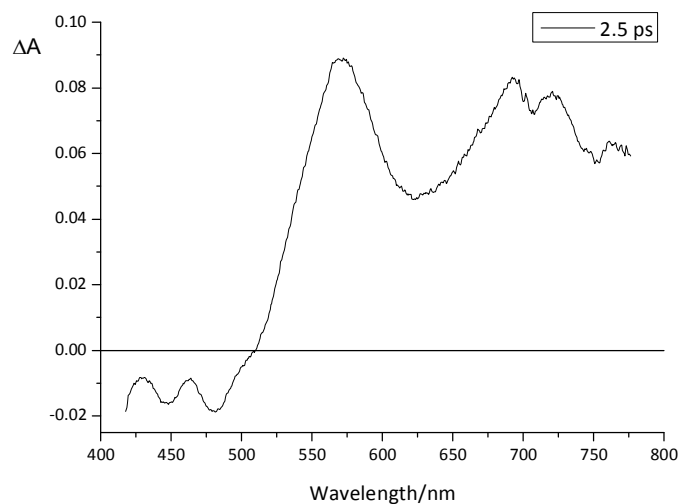
Figure S76. Absorption (a) and emission (b) spectrum of compound **NI3** in *n*-decanol. The concentration of **NI3** is $1.0 \cdot 10^{-5}$ M. Excitation wavelength 470 nm.

8. Transient absorption spectroscopy data of NI1–3

a



b



c

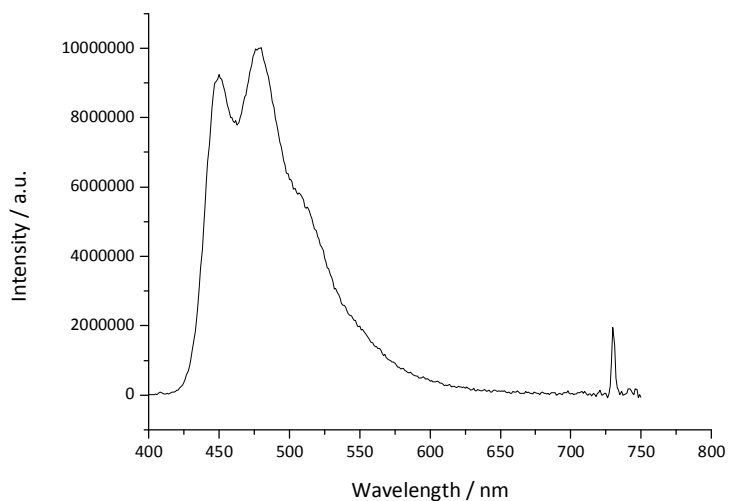
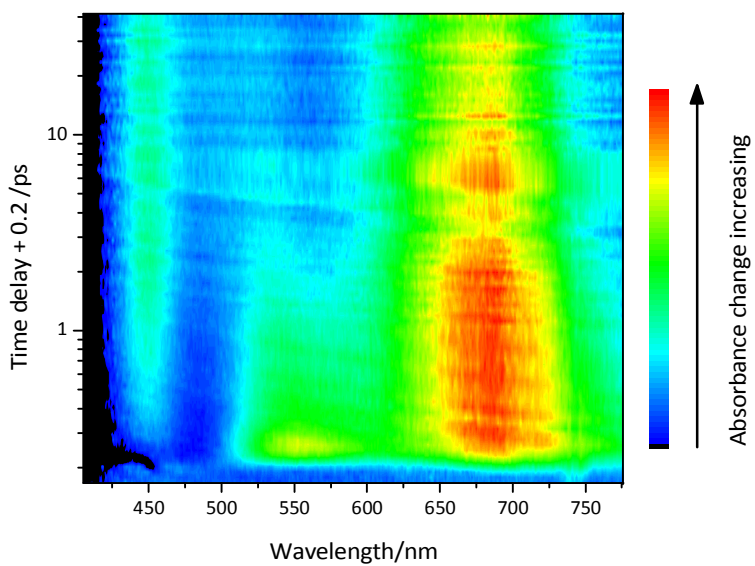
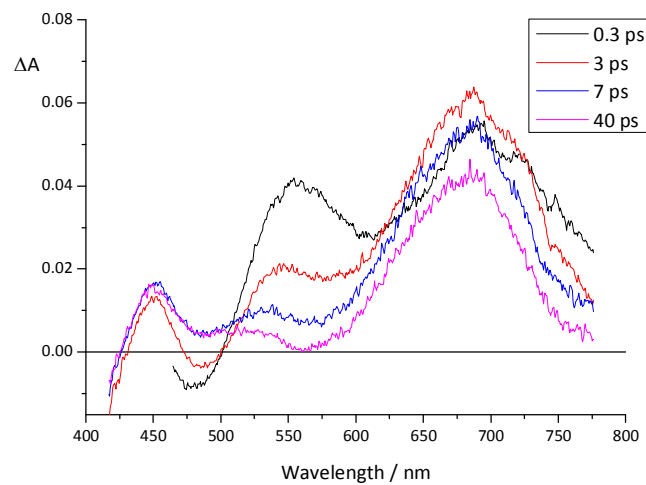


Figure S77. Time-resolved TRABS map (a), TRABS spectrum at 2.5 ps time delay (b) and steady-state fluorescence spectrum (c) of compound NI1 in cyclohexane.

a



b



c

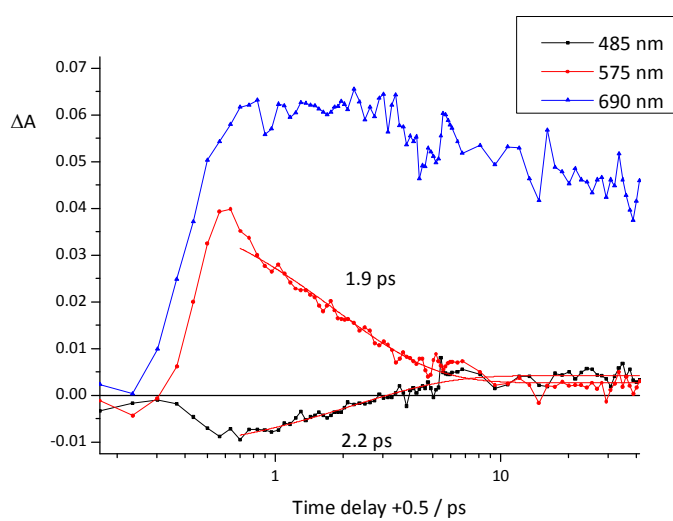
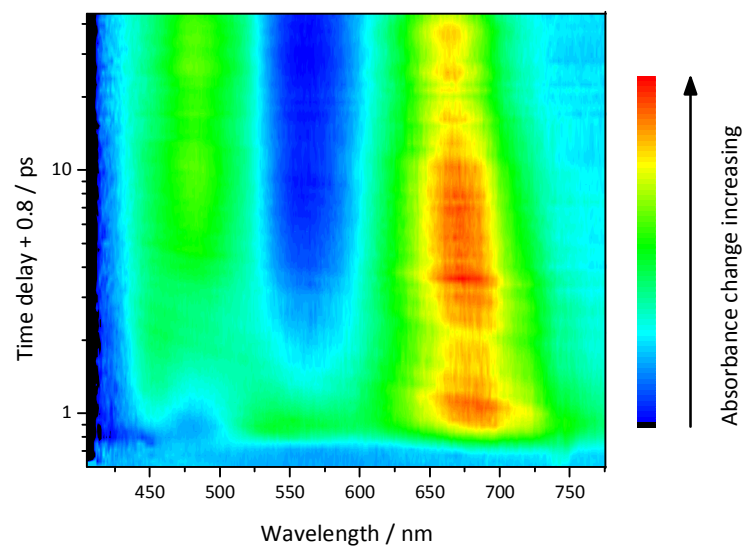
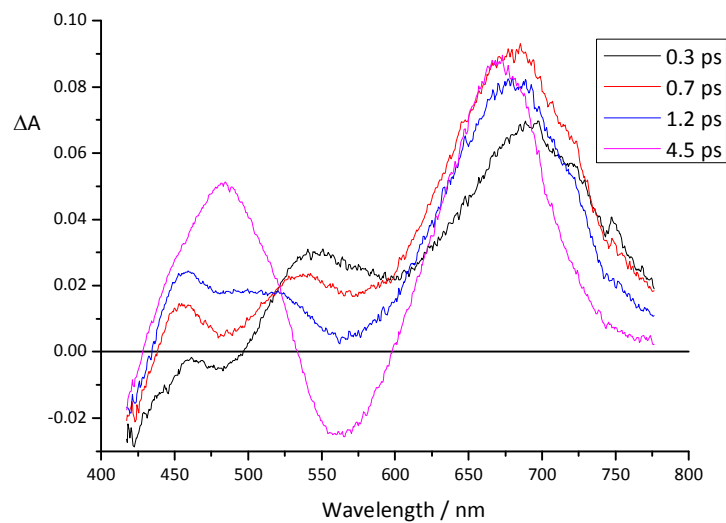


Figure S78. Time-resolved TRABS map (a), TRABS spectrum at different time delays (b) and TRABS kinetic curves at different wavelengths (c) for the compound **N11** in diethyl ether.

a



b



c

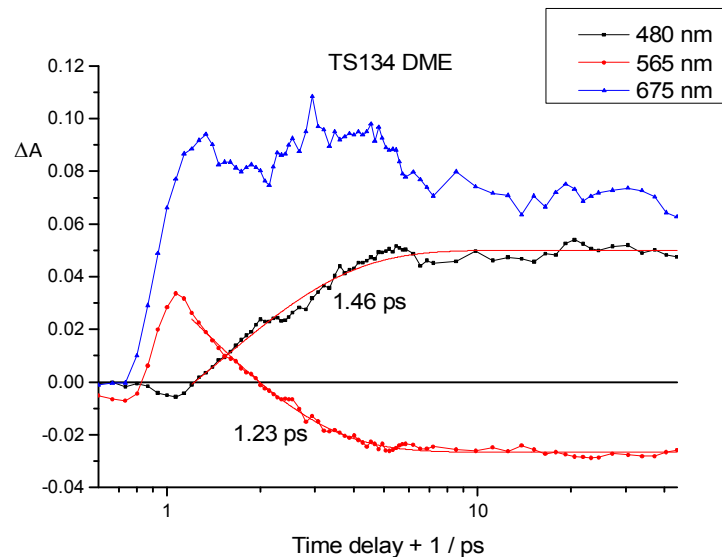
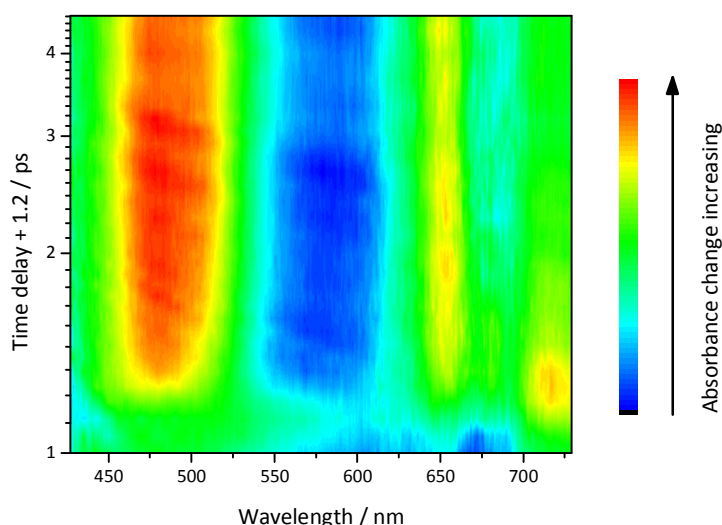
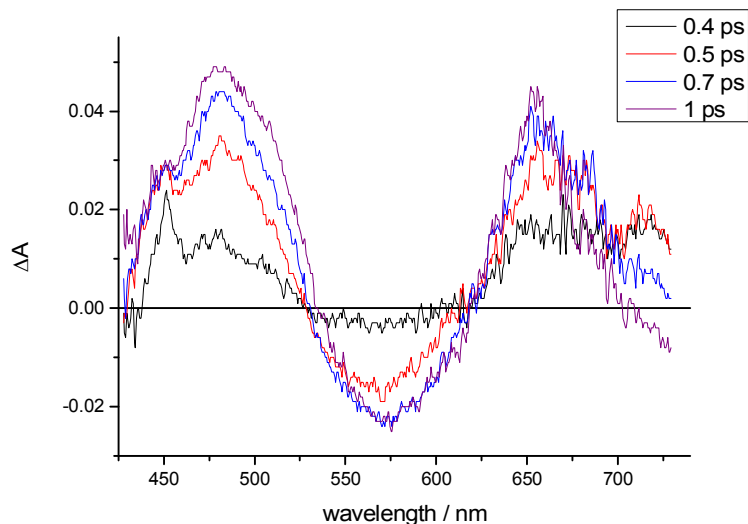


Figure S79. Time-resolved TRABS map (a), TRABS spectrum at different time delays (b) and TRABS kinetic curves at different wavelengths (c) for the compound **NI1** in 1,2-dimethoxyethane.

a



b



c

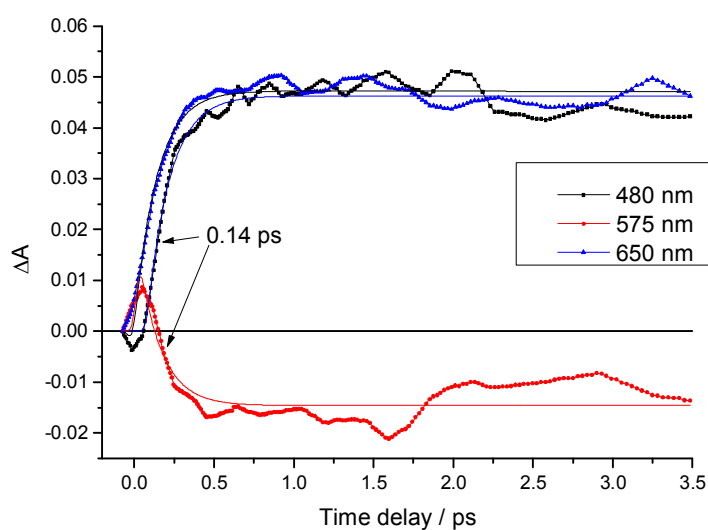
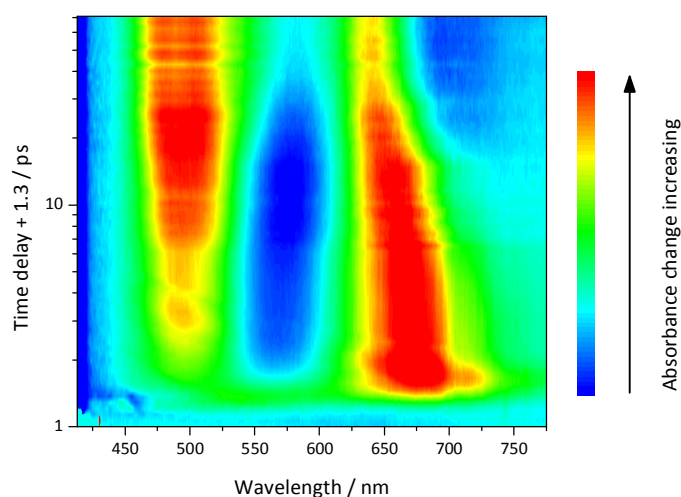
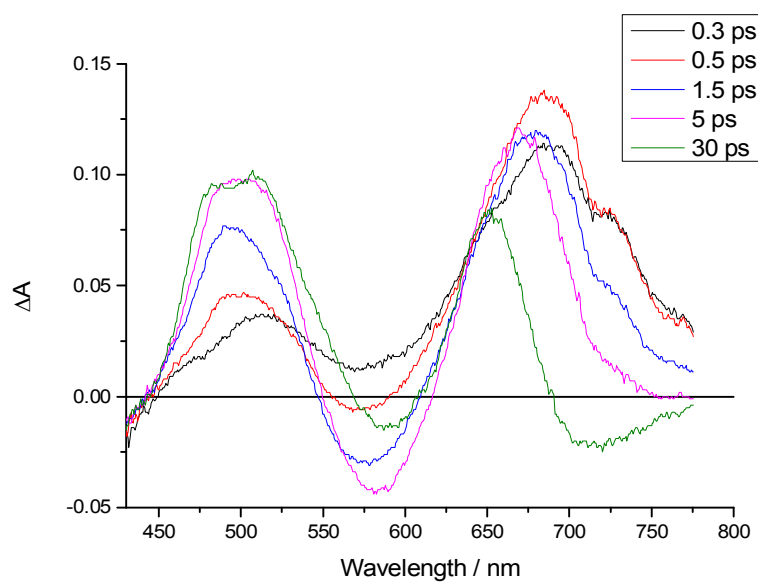


Figure S80. Time-resolved TRABS map (a), TRABS spectrum at different time delays (b) and TRABS kinetic curves at different wavelengths (c) for the compound **N11** in acetonitrile.

a



b



c

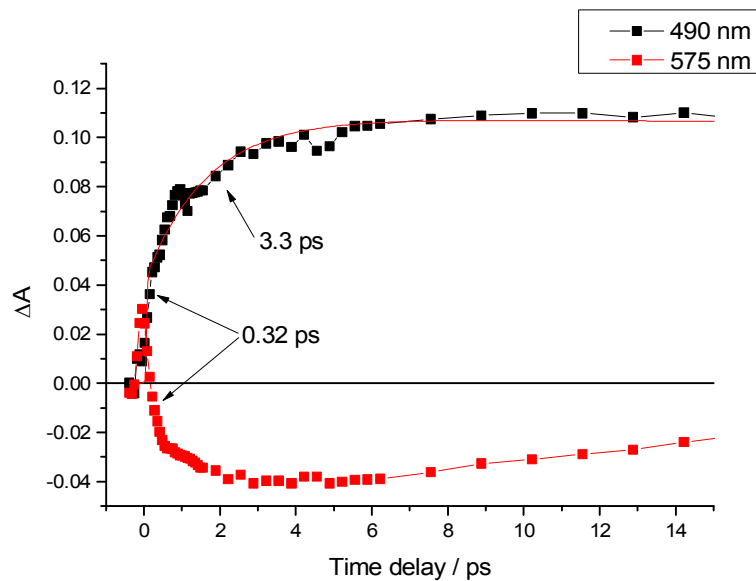
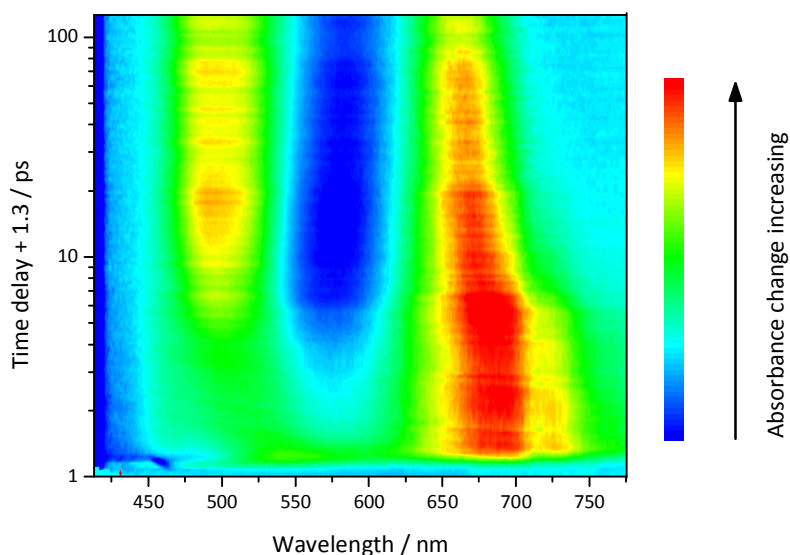
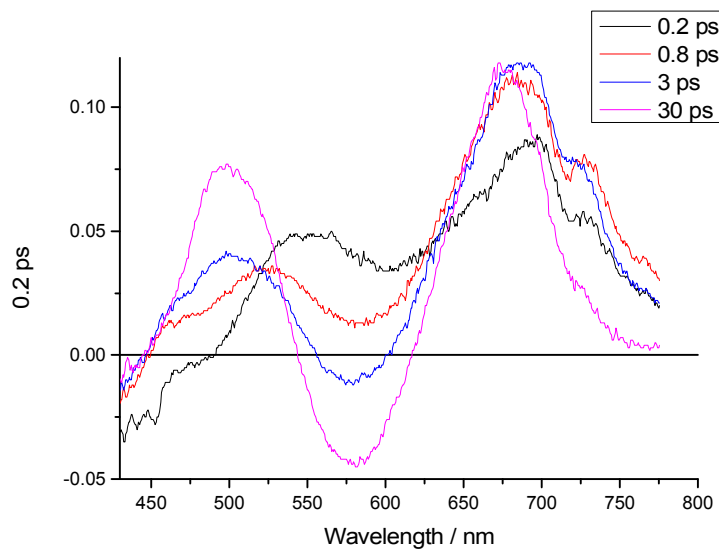


Figure S81. Time-resolved TRABS map (a), TRABS spectrum at different time delays (b) and TRABS kinetic curves at different wavelengths (c) for the compound **N11** in methanol.

a



b



c

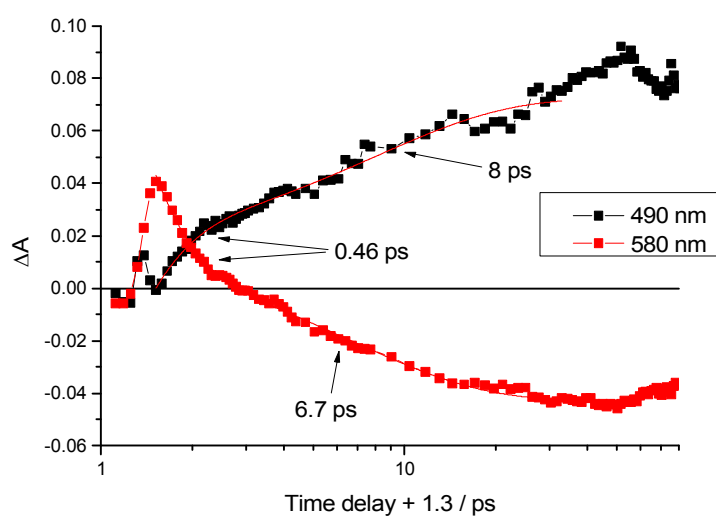


Figure S82. Time-resolved TRABS map (a), TRABS spectrum at different time delays (b) and TRABS kinetic curves at different wavelengths (c) for the compound **N11** in *n*-propanol.

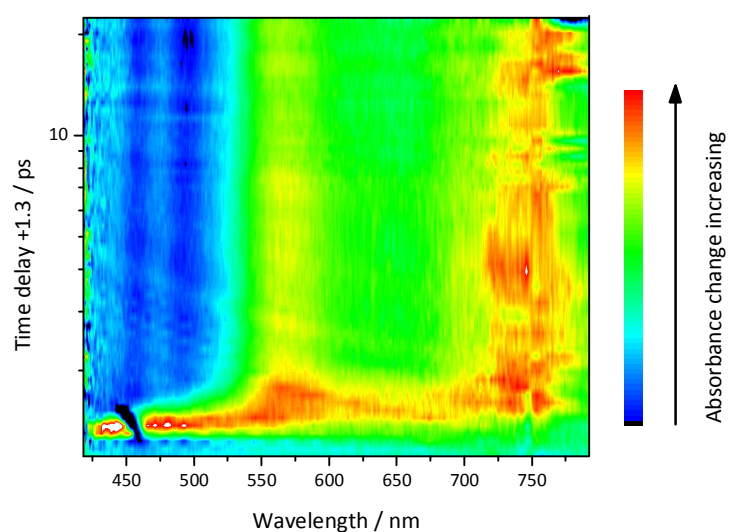
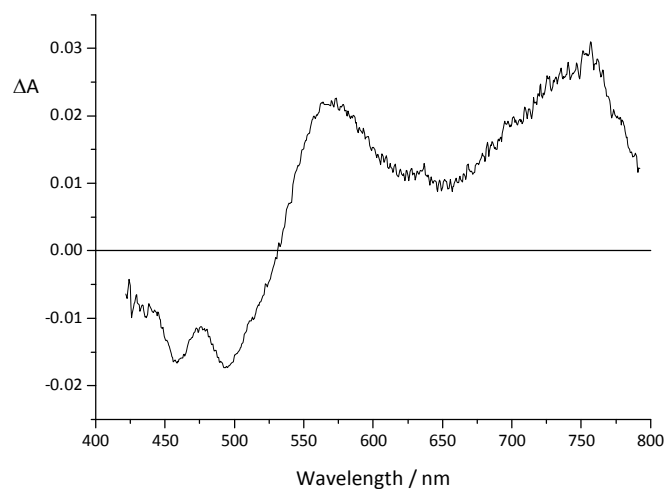
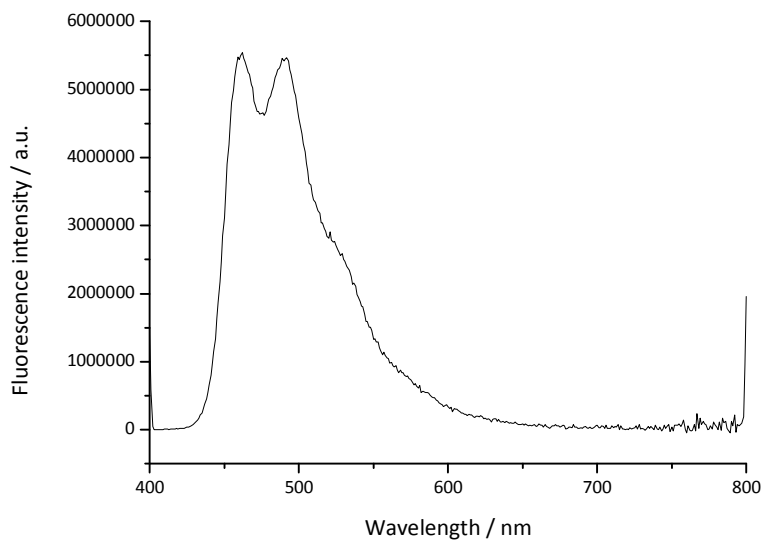
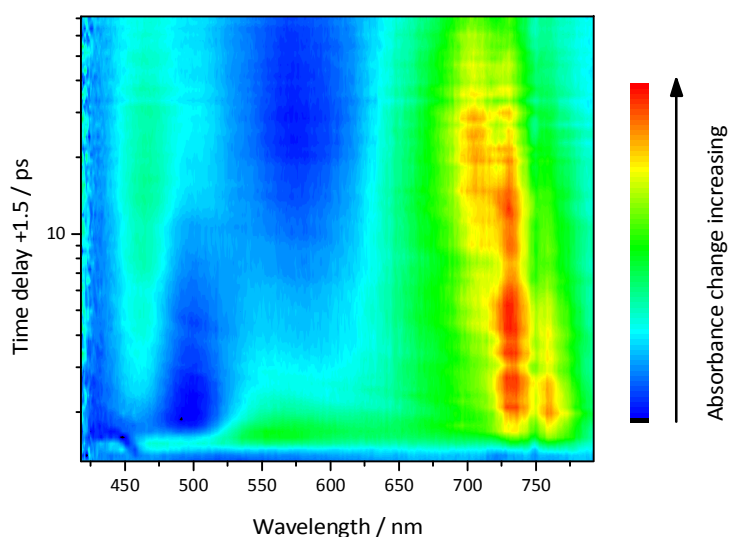
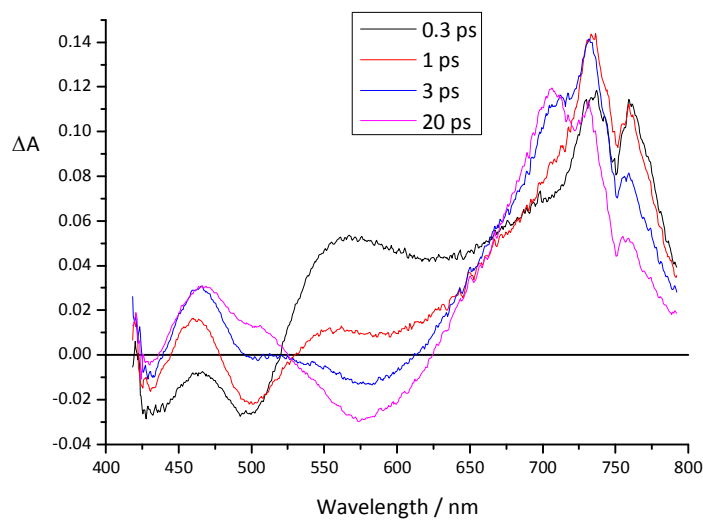
a**b****c**

Figure S83. Time-resolved TRABS map (a), TRABS spectrum (b) and steady-state fluorescence spectrum (c) of compound **N12** in cyclohexane.

a



b



c

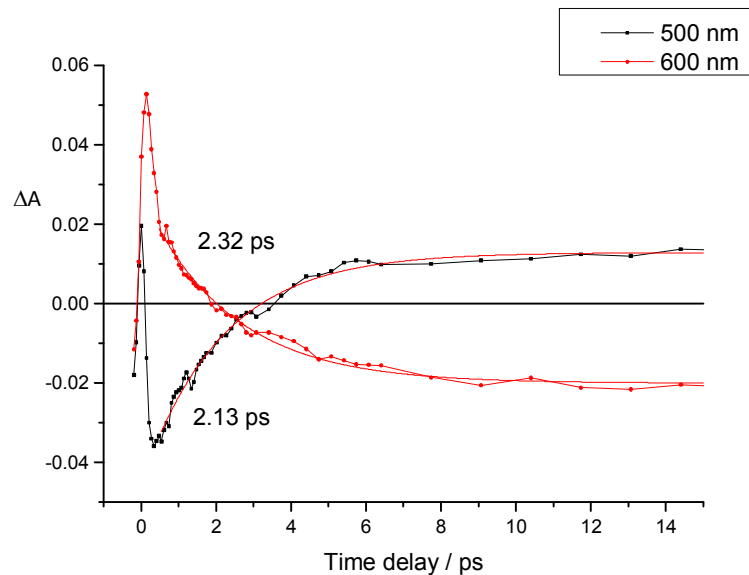
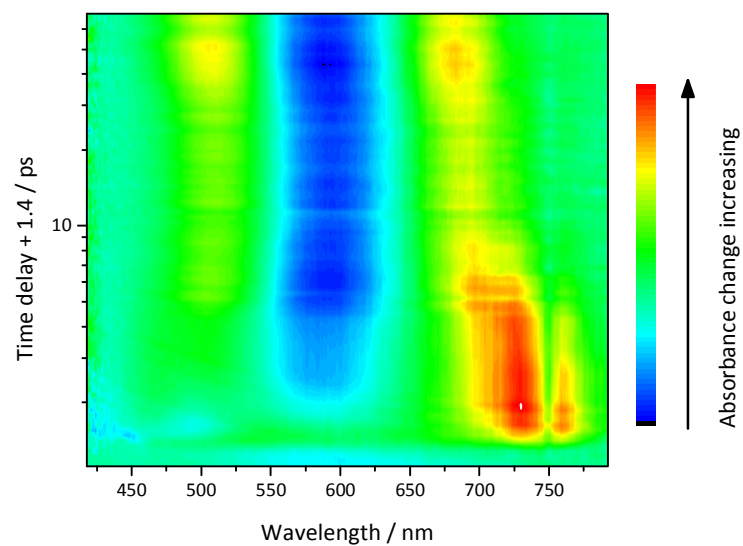
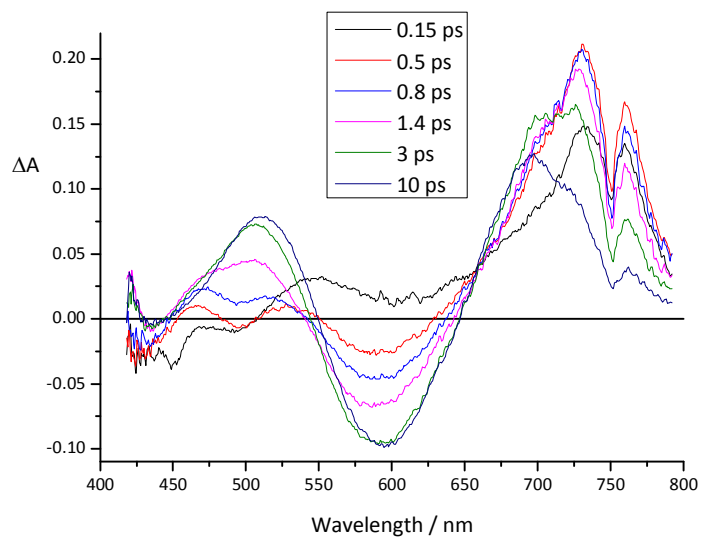


Figure S84. Time-resolved TRABS map (a), TRABS spectrum at different time delays (b) and TRABS kinetic curves at different wavelengths (c) for the compound **N12** in diethyl ether.

a



b



c

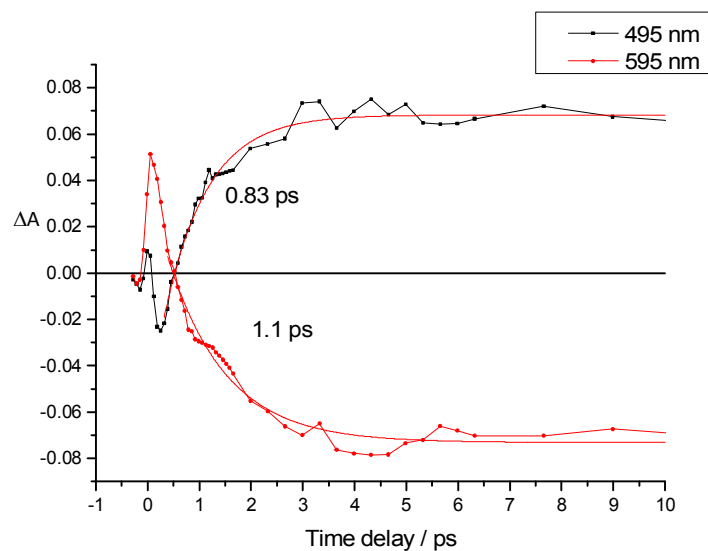


Figure S85. Time-resolved TRABS map (a), TRABS spectrum at different time delays (b) and TRABS kinetic curves at different wavelengths (c) for the compound **N12** in 1,2-dimethoxyethane.

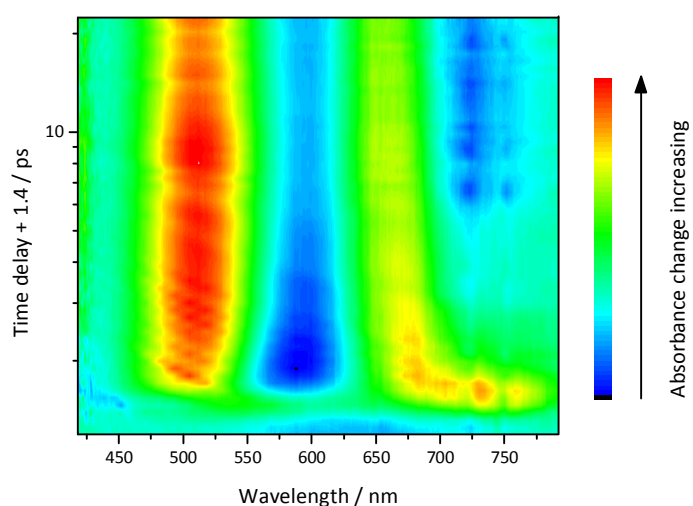
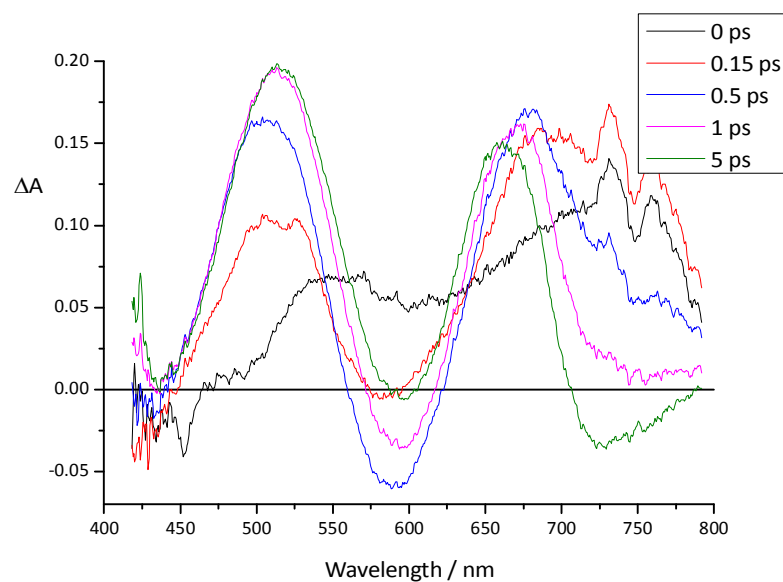
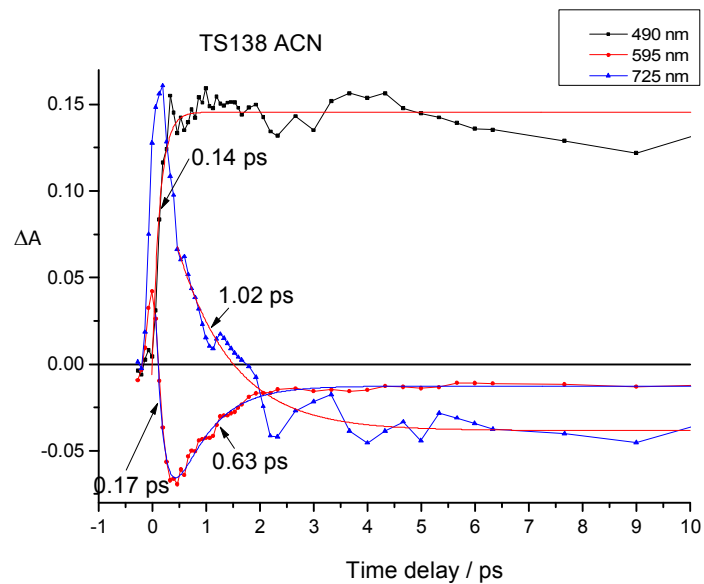
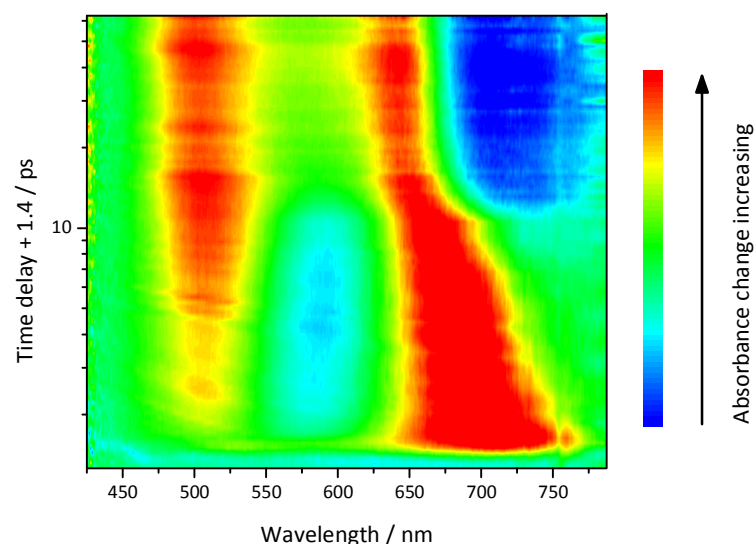
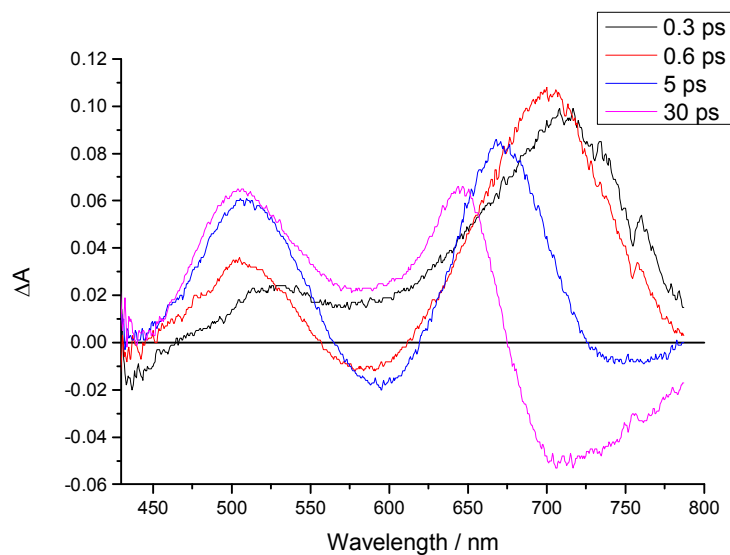
a**b****c**

Figure S86. Time-resolved TRABS map (a), TRABS spectrum at different time delays (b) and TRABS kinetic curves at different wavelengths (c) for the compound **N12** in acetonitrile.

a



b



c

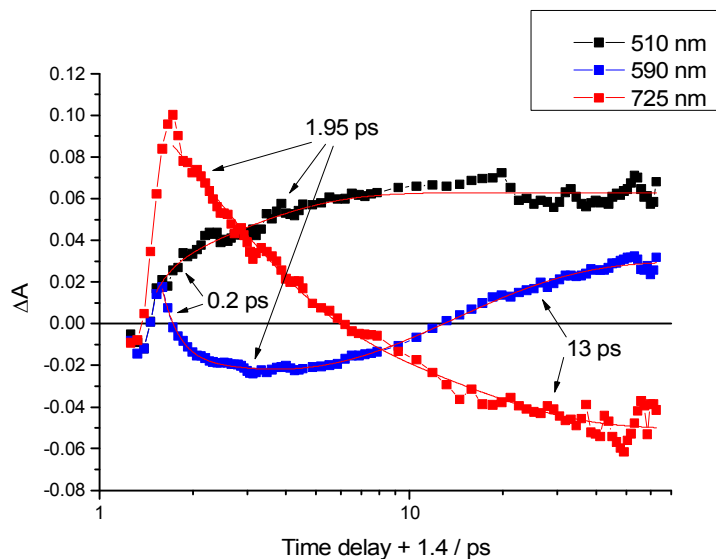
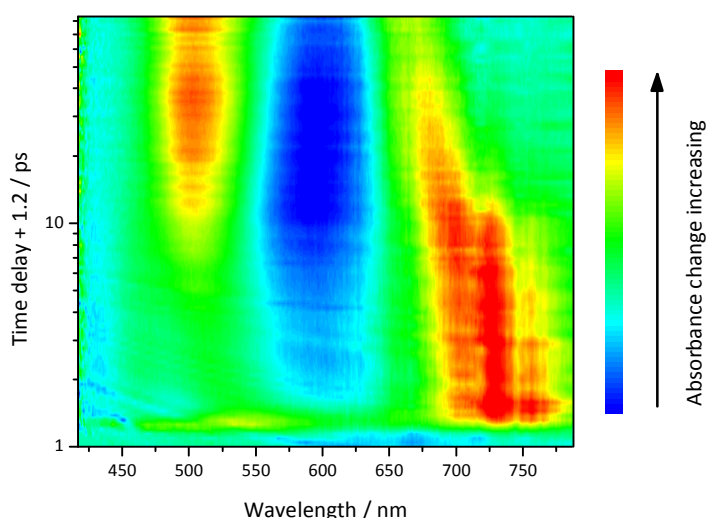
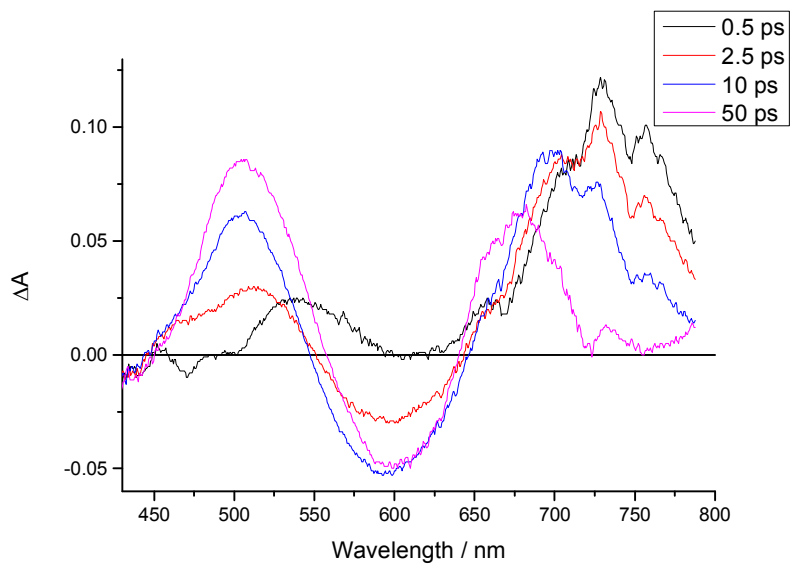


Figure S87. Time-resolved TRABS map (a), TRABS spectrum at different time delays (b) and TRABS kinetic curves at different wavelengths (c) for the compound **N12** in methanol.

a



b



c

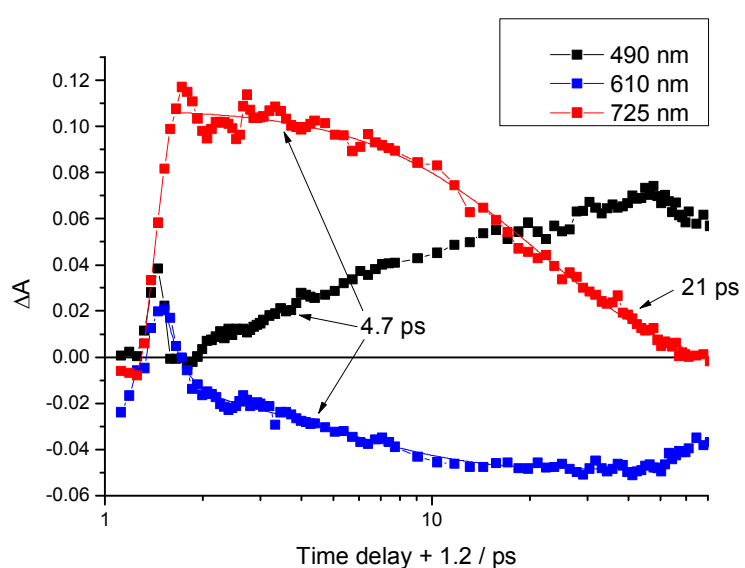
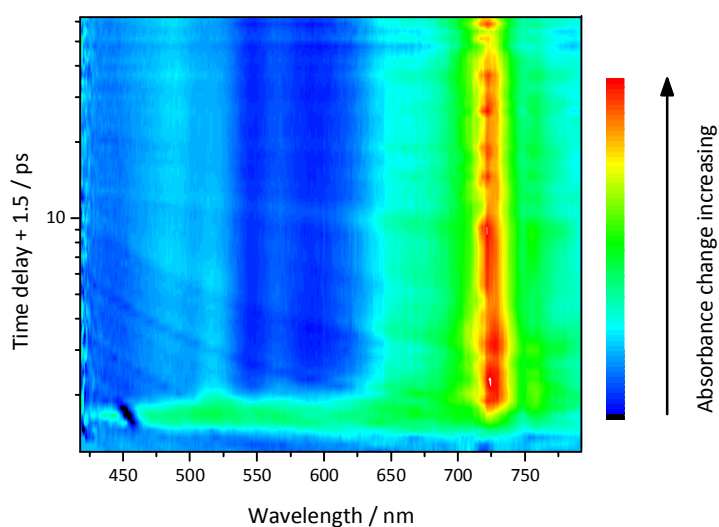
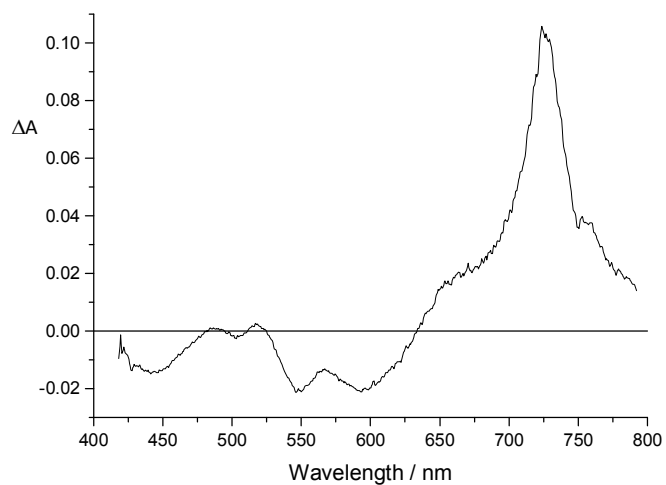


Figure S88. Time-resolved TRABS map (a), TRABS spectrum at different time delays (b) and TRABS kinetic curves at different wavelengths (c) for the compound **N12** in *n*-propanol.

a



b



c

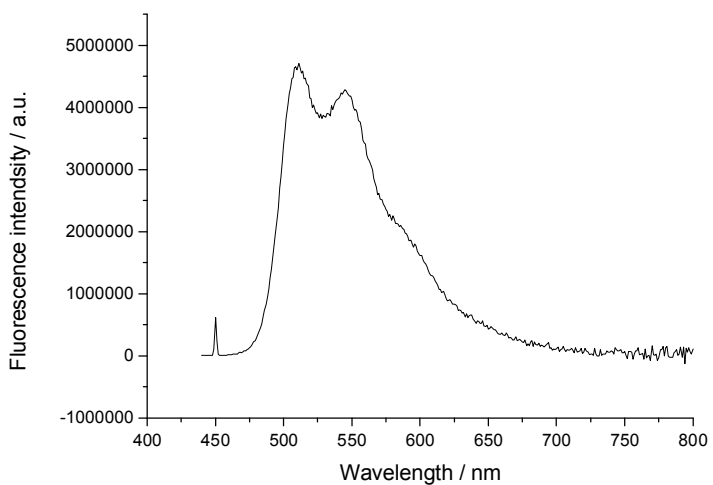
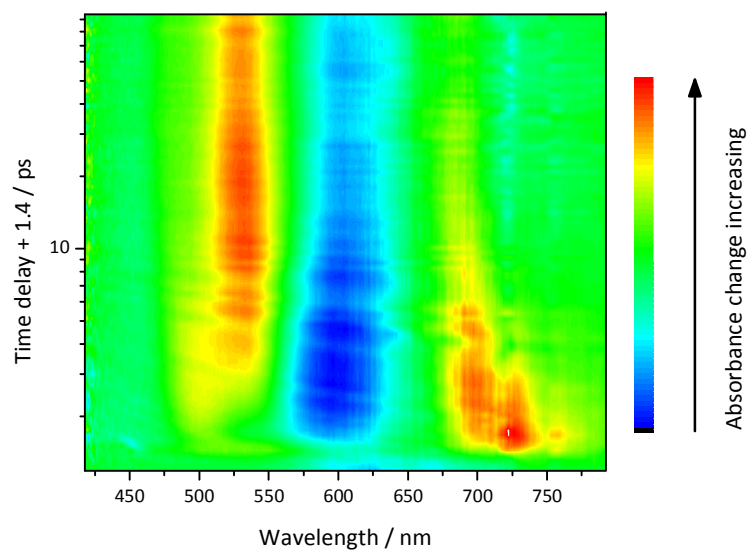


Figure S89. Time-resolved TRABS map (a), TRABS spectrum (b) and steady-state fluorescence spectrum (c) of compound **N13** in cyclohexane.

a



b

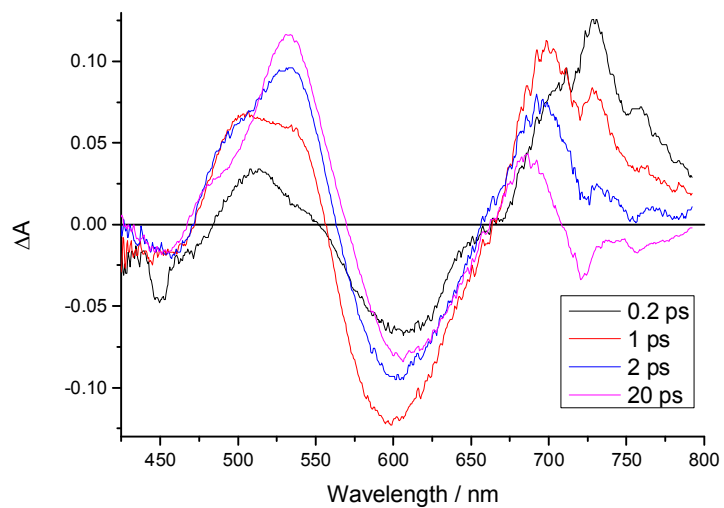
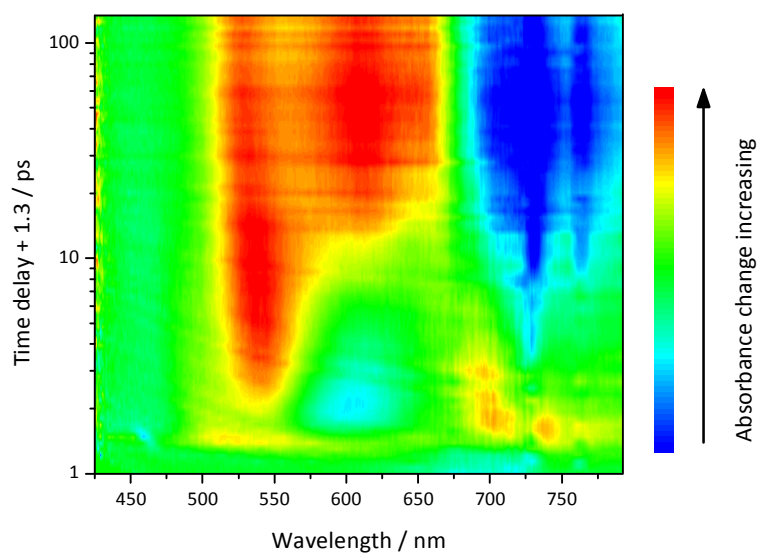


Figure S90. Time-resolved TRABS map (a) and TRABS spectrum at different time delays (b) for the compound NI3 in diethyl ether.

a



b

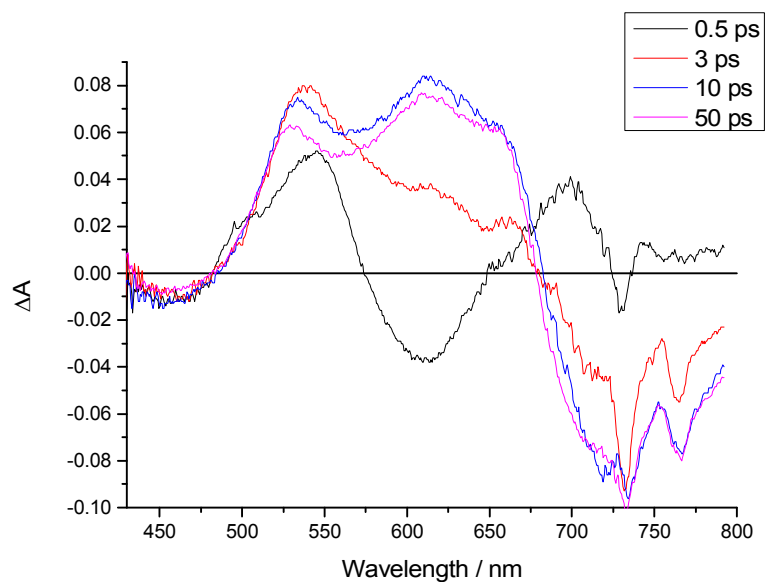
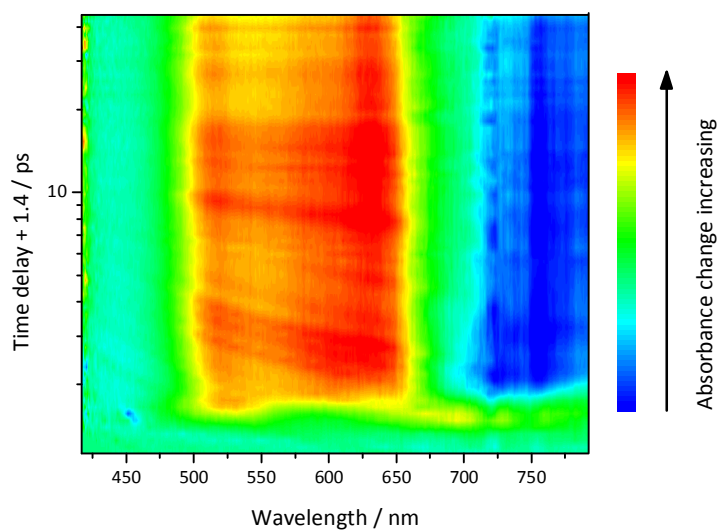


Figure S91. Time-resolved TRABS map (a) and TRABS spectrum at different time delays (b) for the compound NI3 in 1,2-dimethoxyethane.

a



b

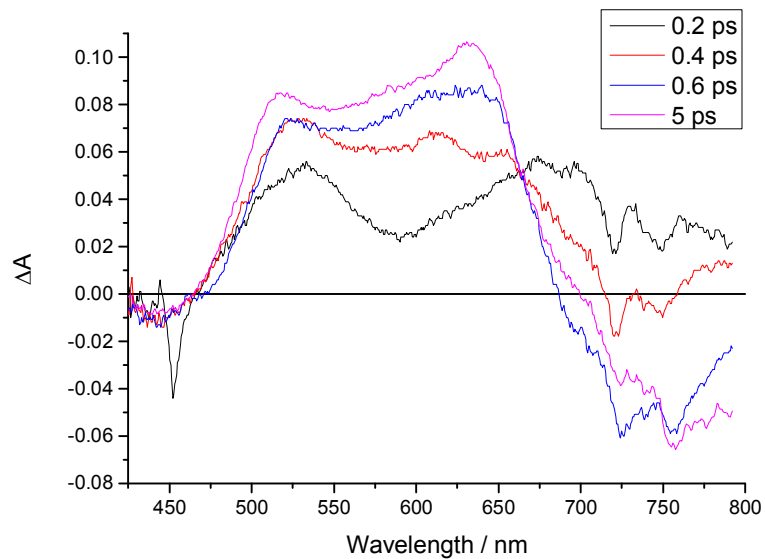
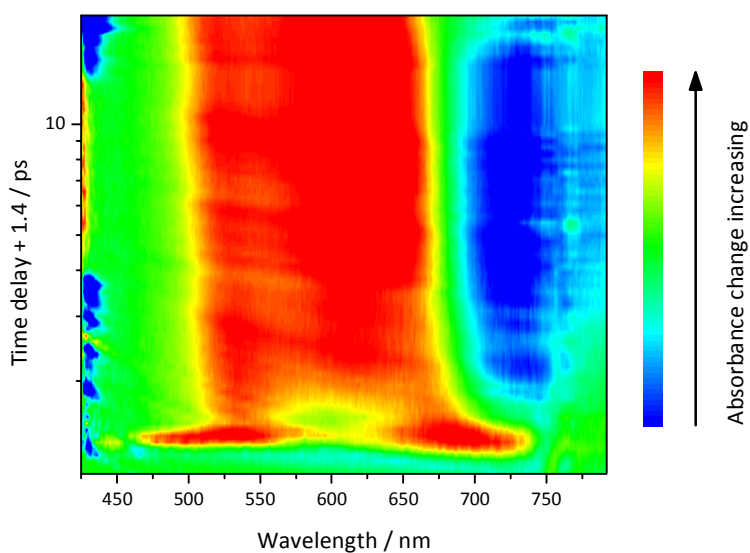


Figure S92. Time-resolved TRABS map (a) and TRABS spectrum at different time delays (b) for the compound **NI3** in acetonitrile.

a



b

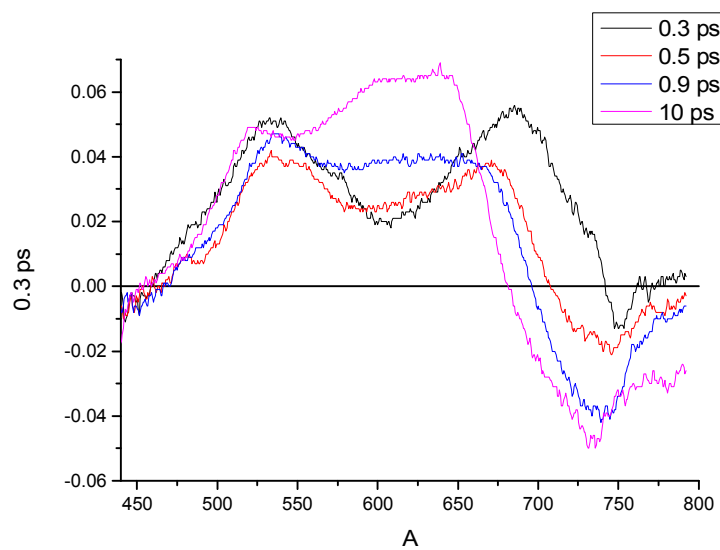
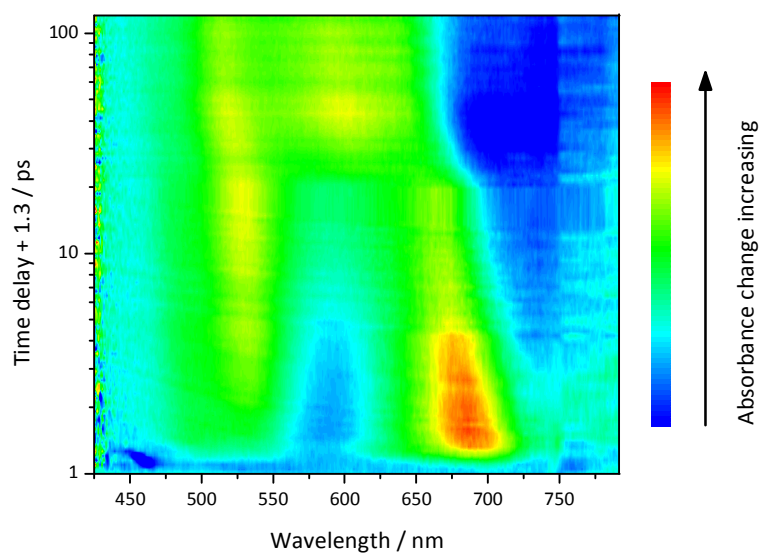


Figure S93. Time-resolved TRABS map (a) and TRABS spectrum at different time delays (b) for the compound **NI3** in methanol.

a



b

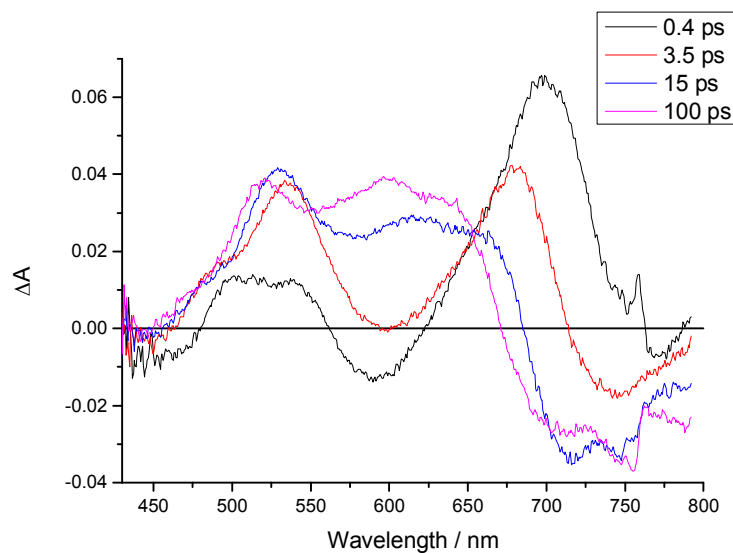
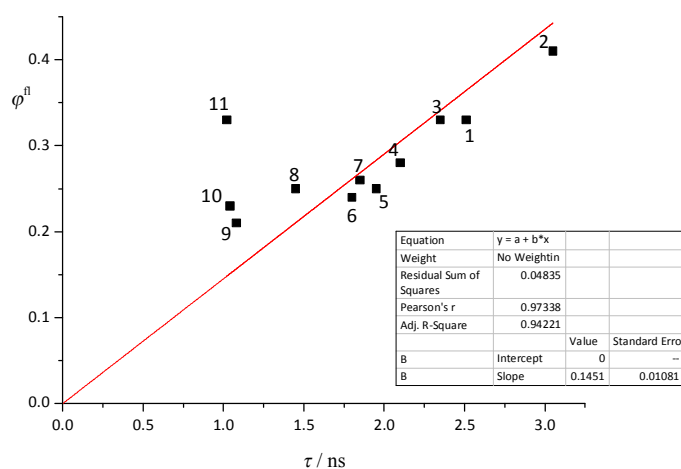


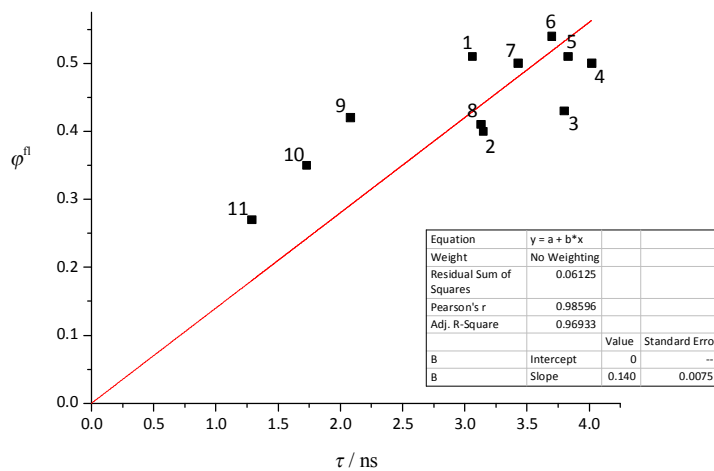
Figure S94. Time-resolved TRABS map (a) and TRABS spectrum at different time delays (b) for the compound NI3 in *n*-propanol.

9. Plots of fluorescence quantum yield *versus* excited state lifetime

a



b



c

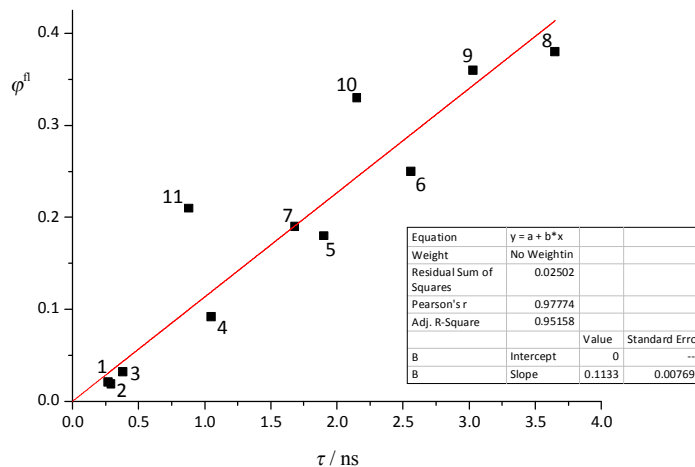


Figure S95. Plot of fluorescence quantum yield (φ^{fl}) *versus* excited state lifetime (τ) for the compound NI1 (a) NI2 (b) and NI3 (c). The solvents are numbered according to the sequence presented in Table 1 (see the manuscript text). The straight lines with zero intercepts represent the best least-square fit to the data. The inserts show the fitting parameters.